ABSTRACT

Title of Thesis: SENSITIVITY OF A SHENANDOAH WATERSHED MODEL TO

DISTRIBUTED RAINFALL DATA

Emily K. Hill, Master of Science, 2013

Directed By: Dr. Kaye L. Brubaker

Department of Civil and Environmental Engineering

Precipitation is a primary input for hydrologic modeling. In this study, the use of spatially varying gridded precipitation data obtained from the North American Land Data Assimilation System (NLDAS) is investigated for possible improvements to stream flow predictions within the Shenandoah River watershed over the use of gage based precipitation data. The sensitivity of hydrologic responses to gridded and gage precipitation data is analyzed using the Hydrologic Engineering Center's Hydrologic Modeling System (HEC-HMS).   Precipitation is the only input which varies between models. Model performance of each precipitation input is assessed by comparing predicted and measured stream flow during the 1995 to 1996 water year and calculating a number of goodness of fit measures. Results indicate that the use of spatially varying gridded precipitation data can improve stream flow predictions within the Shenandoah River watershed. Future research directions include the calibration and validation of the HEC-HMS model using the gridded precipitation data.

SENSITIVITY OF A SHENANDOAH WATERSHED MODEL TO

DISTRIBUTED RAINFALL DATA

by

Emily K. Hill

Thesis submitted to the Faculty of the Graduate School of the

University of Maryland, College Park in partial fulfillment

of the requirement for the degree of

Master of Science

2013

Advisory Committee:

Associate Professor Kaye L. Brubaker, Chair

Professor Richard H. McCuen

Research Professor Gerald E. Galloway, Jr.

Table of Contents

Chapter 1

Introduction

1.1 Context and Motivation

Currently, many hydrologic studies employ gage rainfall data as precipitation inputs to watershed models. However, distributed precipitation data, such as Next-Generation Radar (NexRad) and NASA's North American Land Data Assimilation Systems (NLDAS), are becoming more accessible. Therefore it is important to understand the implications of using currently available distributed rainfall data as precipitation inputs in hydrologic models. This analysis should increase the understanding of the relationship between the chosen precipitation inputs and the hydrological response in a model. In addition, with an increasing focus on climate change impacts in tidally and non-tidally influenced watersheds, watershed impairment due to human interference and water supply demand for an increasing population, the need to understand hydrological parameters and responses is vital in order to make comprehensive water management decisions. The sensitivity of runoff hydrographs to the spatial and temporal variability of forcing data has been a concern of research over the past few decades (Ajami, Gupta, Wagener & Sorooshian, 2004). Since spatially distributed precipitation data can more accurately represent a storm moving through a watershed it is expected that spatially variable data will improve the accuracy of the model-generated discharges and hydrograph shape.

This chapter introduces the project objective and study area. Chapter 2 is a review of relevant technical literature; it includes an introduction to hydrologic modeling and detailed information about the modeling environment and precipitation data set selected for this study: the Hydrologic Engineering Center's Hydrologic Modeling System (HEC-HMS) hydrologic model with HEC's Geospatial Hydrologic Modeling Extension (HEC-GeoHMS) and NLDAS gridded precipitation data. Chapter 3 details the inputs required for the HEC-HMS hydrologic model and

specifics regarding model setup and evaluation metrics. Chapter 4 presents model outputs and related results. Chapter 5 draws conclusions for the study and offers recommendations for further research efforts.

1.2 Project Objectives

The objective of this study is to investigate the sensitivity of a semi-distributed (specifically, HEC-HMS) hydrologic model of the Shenandoah River basin to distributed precipitation data (specifically, NLDAS). This study addresses the following questions:

- How is the modeled hydrological response within the Shenandoah River basin influenced by the use of gridded rainfall data?

- Can gridded rainfall data be used to improve stream flow forecasts within the Shenandoah River basin, compared to gage rainfall data?

1.3 Introduction of the Study Area

1.3.1   Potomac River Basin

The Potomac River basin, comprising the North Branch Potomac – Savage River, South Branch Potomac, Lower Potomac, North Fork Shenandoah, South Fork Shenandoah, Lower Shenandoah, Wills – Evitts – Town Creek, Cacapon, Conococheague – Antietam, Opequon – Back Creek, Monocacy – Catoctin, Goose – Catoctin, Seneca – Anacostia and Occoquan – Accotink watersheds, stretches across Maryland, Pennsylvania, Virginia, West Virginia and the District of Columbia and is approximately 14,670 square miles in area (Fig. 1-1). The Potomac River is the second largest contributor of fresh water to the Chesapeake Bay (Interstate Commission on the Potomac River Basin (ICPRB), 2012).
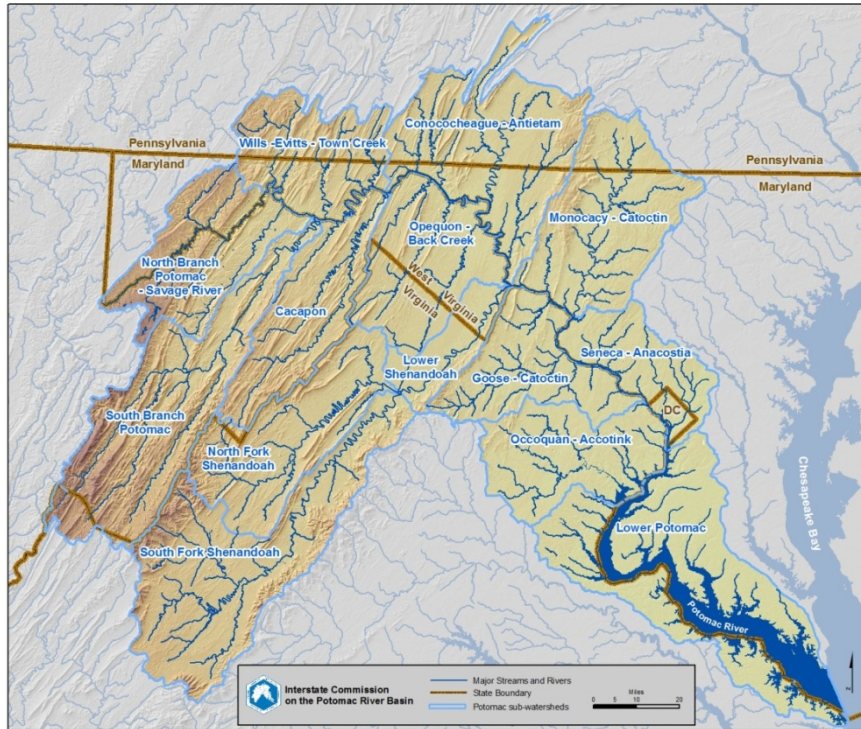
Figure 1-1: Potomac River Basin (ICPRB, 2012)

The Potomac River basin lies within five physiographic regions, the Appalachian Plateau, Ridge-and-Valley, Blue Ridge, Piedmont Plateau and Coastal Plain. The annual rainfall average in the basin ranges from approximately 60 inches in the Appalachian Plateau to approximately 30 inches in the Ridge-and-Valley (Tiruneh, 2007).

The land use within the Potomac River basin is as follows: 58-percent forests, 5-percent developed, 32-percent agricultural and 5-percent water and/or wetlands. According to the 2010 Census, approximately 6.1 million people live within the basin, with 5.4 million residing in the Washington, DC, metropolitan area.

On average 486 million gallons of water per day are withdrawn from the Potomac River to meet the water supply requirements of the Washington, DC, metro area (ICPRB, 2012). The water quality of the Potomac River began deteriorating in the 19th century due to increased mining and agriculture upstream and urban sewage and runoff downstream. Development of cities and other changes in land use have resulted in an increase in direct runoff and

sedimentation, which have led to impairment of local streams and a higher potential of flooding (Wang, 2011).

1.3.2 Shenandoah River Basin

The work presented in this paper focuses on the Shenandoah River basin (Fig. 1-2) which comprises the South Fork Shenandoah, North Fork Shenandoah and Lower Shenandoah watersheds. The Shenandoah River basin is bounded by the Blue Ridge Mountains to the east, Ridge-and-Valley Appalachians to the west, James River basin to the south and its outlet, the Potomac River, to the north. Spanning much of Virginia's western boundary, including Jefferson, Clarke, Warren, Shenandoah, Page, Rockingham, Augusta, and Rockbridge Counties, and stretching into Berkeley and Jefferson Counties, West Virginia, the Shenandoah River basin contains more than 1,400 miles of rivers and streams and is approximately 2,940 square miles in area (University of Virginia (UVAa), date unknown, and Potomac Conservancy, 2013). The Shenandoah River basin is the largest tributary to the Potomac River and therefore plays an important role in not only local water supply but also the water supply of the Washington, DC, metro area (American Rivers, 2006).

The Shenandoah River basin is located in two physiographic regions, the Ridge-and-Valley and Blue Ridge. Due to its location directly east of the Appalachians, the basin lies in a rain shadow. As a result, the basin is among the driest in the region with an annual rainfall average of 33 inches per year (University of Virginia (UVAa), date unknown).
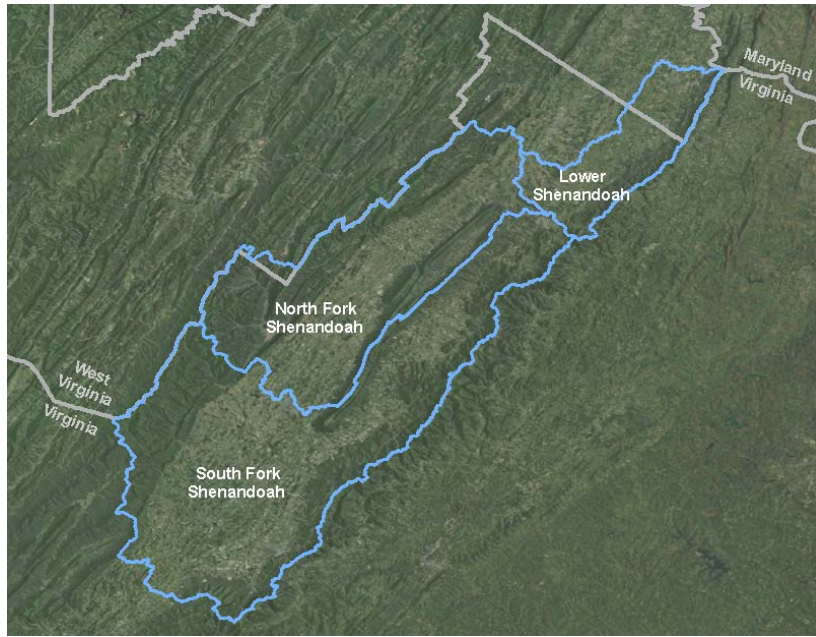
Figure 1-2: Shenandoah River Basin

The land use within the Shenandoah River basin is as follows: 58-percent forests, 3-percent
developed, 38-percent agricultural and 1-percent water and/or wetlands. According to the 2010
Census, over 0.5 million people live in the Shenandoah River basin. Current estimates show the
population in the basin is expected to rise to 0.7 million by 2040 (Virginia Employment
Commission, 2013).

Table 1-1: Potomac and Shenandoah River Basin Characteristics Summary

River Basin	Drainage Area (square miles)	2010 Population (million)	Land Use (%)			
			Forests	Developed	Agricultural	Water
Potomac	14,670	6.1	58	5	32	5
Shenandoah	2,940	0.5	58	3	38	1

As identified by American Rivers 2006, the Shenandoah River basin is currently at threat due
to the increasing population within the basin. The following factors have led to labeling the
Shenandoah River basin one of the most degraded basins within the Potomac River basin: less
than 30-percent of its banks are protected by riparian forests; in 2006, more than 1,300 miles of

rivers and streams in the basin have been identified as failing to meet federal clean water standards because of excess of nutrients, sediment and other pollutants; and river and stream banks have been subject to severe erosion. These are direct results of forests being converted to cropland, agricultural lands being replaced by suburban development, and over-burdened existing waste water and water treatment facilities (Potomac Conservancy, 2013 and American Rivers, 2006). Recently, conservation efforts within the Shenandoah River basin to return the system of rivers and streams to their native form have been effective (Wang, 2011).

Chapter 2

Literature Review

2.1 Introduction of a Watershed

A watershed is the area of land where all the water within its limits, both surface and subsurface, flows into the same place. Watersheds come in all shapes and sizes. They cross county, state and national boundaries (Environmental Protection Agency, 2012). Topography drives watershed boundaries because surface water flows downhill. A watershed is bounded by ridgelines, mountains, and hills. The boundary, or watershed divide, can be defined by connecting the highest points surrounding the drainage area (University of Arizona, 2007). Figure 2-1 shows a typical watershed. Each particular watershed has its own network of stream channels that drain water from and through the basin. The characteristics of that drainage network play a great part in determining how water moves through the basin and the consequent impacts on water quantity and quality. Large watersheds can be broken into smaller drainage basins, called subbasins, in order to better assess the topographic and hydrologic characteristics of the watershed. It is important to grasp the concept that individual drainage basins are not self-contained entities; they are pieces of a puzzle incorporated into larger surrounding watersheds that represent only a small portion of the greater hydrologic cycle (University of Delaware Water Resources Agency, date unknown).

Produced by Lane Council of Governments
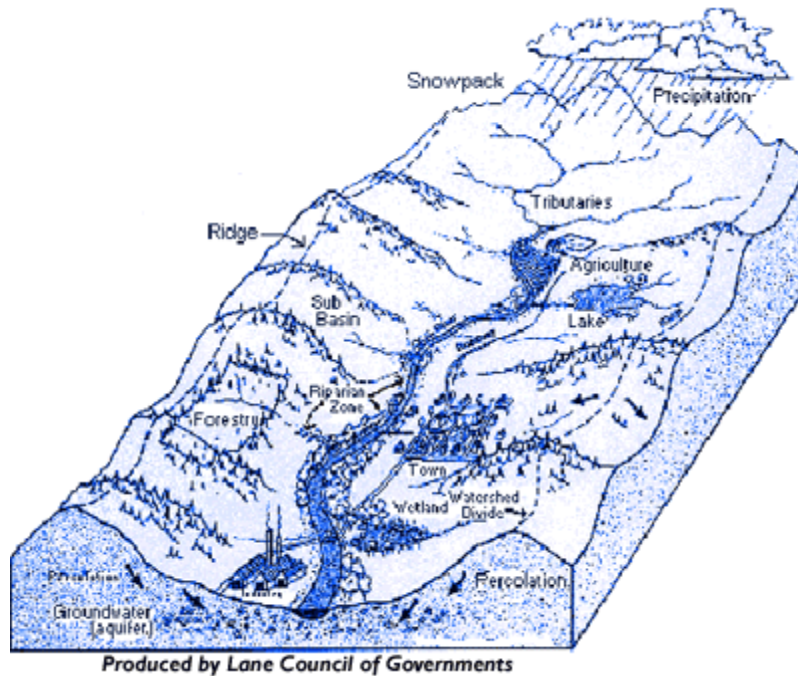
Figure 2-1: Graphical Depiction of a Watershed (EPA, 2012)

2.2 Overview of Hydrologic Modeling

Hydrologic models are simplified, conceptual representations of part of the hydrologic cycle. Hydrologic models use physics-based and empirical methods to convert rainfall into runoff and describe the flow of water over land surface (and in some cases into the soil and through the subsurface) and routing of water once it has entered a river system. Commonly, hydrologic modeling is used to estimate runoff from a watershed for hydraulic and hydrologic design projects. The most widely used application of hydrologic models is to determine the design or flood discharge of watershed (Paudel, Nelson & Downer, 2009).

In 1959, the Stanford Watershed Model was developed as the first hydrologic modeling environment to take advantage of the advent of computers to describe quantitatively the hydrologic processes that occur within a watershed (Duan, Gupta, Sorooshian, Rousseau & Turcotte, 2003). With increased understanding of the physics of watersheds and increased

computational power, many complex modeling environments have been developed since the Stanford Watershed Model (Wang, 2011)

Model types can be divided into three categories: lumped, semi-distributed and distributed (Fig. 2.2). In terms of resolution and sophistication, these models can be ranked on an ascending scale from lumped to distributed models (Paudel, Nelson & Downer, 2009).
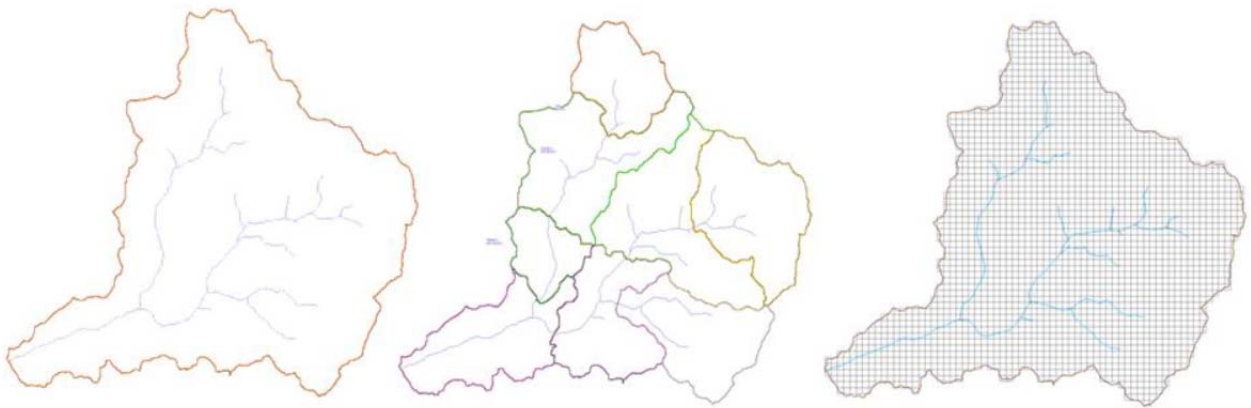
Figure 2-2 Graphical Representations of Lumped, Semi-Distributed and Distributed Hydrologic Models (Paudel, Nelson & Downer, 2009)

The following sections discuss lumped, distributed and semi-distributed models. Distributed models are discussed prior to semi-distributed since a fundamental understanding of lumped and distributed models is necessary.

2.2.1 Lumped Hydrologic Models

Lumped hydrologic models characterize the hydrologic behavior of a watershed as a single system, meaning that input data are spatially averaged over a watershed and model equations and parameters represent the response of the entire watershed as a whole (Shah, O'Connell & Hosking, 1996). They first were developed in the 1960's and applied in small to midsized watersheds where historical discharge measurements are available (Ajami, Gupta, Wagener & Sorooshian, 2004).

Limitations when using a lumped model include the assumption that rainfall is uniformly distributed over a watershed both spatially and temporally in order to develop a single hydrograph. Another shortcoming of lumped models is that their parameters are not necessarily directly related to the physical characteristics of the catchments since the parameters are assumed to be homogeneous over a watershed. Despite the simplified approach used by lumped hydrologic models, they produce runoff simulations of acceptable accuracy for numerous applications (Shah, O'Connell & Hosking, 1996). Due to this and the fact that lumped models require fewer parameters to be defined, these models are the most commonly used in practice (Paudel, Nelson & Downer, 2009).

Several lumped hydrologic modeling environments currently available are: Hydrologic Modeling System (HEC-HMS), MIKE 11 RR and Hydrologic Simulation Program-Fortran (HSPF).

2.2.2 Distributed Hydrologic Models

Distributed hydrologic models are those which divide the entire watershed into grid cells and flows are routed from one grid cell to another using the differential equations that describe the physics of flow. This allows the natural heterogeneity of a watershed to be incorporated on the scale of a grid cell. The cell resolution is chosen to represent the spatial variation of all the input data such as rainfall (Paudel, Nelson & Downer, 2009). However, the resolution of grid cells may be restricted by the resolution of topographic, land cover, or soil data, for example.

For watersheds with numerous parameters each with inherent uncertainties, distributed hydrologic models are preferred due to their capability to better incorporate the variation and uncertainties involved in defining the hydrological response to rainfall. While distributed models can simulate both spatial and temporal variability in a watershed, this often means that there are more computational requirements (Paudel, Nelson & Downer, 2009). There are ongoing studies

to address if distributed models show significant improvement over the traditional lumped models (Smith, et al., 2004).

Several distributed hydrologic modeling environments currently available are: Storm Water Management Model (SWMM), MIKE SHE, Precipitation-Runoff Modeling System (PRMS) and Gridded Surface and Subsurface Hydrologic Analysis (GSSHA).

2.2.3 Semi-Distributed Hydrologic Models

Semi-distributed models are models which have attributes of distributed models as well as lumped models (University of Saskatchewan, 2004). These models discretize the watershed into homogenous subbasins based on topography or drainage area size (Paudel, Nelson & Downer, 2009). GIS technology has made it possible to transform lumped models into semi-distributed models. With the availability of finer resolution watershed parameters from nationwide geodatabases, modelers are able to transform lumped parameters into spatially distributed parameters (Song-James, date unknown).

Some researchers suggest that semi-distributed models combine the advantages of both types of modeling. While semi-distributed models do not represent a spatially continuous distribution of variables, they do discretize watersheds to a degree thought to be useful to the individual modeler using a set of lumped models. Therefore it can represent important features of a catchment while reducing the data, time and cost of using a distributed model (Pechlivanidis, Jackson, Mcintyre & Wheater, 2011).

Several semi-distributed hydrologic modeling environments currently available are: HEC-HMS when the MODClark runoff transform method is used with distributed precipitation data, the variable infiltration capacity (VIC) model and TOPMODEL.

2.3 Current Semi-Distributed Hydrologic Modeling Environments

This section introduces the basic modeling capabilities of the semi-distributed hydrologic modeling environments, VIC, TOPMODEL, and HEC-HMS used in semi-distributed form. These models are considered semi-distributed models since they used both distributed and lumped parameters. HEC-HMS was selected for use in this study; it is described in more detail.

2.3.1 VIC

The VIC modeling environment is used to build large-scale, semi-distributed models that have both hydrologic and land surface modeling capabilities. Based on the work of Liang, Lettenmaier, Wood, and Burges (1994), it was developed at the University of Washington and Princeton University. Within the continental United States, VIC models have been applied to the Columbia, Ohio, Arkansas and Mississippi River basins.

The land surface of the VIC model is modeled as a grid of large (> 1 kilometer), flat, uniform cells. Since many land surface datasets have a smaller resolution, e.g. elevation and land cover, sub-grid nonuniformity is handled by statistical distributions. Inputs, such as precipitation and atmospheric forcings, can be gaged or gridded observations that are daily or sub-daily time series and can be processed on a daily or sub-daily time step. At a minimum, VIC requires daily precipitation, maximum and minimum air temperature and wind speed (University of Washington (UW), 2009a). VIC distributes precipitation data throughout all or a portion of a grid cell as a function of the intensity of the precipitation event. Fractional coverage of a grid cell by a precipitation event is based on the relationship:

$$\mu = (1 - e^{-aI}) \qquad\qquad 2\text{-}1$$

where *I* represents the grid cell average precipitation intensity and *a* is a coefficient which includes the effects of grid cell size and geographic variations. As the grid cell size increases, *a* decreases, thus decreasing the fractional coverage of the grid cell (UW, 2009b).

In the VIC model, each grid cell is modeled independently without consideration for horizontal water flow. This means that the VIC model simulates a time series of runoff only for each grid cell. Therefore a stand-alone routing model was developed by Lohmann, et al., (1996 and 1998) to transport grid cell surface runoff and base flow to the outlet of that grid cell and then to the river system. In this routing model, water is not allowed to flow from the channel network back into the grid cell. Once it reaches the channel it is no longer part of the water budget (no infiltration or evaporation) (Gao, et al., 2010). A unit hydrograph representing the distribution of travel times of water from its point of origin to the channel network is computed for each grid cell (UW, 2009a). Then by assuming all runoff exits a grid cell in a single flow direction, a channel routing based on the linearized Saint-Venant equation,

$$(\frac{\partial Q}{\partial t} = D\frac{\partial^2 Q}{\partial x^2} - C\frac{\partial Q}{\partial x})$$

2-2

where *C* and *D* are parameters which denote wave velocity and diffusivity, is used to calculate the discharge at the watershed outlet (Gao, et al., 2010). The VIC approach is illustrated in Figure 2-3.
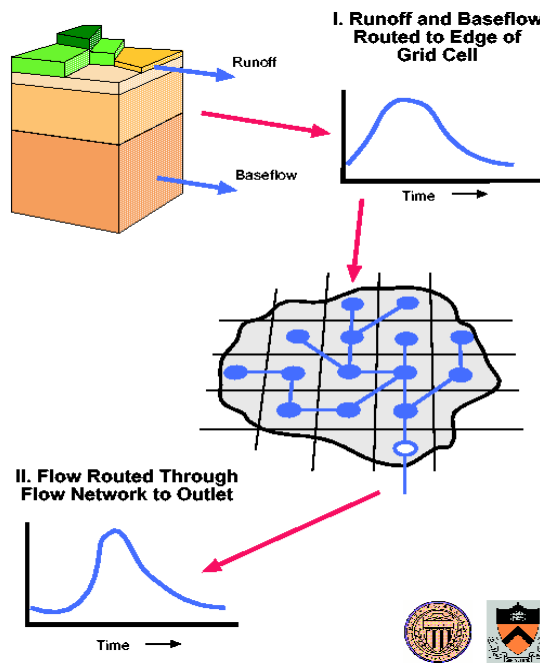
Figure 2-3: Schematic of VIC Channel Routing Model (UW, 2009a)

13

2.3.2 TOPMODEL

TOPMODEL is a semi-distributed hydrologic model which uses a set of programs for rainfall-runoff modeling in watersheds where gridded topographic data is available (Montesinos-Barrios & Beven, date unknown). TOPMODEL was developed by the Hydrology and Fluid Dynamics Group at Lancaster University in the United Kingdom. It has been applied to watersheds worldwide due to its applicability to a large range of basins (Nourani, Roughani & Gebremichael, 2011).

Data for TOPMODEL is read in ASCII format, while watershed topography is defined by gridded elevation data. At a minimum, TOPMODEL requires inputs for mean soil surface transmissivity, a transmissivity profile decay constant, a root zone storage capacity, an unsaturated zone time delay, a main channel routing velocity, internal subbasin routing velocities and rainfall (Montesinos-Barrios & Beven, date unknown). There are three options available in TOPMODEL: 1. hydrograph prediction where after model runs hydrographs are displayed and parameter values can be changed on screen and the model run again; 2. sensitivity analysis of objective functions to parameter changes where a range of parameter values are tested; and 3. Monte Carlo analysis where a large number of runs of the model can be made using random samples of the parameters (Lancaster University, 2005).

In TOPMODEL, topographic information is used in the form of an index that describes the tendency of water to accumulate and to be moved down slope by gravitational forces (Nourani, Roughani & Gebremichael, 2011). The distribution of the topographic index, λ, is used as an index of hydrologic similarity as follows:

$$\lambda_i = \ln\left(\frac{a_i}{tan\beta_i}\right) \qquad\qquad 2\text{-}3$$

where *a* is the area draining through a grid square per unit length of a contour and *tanβ* is the

local surface slope. Areas with hydrological similarity, class areas, are then used to calculate

storage deficits and discharge at each time step since they are assumed to respond in a

hydrologically similar way. Baseflow is defined as:

$$\overline{\hspace{3cm}}$$ 2-4

where Q_S is the discharge when the watershed is saturated, *S* is the storage deficit and *m* is a

parameter representing the rate of decline of the watershed recession curve. Flow routing is

through each cell by through a time-area function using the following equation

$$\overline{\hspace{3cm}}$$ 2-5

where *k* is a class area (main channel, hillslopes, etc.), tc_k is the time of concentration, *V* is a

velocity parameter, *l* is the flow path length from a class area to the watershed outlet and *N* is the

total number of classes which the time-area function is composed (Da Silva, Yamashiki &

Takara, 2010). The TOPMODEL topographic and flow concepts are shown in Figure 2-4.
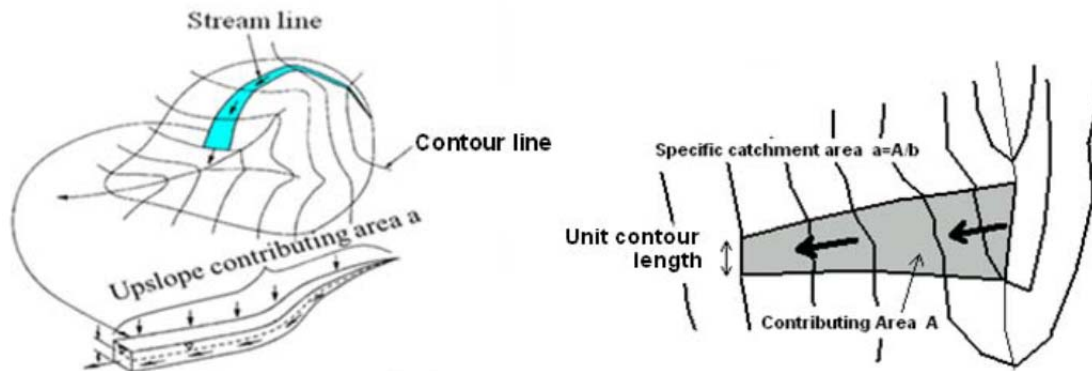

Figure 2-4: Accumulated Runoff Contributing Area per Unit Contour Length (Nourani, Roughani & Gebremichael, 2011)

2.3.3 Hydrologic Engineering Center's Hydrologic Modeling System (HEC-HMS)

The Hydrologic Engineering Center's Hydrologic Model System (HEC-HMS) was selected

for this project because it is widely used in practice and has the capacity to ingest gridded

precipitation data. This section provides the details of HEC-HMS that allow the reader to understand and interpret the study results.

2.3.3.1 Introduction of HEC-HMS

HEC-HMS is designed to simulate the precipitation-runoff processes of dendritic watershed systems. It is designed to be applicable in a wide range of geographic areas for solving a broad range of problems, from large river basin water supply and flood hydrology to small urban or natural watershed runoff. Hydrographs produced by the program can be used directly or in conjunction with other software for studies of water availability, urban drainage, flow forecasting, future urbanization impact, reservoir spillway design, flood damage reduction, floodplain regulation, wetlands hydrology, and systems operation. The HEC-HMS modeling environment was developed by the U.S. Army Corps of Engineers as a successor to HEC-1 (HEC, 2010a).

HEC-HMS in its semi-distributed form uses gridded topographic information to discretize a watershed into subbasins and incorporates the use of gridded precipitation data (Zhang, Wang, Wang, Li & Wang, 2013). The following sections will discuss the components and calculations methods utilized by HEC-HMS.

2.3.3.2 Basic Components of HEC-HMS

A HEC-HMS model is composed of four elements – subbasin; reach; reservoir; and network elements. These four elements, plus the meteorologic model, wholly represent a modeled watershed and are introduced in this section.

1. Subbasin Elements – A subbasin is an element that usually has no inflow and only one outflow. It is one of only two ways to produce flow in the watershed model. Outflow is computed from meteorological data by subtracting losses, transforming excess precipitation and adding baseflow. Subbasin elements represent the subdivided areas of a watershed.

16

2. Reach Elements – A reach element is an element with one or more inflow and only one outflow. Inflow comes from other elements in the watershed model. If there is more than one inflow, all inflow is added together before computing the outflow. Outflow is computed using one of the available methods for simulating open channel flow. Reach elements represent rivers and streams.

3. Reservoir Elements – A reservoir is an element with one or more inflow and one computed outflow. Inflow comes from other elements in the watershed model. If there is more than one inflow, all inflow is added together before computing the outflow. It is assumed that the water surface in the reservoir element is level. Several methods are available for defining storage properties of the reservoir. Reservoir elements represent reservoirs, lakes and ponds. (HEC 2010) Reservoir elements are not utilized in this study.

4. Network Elements – Network elements include source, junction, diversion and sink elements. Source elements provide a way to add measured inflows to the flow network, or to represent upstream boundary conditions. Junction elements are used in the flow network to combine multiple inflows, often at a confluence. The diversion element is used to represent locations in the flow network where water is withdrawn from the channel and discharged elsewhere. Sink elements represent the outlet of a watershed. Source elements are the second way to produce flow in the watershed model. Source and diversion elements are not utilized in this study.

5. Meteorologic Model – The meteorologic model is used to represent the external vertical forcings that drive watershed hydrology during a simulation (for example, precipitation and potential evapotranspiration). (HEC, 2010a)

The following section introduces the basic modeling functions of HEC-HMS. For this study, since reservoir elements, diversion elements and snowmelt are not utilized, they will not be addressed in further sections.

2.3.3.3 Basic Modeling Methods of HEC-HMS

For each model element, HEC-HMS offers of variety of methods to calculate the hydrological response to input data, including precipitation. This section will introduce the methods available for each model element. Only those methods chosen for this study will be discussed in detail.

1. Subbasin Elements Methods

    a. Canopy method – Used to represent the presence of plants in the landscape and for reductions in rainfall based on plant interception. When rainfall occurs, the canopy interception storage fills first. Precipitation intercepted becomes available to be evaporated, thereby reducing the precipitation available for direct flow. Water in canopy interception storage is held until it is removed by evaporation.

    b. Surface method – Used to represent the ground surface where water may accumulate in depression storage areas. Net precipitation accumulates in the depression storage areas and infiltrates as the soil has capacity to accept water, thereby reducing the precipitation available for direct flow. Water in surface interception storage is precipitation not captured by canopy interception and in excess of the infiltration rate. Precipitation is held in surface interception storage until it is removed by infiltration and evapotranspiration.

    c. Loss method – Infiltration calculations are performed by a loss method. Twelve different loss methods are available. Two which were investigated for use in this

study are the Soil Conservation Service (SCS) Curve Number (CN) and Soil

Moisture Accounting (SMA).

i. SCS CN loss method

The subbasin SCS CN method, HEC-HMS computes incremental

precipitation during a storm by recalculating the infiltration volume at the

end of each time interval based on the CN and percent impervious area of

the subbasin. Infiltration during each time interval is the difference in

volume at the end of two adjacent time intervals (HEC, 2010a). Runoff

using the SCS CN method is determined by the following equation:

$$Q = \frac{\left[P - 0.2\left(\frac{1000}{CN} - 10\right)\right]^2}{P + 0.8\left(\frac{1000}{CN} - 10\right)} \qquad \text{2-6}$$

where Q is runoff (in.) and P is precipitation (in.) (NRCS, 1986). The

SCS loss method is intended for event simulations.

ii. SMA loss method

The SMA loss method is based on the USGS's Precipitation Runoff

Modeling System (Leavesley, Litchy, Troutman & Saindon, 1982). The

model simulates the movement of water through, and storage of water on

or in the surface and groundwater layers. The SMA loss method uses

three layers to represent the dynamics of water movement in the soil.

Layers include soil storage, upper groundwater and lower groundwater.

The soil storage layer is subdivided into tension and gravity storage.

Groundwater layers are intended to represent shallow interflow processes.

The layers and processes are summarized in Figure 2-5. The SMA loss

method is well suited for continuous simulation since it can simulate both

wet and dry weather conditions. Canopy and surface infiltration storage

are used in conjunction with the SMA loss method.
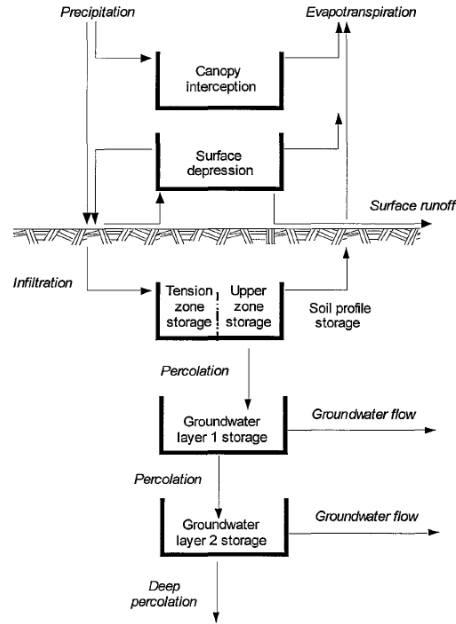
Figure 2-5: SMA Loss Method Schematic (HEC, 2000)

d. Transform method – Surface runoff calculations are performed by a transform

method. Seven methods are available in HEC-HMS. Two which were

investigated for use in this study are SCS Unit Hydrograph (UH) and Clark's UH.

The SCS unit hydrograph transform method has been evaluated for use in HEC-

HMS using gage rainfall data; it is not well suited for gridded precipitation data.

Therefore, the Clark's UH transform method for gaged precipitation data and

ModClark transform method for gridded precipitation data are utilized in this

study.

Clark's UH derives a watershed UH by explicitly representing the short-term

attenuation of precipitation and translation of precipitation to runoff. Outflow,

O_t, is computed as:

$$O_t = C_A I_t + C_B O_{t-1} \qquad\qquad 2\text{-}7$$

where R is constant linear reservoir parameter, Δt is the model time step, I_t is

inflow into storage, and C_A and C_B are routing coefficients computed as

$C_A = \frac{\Delta t}{R + 0.5\Delta t}$ and $C_B = 1 - C_A$.

The ModClark method is a linear, quasi-distributed transform method based

on the Clark conceptual unit hydrograph. It fundamentally represents the

subbasin as a collection of grid cells. While the Clark method uses a time-area

curve and the time of concentration to develop a translation hydrograph, the

ModClark method eliminates the time-area curve and instead uses a separate

travel time index for each grid cell (HEC, 2000). The travel time index for each

cell is scaled by the overall time of concentration. Excess precipitation falling on

each grid cell is lagged by the scaled time index and then routed through a linear

reservoir. Final hydrographs are the outputs from the linear reservoirs of the cells
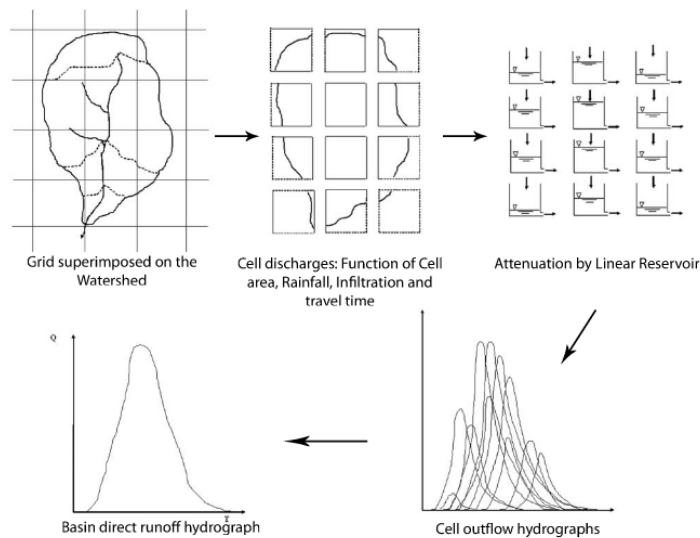
(Figure 2-6).

Figure 2-6: ModClark Conceptual Model (Kull & Feldman, 1998)

e. Baseflow method – Subsurface calculations are performed by a baseflow method. Four methods are available in HEC-HMS. The linear reservoir baseflow method uses a linear reservoir to model the recession after a storm event. It conserves mass within the subbasin. The infiltration computed by the loss method is connected as the inflow to the linear reservoir. When used with the SMA loss method, infiltration is connected to the lateral outflow of the groundwater layers.

2. Reach Elements

a. Routing method – While a reach conceptually represents a segment of stream, the calculations are performed by a routing method contained within the reach. Six methods are available in HEC-HMS. Two which were investigated for use in this study are Muskingum-Cunge and Kinematic Wave. The kinematic wave routing method is best suited to steep slopes and engineered channels (HEC, 2010a). The Muskingum-Cunge is applicable to a wide range of applications; therefore this routing method is used for this study. The Muskingum-Cunge routing method is based on the conservation of mass and the diffusion representative of the conservation of momentum. It is sometimes referred to as a variable coefficient method because the routing parameters are recalculated every time step based on channel properties and depth of flow. It represents attenuation of flood waves and can be used in reaches with small slopes. The governing equation to determine discharge during the Muskingum-Cunge routing method is:

$$\frac{\partial Q}{\partial t} + c \frac{\partial Q}{\partial x} = \frac{q_o}{2S_o} \frac{\partial^2 Q}{\partial x^2} \qquad\qquad 2\text{-}8$$

where Q is discharge (cfs), c is wave celerity (ft/sec), q_o is average discharge per unit channel width (ft^2/sec) and S is storage (ft^3) (HEC, 2000).

b. Loss/Gain Method – The loss/gain method represents losses from the channel, additions to the channel from groundwater or bi-directional water movements. A loss/gain method is optional and is not utilized in this study.

3. Network Elements

a. Junctions – Elements with one or more inflows and only one outflow, used to represent stream confluences in this study. All inflow is added together to produce the outflow by assuming zero storage at the junction. There is no spatial extent or physical properties associated with junctions therefore no computational methods are needed.

b. Sinks – Elements with one or more inflows but no outflow, used to represent the outlet in this study. Multiple inflows are added together to determine the total amount of water entering the elements. There are no spatial extents or physical properties associated with sinks therefore no computational methods are needed.

4. Meteorologic Model – The meteorologic model is one of the main components of a HEC-HMS model. Its principal purpose is to prepare meteorologic inputs for subbasins.

a. Precipitation method – Represents the choice of precipitation data. Gridded precipitation data and gage precipitation data are used in this study. Gridded precipitation data are inserted directly into a HEC-HMS and require no spatial adjustment. Generally, since gage precipitation data are not available on a subbasin basis the precipitation must be adjusted within HEC-HMS. The inverse distance method is used in this study. The inverse distance method relies on gages that are positioned within and around a watershed to provide adequate spatial resolution of precipitation within the watershed. Weights are computed and assigned to each gage in inverse proportion to the square of the gage's distance from each subbasin centroid.

b. Evapotranspiration method – Represents a combination of evaporation and from the ground surface and transpiration by vegetation. Evapotranspiration is often responsible for returning 50% of precipitation back to the environment. The monthly average method is designed to work with average depth of evaporation water each month. (HEC, 2010a)

The following section introduces the inputs required for the elements and meteorologic model, as identified in this section as being utilized, in HEC-HMS.

2.3.3.4 Input Requirements of HEC-HMS

1. Subbasin Inputs

   a. Area (mi^2)

   b. SCS CN loss method

      i. CN prepared from land cover and soil surveys

      ii. Percent impervious area (%) – Defines the percentage of the subbasin which is impervious area.

   c. SMA loss method

      i. Soil (%), groundwater 1 (%) and groundwater 2 (%) – initial condition of the soil, upper groundwater layer and lower groundwater layer specified as a percentage of the maximum possible soil water storage that is full of water at the beginning of the simulation.

      ii. Maximum infiltration (in./hr) – the upper bound of infiltration from the surface storage into the soil. The actual infiltration in a particular time interval is a linear function of the surface and soil storage.

      iii. Impervious area (%) – percentage of the subbasin which is directly connected impervious area.

iv. Soil storage (in.) – represents the total storage available in the upper soil layer. If set to 0, infiltrated water is passed directly to groundwater.

v. Tension storage (in.) – represents the amount of water storage in the soil that does not drain under the affects of gravity. Percolation from the soil layer to the upper groundwater layer occurs when the soil storage exceeds the tension storage. Water in tension storage is removed by evapotranspiration.

vi. Soil percolation (in./hr), groundwater 1 percolation (in./hr) and groundwater 2 percolation (in./hr) – sets the upper bound on the percolation from the given layer into the layer located directly below. The actual percolation rate is a linear function of the current storage in the given layer and the current storage in the layer located directly below.

vii. Groundwater 1 storage (in.) and groundwater 2 storage (in.) – represent the total storage in the upper and lower groundwater layers. If set to 0, water percolated from the soil passes directly to the lower groundwater layer or deep percolation.

viii. Groundwater 1 coefficient (hr) and groundwater 2 coefficient (hr) – time lag on a linear reservoir for transforming water in storage to become lateral outflow available to become baseflow.

d. Clark's UH and ModClark transform method

i. Time of concentration, T_c, (hr) – Defines the maximum travel time in the subbasin. The grid cell in the subbasin with the largest travel time index sets the T_c value for the subbasin. All other grid cells have a scaled T_c based on the ratio of the grid cell's travel time index to the maximum travel time index.

  ii. Storage coefficient (hr) – Index of the temporary storage of precipitation excess in the watershed as it drains to the outlet point.

 e. Baseflow method

  i. Initial Discharge (cfs) – Represents observed initial baseflow within a subbasin.

  ii. Groundwater 1 and 2 Coefficient (hr) – Time constant for the linear reservoir in each groundwater layer. Gives a sense of the response time of the subbasin.

  iii. Groundwater 1 and 2 Reservoirs – Can be used to route the baseflow through several sequential reservoirs. Attenuation of the baseflow increases as the number of reservoirs increases.

2. Reach Inputs

 a. Muskingum-Cunge routing method

  i. Length (ft) – Total length of the reach element

  ii. Slope (ft/ft) – Average slope for the reach element

  iii. Manning's n – Average value for the reach element. Typically estimated through calibration, using engineering judgment and knowledge of the river/stream properties.

  iv. Shape – Specifies the cross section shape of the reach element. Five options are available: circular, triangle, rectangle, trapezoid and 8-point cross section.

3. Meteorologic Inputs

 a. Precipitation data (in.)

 b. Evapotranspiration rates (in./month) (HEC, 2010a).

Many of the input parameters used in this study have been determined using Geographic Information Systems (GIS) capabilities. The program, HEC-GeoHMS, which has been developed by the Army Corps of Engineers to aid in the development of inputs for HEC-HMS is described in Section 2.5 and Chapter 3.

2.3.3.5 Output Files of HEC-HMS

The output from HEC-HMS simulations are grouped into two categories: summary and individual output. Summary outputs give a high level overview of HEC-HMS outputs which include peak discharges from subbasin and reach elements and associated time and volume. An example is shown in Figure 2-7.

Figure 2-7: Example HEC-HMS Global Summary Results
(HEC, 2010a)

Individual outputs give detailed information at specific elements. These outputs include hydrographs (Figure 2-8A) and time-series data (Figure 2-8B).
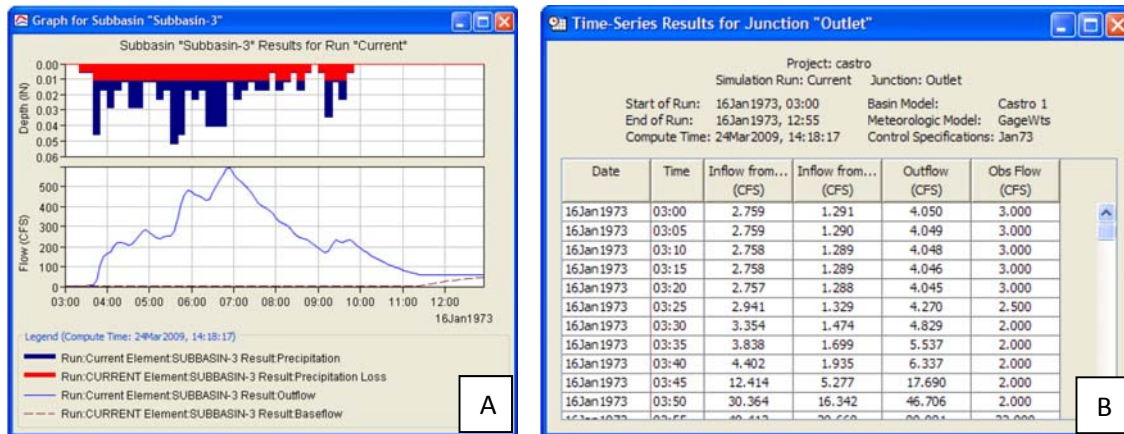
Figure 2-8: Example HEC-HMS Individual Results for a Subbasin and Junction
(HEC, 2010a)

2.4 Introduction of Rainfall Data

The most important input information for a hydrologic model is precipitation. The most

common form applied in modeling is gage data. Gage data is input as point data and generally

assumed to be constant across a subbasin. This type of modeling does not accurately represent

the spatial variation that occurs in reality. Rainfall data obtained through radar observations can

be input as gridded data and is assumed to be a better representation of spatial variation across

subbasins (McMillan, Jackson, Clark, Kavetski & Woods, date unknown). As indicated in

Chapter One, the sensitivity of runoff hydrographs to the spatial and temporal variability of

rainfall data has been a concern of research over the past few decades (Ajami, Gupta, Wagener &

Sorooshian, 2004). This section introduces NASA's North American Land Data Assimilation

System (NLDAS) which is used in the semi-distributed HEC-HMS model developed for this

study.

2.4.1 NLDAS

2.4.1.1 Introduction of NLDAS

The NLDAS integrates a large quantity of observation-based and model reanalysis data,

including forcing data for total hourly precipitation in kg/m, to drive four offline land-surface

models (LSMs), NASA's Mosaic, NOAA's Noah, the NWS Office of Hydrological

Development (OHD)'s SAC and Princeton's implementation of VIC (NASA, 2013a).

Reanalysis is a systematic approach to produce data for climate monitoring and research.

Reanalyses are created by an unchanging data assimilation scheme and models which contain all

available observations over the period being analyzed. The unchanging scheme provides a

consistent estimate of the data state at each time step (National Center for Atmospheric Research,

undated). The Mosaic and Noah LSMs are coupled land-atmosphere modeling systems, while

SAC and VIC are hydrologic models (Xia, Ek, Wei & Meng, 2012). NLDAS consists of two

datasets, Phase 1 and Phase 2, both which contain forcing data in 1/8th-degree grid spacing

(approximately 14 km) over central North America, enabled by NASA's Land Information

System (LIS), a software framework for high performance land surface modeling and

assimilation (NASA, 2013b). Phase 1 contains hourly data from August 1, 1996, to December

31, 2007, while Phase 2 contains hourly and monthly data from January 01, 1979, to present

(Goddard Earth Sciences Data and Information Services Center (GES DISC), 2013). Currently,

the lag time for real-time availability for NLDAS forcing data is 4-5 days (Xia, Ek, Wei & Meng,

2012). The analysis presented in this study utilizes the Phase 2 data which is discussed herein.

For more information regarding Phase 1, the reader may refer to the NLDAS website at

ldas.gsfc.nasa.gov/index.php.

NDLAS Phase 2 (NLDAS-2) is a collaborative project among NCEP's Environmental

Modeling Center (EMC), NASA's Goddard Space Flight Center (GSFC), Princeton University,

OHD, the University of Washington and NCEP's Climate Prediction Center (CPC). NASA's

GSFC led the development of the algorithm to generate the forcing data and produced the data

for the January 1, 1979 to December 31, 2007, timeframe (GES DISC, 2013).

NLDAS-2 forcing data is available via FTP access through the GrADS Data Server (GDS)

and via Giovanni and Mirador Services – all through the GES DISC. NLDAS-2 forcing data are

stored an provided in the GRIdded Binary (GRIB) format, but can be converted to Network Common Data Form (NetCDF) files during the download process. GRIB files are a concise data format commonly used in meteorology to store historical and forecast weather data. GRIB files contain information related to gridded fields, including grid time and spatial data (National Oceanic and Atmospheric Administration (NOAAa), date unknown). NetCDF is an interface for array-oriented data access and a library that provides an implementation of the interface; data in this format can be opened in ArcGIS through the Multidimension Tools toolbox (National Oceanic and Atmospheric Administration (NOAAb), date unknown). Two sets of forcing data are available, a primary (default) forcing dataset (File A) and a secondary (optional) forcing dataset (File B) (GES DISC, 2013). The forcing variables (parameters) contained in File A are listed in Table 2-1. This study utilizes the total hourly precipitation forcing data contained in File A.

Table 2-1: Parameters Available in the NLDAS-2 File A

PDS IDs	Full Name	Unit	Time
61	Precipitation hourly total	kg/m^2	Hourly backward-accumulated
157	180-0 mb above ground Convective Available Potential Energy	J/kg	Hourly instantaneous
153	Fraction of total precipitation that is convective	unitless	Hourly backward-accumulated
205	LW radiation flux downwards (surface)*	W/m^2	Hourly instantaneous
204	SW radiation flux downwards (surface)	W/m^2	Hourly instantaneous
228	Potential evaporation	kg/m^2	Hourly backward-accumulated
1	Surface pressure*	Pa	Hourly instantaneous
51	2-m above ground Specific humidity*	kg/kg	Hourly instantaneous
11	2-m above ground Temperature*	K	Hourly instantaneous
33	10-m above ground Zonal wind speed	m/s	Hourly instantaneous
34	10-m above ground Meridional wind speed	m/s	Hourly instantaneous

Source: GES DISC, 2013

2.4.1.2 NLDAS Precipitation Forcing Data

The total hourly precipitation contained in File A is derived from Climate Prediction Center (CPC) daily gage data (with the PRISM topographic adjustment as introduced by Daly, Neilson & Phillips, 1994), hourly Doppler Stage II radar precipitation data, half-hourly CPC Morphing

Technique (CMORPH) data and 3-hourly North American Regional Reanalysis (NARR) precipitation data (NASA, 2013a). The Precipitation-elevation Regressions on Independent Slopes Model (PRISM) is a method to distribute point measurements of monthly and annual average precipitation to regularly spaced grid cells (Daly, Neilson & Phillips, 1994). Reflecting the strengths of each dataset, hourly NLDAS-2 precipitation is derived by using the Doppler radar or CMORPH products to temporally disaggregate the daily gage products. This process capitalizes on the accuracy of the daily gage product and on the temporal and spatial variations of the Doppler radar and CMORPH products (NASA, 2013a).

Over the continental United States (CONUS), CPC PRISM-adjusted $1/8^{th}$ degree daily gage analyses serves as the backbone of the NLDAS-2 hourly precipitation forcing. These gage-only precipitation analyses are first processed to fill any missing values and then are separated in hourly fields. This is done by deriving hourly disaggregation weights from NWS real-time, 4-km Stage II radar (from 1996 to present) and 8-km CMORPH (from 2002 to present) hourly precipitation analyses. (NLDAS, 2013) The Stage II product consists of Weather Surveillance Radar-1988 Doppler (WSR-88D) radar based precipitation estimates that have been bias corrected using hourly multi-agency gaged data and complied into a national product over CONUS (Fulton, Breidenbach, Seo, Miller & O'Bannon, 1998). The compiled data are interpolated to $1/8^{th}$ degree (approximately 14 km). Gaps, which account for approximately 13% of CONUS due to lack of radar coverage and equipment maintenance, are filled with the nearest neighbor Stage II data. If Stage II data is not available, CMORPH data are used. For gage precipitation analyses prior to the availability of Stage II and CMORPH data, CPC Hourly Precipitation Dataset (HPD) or NARR data are used instead. Table 2-2 shows the ranking of data choice (Goddard Earth Sciences Data and Information Services Center (GES DISC), 2013).

Table 2-2: Summary of Datasets for NLDAS-2

Dataset	Years	CONUS
CPC daily gage analysis	1979 - present	1/8th-degree PRISM-adjusted analysis
Stage II Doppler hourly 4-km radar data	1996 - present	1st choice to temporally disaggregate
CMORPH satellite-retrieved half-hourly 8-km analysis	2002 - present	2nd choice to temporally disaggregate
CPC HPD 2x2.5-degree hourly gage analysis	1979 - present	3rd choice to temporally disaggregate
NARR/R-CDAS 3-hourly 32-km model-simulated precipitation	1979 - present	4th choice to temporally disaggregate

Source: NASA, 2013a

2.5 Introduction of HEC-GeoHMS

Recent advances in GIS have opened many opportunities for enhancing hydrologic modeling of watershed systems. With the increasing availability of spatial information from government agencies, commercial vendors and private companies, coupled with the powerful spatial algorithms, the integration of GIS with hydrologic modeling improves accuracy for both lumped and distributed parameters. In addition, hydrologic modeling has evolved to consider distributed rainfall data and advanced techniques for modeling watersheds on a grid level to provide more detail than the traditional lumped approach. HEC-GeoHMS has been developed as a geospatial hydrology toolkit for engineers and hydrologists. HEC-GeoHMS is a set of ArcGIS tools specifically designed to process geospatial data and create input files for HEC-HMS. It includes integrated data management and a graphical user interface (GUI). Through the GUI, which consists of menus, tools and buttons, the user can analyze terrain information, delineate subbasins and stream and prepare hydrologic parameters. The relationship between GIS, HEC-HMS and HEC-GeoHMS is illustrated in Figure 2-9 (HEC, 2010b).
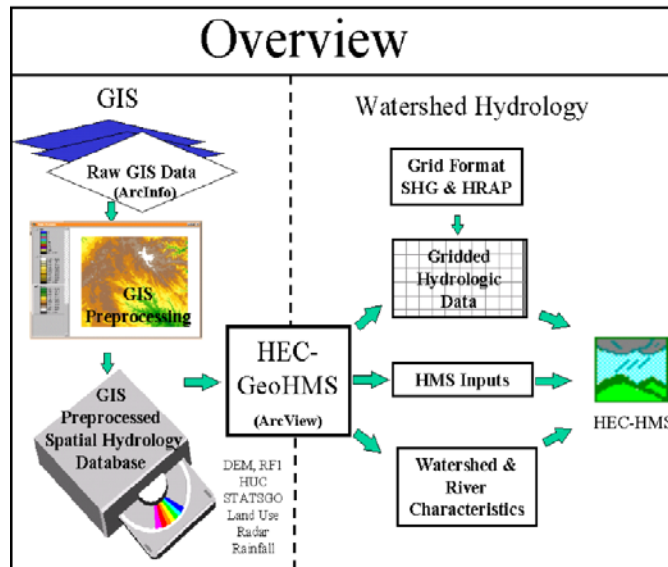
Figure 2-9: Overview of GIS and Hydrology Programs (HEC, 2010b)

2.5.1 Basic Steps of HEC-GeoHMS

1. Data Collection – This step includes collecting datasets which are necessary to construct a HEC-HMS model. Examples of data collected and their sources include the following:

    a. Digital Elevation Models (DEM) can be obtained from the USGS National Elevation Dataset (NED). NED is a raster product primarily derived from 10- and 30-meter DEMs, from higher resolution data sources such as light detection and ranging (LiDAR) and high-resolution imagery. NED data is currently available as 1 arc-second (approximately 30 meters) for the CONUS and at 1/3 and 1/9 arc-seconds (approximately 10 and 3 meters) for parts of the United States (USGS, 2013a).

    b. Land cover and percent impervious surface data, can both be obtained from the Multi-Resolution Land Characteristics Consortium's (MRLC) National Land Cover Database (NLCD). The NLCD has land cover and percent impervious surface data for 1992, 2001 and 2006 at a resolution of 1 arc-second (approximately 30 meters) (USGS, 2012).

c. Soil data can be obtained from the Natural Resources Conservation Service's (NRCS) Soil Survey Geographic Database (SSURGO). The SSURGO database contains information about soil as collected by the National Cooperative Soil Survey over the course of a century by in situ soil observations. The SSURGO datasets consists of map data, tabular data and source information (NRCS, date unknown).

d. Hydrography data (the location of streams, rivers, and water bodies) can be obtained from the USGS National Hydrography Dataset (NHD). The NHD is the surface water component of The National Map. It is a digital vector dataset used by GIS and contains features such as lakes, streams, rivers, dams and stream gages (USGS, 2013b).

2. Data Assembly – This step includes converting data collected during Data Collection into a common format, grid files for terrain, land cover, etc. and vector shapefiles for hydrography, gage locations, etc., and common projection.

3. Terrain Processing – This step includes computing flow direction and accumulation, defining streams and delineating watersheds/subbasins based on the DEM assembled in Data Assembly.

4. HMS Project Setup – This step includes defining the study area in GIS that will be used to develop the HEC-HMS hydrologic model. The user defines the outlet of the watershed to be analyzed and HEC-GeoHMS copies all data upstream of that location to a new workspace.

5. Basin Processing – At this step, the stream and subbasin delineations as determined in Terrain Processing can be modified as necessary to meet the study objectives. For example, during this step, the subbasins can be modified to capture stream gage locations.

6. Stream and Watershed Characteristics – This step includes determining the physical characteristics for subbasins, including longest flow paths and river and subbasin slopes. These parameters are stored in attribute tables and can be exported in order to determine hydrologic parameters outside of HEC-GeoHMS.

7. Hydrologic Parameters – The step includes estimating the values of hydrologic parameters, selecting the HEC-HMS processes described in Section 2.2 and creating grid-based representation of the watershed for use with distributed rainfall data. Hydrologic parameters which are estimated during this step include time of concentration, lag time, curve number and percent impervious. All hydrologic parameters are stored in the attribute table of the stream and/or subbasin shapefiles. Time of concentration calculations are initially estimated in HEC-GeoHMS and then exported to an excel spreadsheet for revisions as necessary. The revised values are then imported back into HEC-GeoHMS and stored in the subbasin attribute table.

8. HEC-HMS Model Files – This step produces files that are used directly in HEC-HMS, including background shapefiles, basin schematic, watershed model file and a project file. Once a data check is completed, the user can import necessary files to a HEC-HMS model (HEC, 2010b).

2.6 Current Studies

In the past 10 years, numerous studies have utilized gridded forcing data in studies. Knebl, Yang, Hutchison, and Maidment (2005) and Neary, Habib, and Fleming (2004) used NEXRAD gridded precipitation data as inputs for HEC-HMS to model the San Antonio (Texas) River Basin and a watershed in middle Tennessee. Pan, et al., (2003) used NLDAS gridded snow data from the LSM models to make comparisons to observed data from the Natural Resources Conservation Service's Snowpack (SNOTEL). Sullivan and Maidment (2013) analyzed NLDAS gridded soil

moisture data to assess drought periods in Texas for decision making purposes. Luo, et al., (2003) made comparisons between NLDAS gridded precipitation data and local precipitation data in the Southern Great Plains; no hydrologic modeling was completed. Nan, et al., (2010) made comparisons between NLDAS gridded precipitation data and NEXRAD precipitation data in the Ohio River Basin; no hydrologic modeling was completed. To the author's knowledge no studies have used NLDAS gridded precipitation data as inputs for a HEC-HMS hydrologic model.

Chapter 3

Methods and Model Setup

Two HEC-HMS hydrologic models were created as part of this study: one using

precipitation gage data, the other using NLDAS gridded precipitation data. All other parameters

used in the hydrologic model were identical. The following sections describe the methods used

in the hydrologic model development and analysis.

3.1 GIS Watershed Processing

At a minimum, the data required to build a HEC-HMS hydrologic model are elevation, land

cover, percent impervious area, soil and hydrography information. These datasets were used to

determine stream/subbasin characteristics and hydrologic parameter estimations. HEC-GeoHMS

was utilized to process these datasets for use in HEC-HMS. The following sections detail the

methods used in ArcGIS and HEC-GeoHMS used to set up and estimate parameters for the HEC-

HMS hydrologic model.

3.1.1 Data Collection and Assembly

Data collection and assembly is required prior to using HEC-GeoHMS. The tools described

in this section are contained within the ArcGIS toolboxes. The following are the data obtained,

their sources and assembly required for use with the HEC-GeoHMS tools.

1. DEMs were obtained from the USGS National Elevation Dataset. The DEMs obtained

    have a resolution of 1/3 arc-second (approximately 10 m) and were flown by the USGS

    between 1999 and 2009. DEMs are not supplied as contiguous raster over the

    Shenandoah River basin and the individual raster tiles must be joined to produce a

    seamless elevation raster. This was done using the Raster, Mosaic to New Raster tool

within the Data Management toolbox in ArcGIS and is referred to as the raw DEM in future sections.

2. Land cover and percent impervious surface data were both obtained from the MRLC National Land Cover Dataset. The land cover and percent impervious data have a resolution of 1 arc-second (approximately 30 m) and were obtained by MRLC in 2001. Land cover and percent impervious data are supplied as a single raster for the entire CONUS.

3. Soil data were obtained from the NRCS SSURGO Database. SSURGO data are stored in a polygon shapefile and were published by NRCS 2002. SSURGO data are not supplied as a contiguous shapefile over the Shenandoah River basin and the individual shapefiles were joined to produce a single shapefile. This was done using the General, Merge tool within the Data Management toolbox in ArcGIS.

4. Hydrography data were obtained from the USGS National Hydrography Dataset. Hydrography data are a polyline shapefile and is not dated. The hydrography data are supplied by 8-digit Hydrologic Unit Code (HUC) subbasins. The hydrography shapefiles for the North Branch, South Branch and Lower Shenandoah basins (HUC Subbasins 0207006, 0007 and 0005 respectively) were obtained. Since hydrography data are not supplied as a contiguous shapefile over the Shenandoah River basin and the individual shapefiles were joined to produce a single shapefile. This was done using the General, Merge tool within the Data Management toolbox in ArcGIS.

Once the datasets had been downloaded and compiled as contiguous features over the entire Shenandoah River basin, a projection was defined. The Shenandoah River basin falls within the jurisdiction of the ICPRB. The ICPRB has numerous completed or ongoing studies that have utilized the geographic and projected coordinate systems shown in Figure 3-1. Therefore, these were utilized for this study. Raster datasets were projected using the Projections and

Transformations, Project Raster tool within the Data Management Toolbox. Polygon datasets were projected using the Projections and Transformations, Project tool within the Data Management Toolbox.

```
NAD_1983_UTM_Zone_18N
Projection: Transverse_Mercator
False_Easting: 500000.000000
False_Northing: 0.000000
Central_Meridian: -75.000000
Scale_Factor: 0.999600
Latitude_Of_Origin: 0.000000
Linear Unit: Meter

GCS_North_American_1983
Datum: D_North_American_1983
```

Figure 3-1: Geographic and Projected Coordinate System for Study Area

The datasets were clipped to the Shenandoah River basin once the projection was completed. For raster and polygon datasets, a boundary shapefile is needed to define the limits of data to be retained. The merged HUC Subbasins was used as the boundary shapefile. Raster datasets were clipped using the Extraction, Extract by Polygon tool within the Spatial Analyst toolbox. Polygon datasets were clipped using the Extract, Clip tool within the Analysis toolbox.

3.1.2 Terrain Processing and Watershed Delineation

Prior to setting up a HEC-HMS project within HEC-GeoHMS, the raw DEM must be processed to create datasets that serve as the spatial database of the hydrologic model. The tools described in this section are found under the Terrain Processing menu in HEC-GeoHMS.

1. To ensure that the true channel is represented and flow is conveyed along the channel, the elevations of cells in the raw DEM that coincide with flow lines contained in the hydrography shapefile were artificially lowered. This was done using the DEM Reconditioning tool.

2. Since the raw DEM and the hydrography dataset were checked to ensure that artifacts did not exist, the Fill Sink tool was used to fill any potential sinks contained with the raw DEM or created during the reconditioning process.   The resulting DEM (Figure 3-2) is referred to as the hydro DEM.
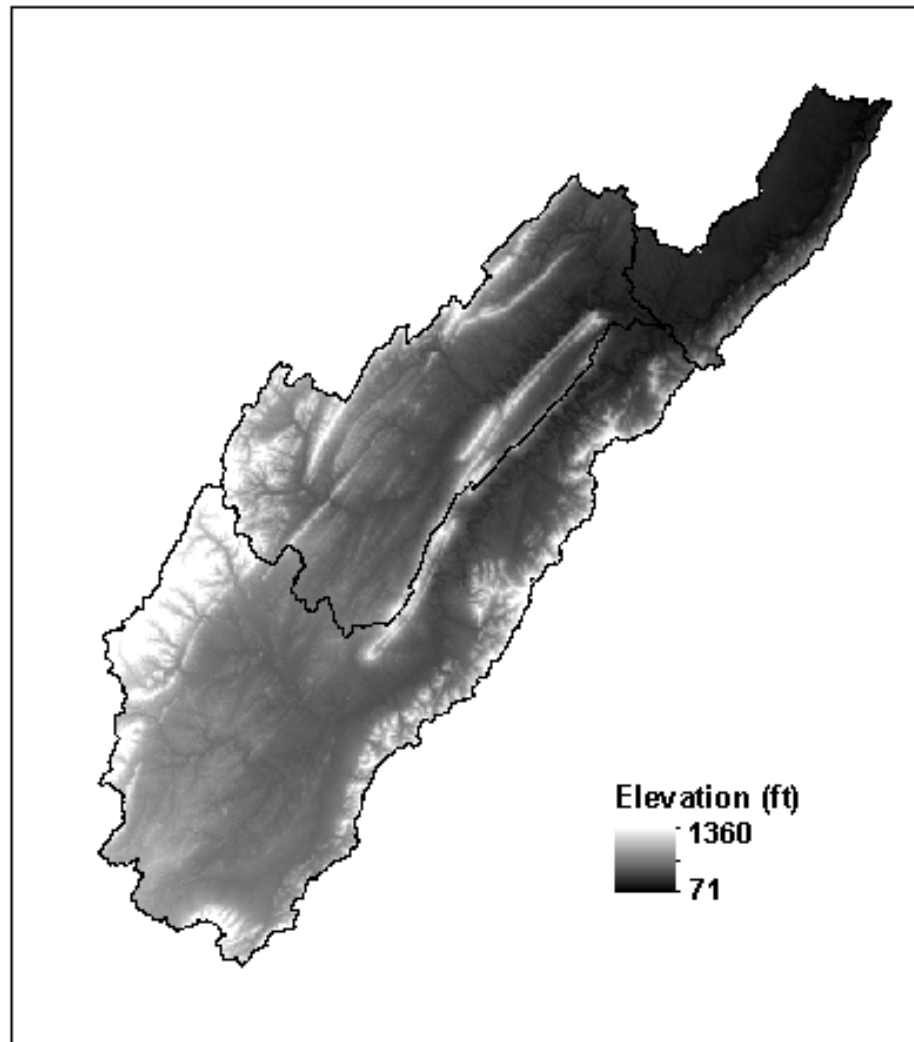
Figure 3-2: Digital Elevation Model for the Shenandoah Watershed

3. The hydro DEM was used to determine the flow direction within each cell using the Flow Direction tool. This tool determines the steepest descent within each cell within the hydro DEM and creates a new raster which assigns a flow direction ID for each cell; 1 =

east, 2 = southeast, 4 = south, 8 = southwest, 16 = west, 32 = northwest 64 = north and

128 = northeast. A value 255 is assigned to cells where a distinct flow direction cannot

be determine and is often indicates that a sink exists within the DEM. A review of the

flow direction grid (Figure 3-3) revealed that none of the cells were assigned a value of

255.
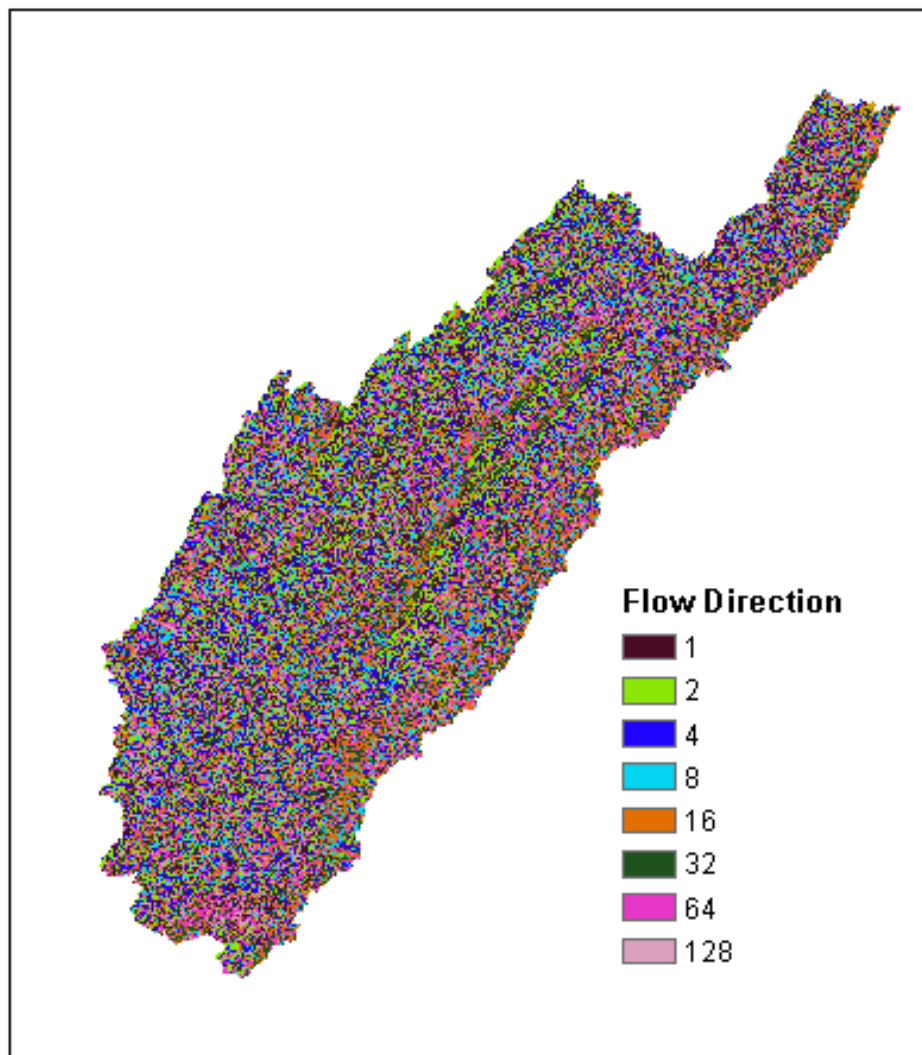
Figure 3-3: Flow Direction Grid for the Shenandoah Watershed

4. A flow accumulation grid was created using the Flow Accumulation tool and flow

    direction grid. The number associated with a cell in the flow accumulation grid

represents the total number of cells draining to that specific cell. Upstream drainage areas can be determined by multiplying the flow accumulation number at any given cell by the cell area (100 m^2).

5. A stream network grid was defined using the flow accumulation grid and a user-specified threshold. The threshold defines the flow accumulation needed before a stream is initiated. The default for this threshold is 1% of the largest drainage area with the hydro DEM. The larger the threshold the fewer the subbasins. The 1% default for threshold was used in the Stream Definition tool to create the stream network grid.

6. A segmented version of the stream network grid was created using the Stream Segmentation tool. This segmented stream network grid creates the initial reaches for the HEC-HMS hydrologic model.

7. A subbasin (catchment) grid was created from the flow accumulation grid and segmented stream network grid using the Catchment Grid Delineation tool. This creates an initial gridded form of the subbasins for the HEC-HMS hydrologic model. Fifty-seven subbasins were created within the Shenandoah River basin.

8. Subbasins in gridded form are not usable in HEC-HMS; therefore, the subbasin grid was converted to a polygon shapefile through the Catchment Polygon Processing tool. During this step the area of each subbasin was stored within the shapefile's attribute table. The catchment shapefile must be created within a geodatabase to comply with ArcGIS structuring and avoid errors.
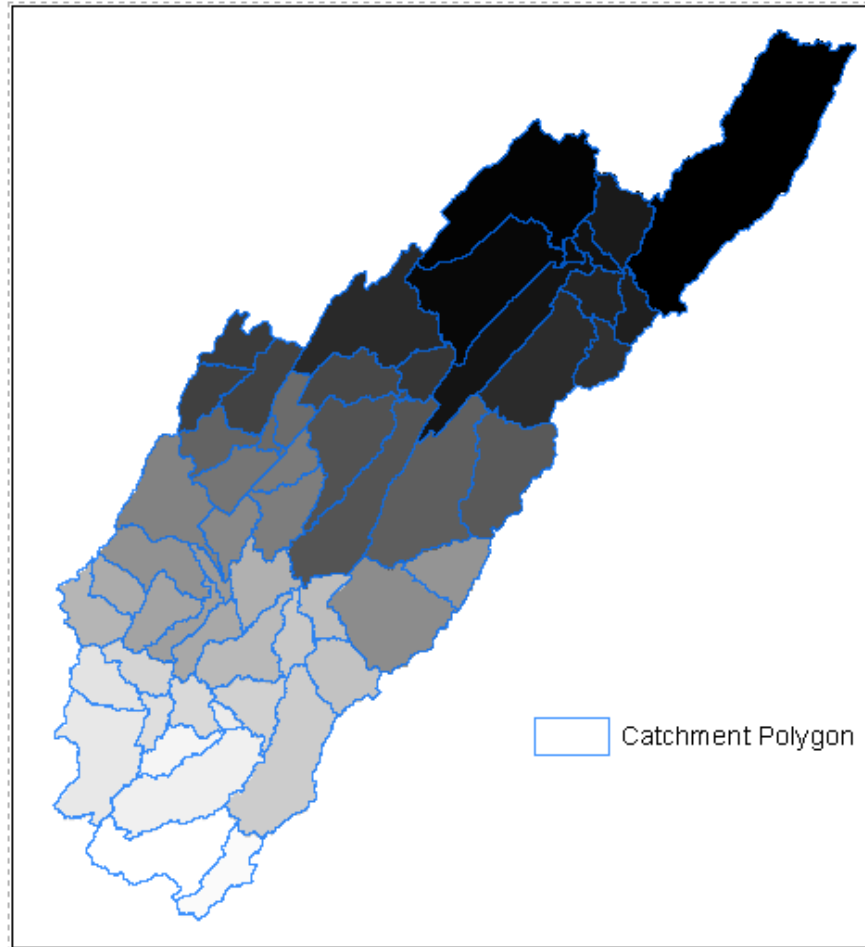
Figure 3-4: Catchment Polygons for the Shenandoah Watershed as Determined in HEC-GeoHMS

9. Stream segments in gridded from are not usable in HEC-HMS; therefore, the stream segmentation grid was converted to a polyline shapefile through the Drainage Line Processing tool. The drainage line shapefile must be created within a geodatabase to comply with ArcGIS structuring and avoid errors.

10. The last step before creating a HEC-HMS project within ArcGIS was to combine the upstream subbasins at every stream confluence using the Watershed Aggregation tool. This does not have any hydrologic significance but improves the computational performance of HEC-GeoHMS during the HEC-HMS project setup. The watershed

aggregation shapefile must be created within a geodatabase to comply with ArcGIS
structuring and avoid errors.

3.1.3 HEC-HMS Project Setup

Once the terrain processing of the raw DEM was finalized, a separate workspace within
ArcGIS was created for the HEC-HMS project, which was accomplished through the HEC-HMS
project setup menu. The Start New Project tool creates the new workspace based on the stream
definition created during the terrain processing and a user-specified outlet location. For this
study, the outlet was specified at the downstream end of the Shenandoah River Basin. Next, the
Generate Project tool was used to transfer the raw DEM and rasters/shapefiles derived during the
terrain processing to the new workspace. In addition, a project point (outlet location), river
polyline (reaches), and subbasin polygon (subbasin) shapefiles were created. The river and
subbasin shapefiles were set up to contain the stream/subbasin characteristics and hydrologic
parameters required by the HEC-HMS hydrologic analysis.

3.1.4 Basin Processing

Once the HEC-HMS project has been set up in ArcGIS, the Basin Processing menu is
available to make modifications, merges and subdivides, to the subbasin delineations. Based on a
visual inspection of the watershed and subbasins created, it was determined that merging of
subbasins was not required. However, since the initial subbasin divides did not account for
USGS gage locations, the subbasins were further divided using the Import Batch Points and
Delineate Batch Points tools. A point shapefile of the USGS stream gage locations was imported
using the Import Batch Points tool. The batch points representing the USGS stream gage
locations were used in the Delineate Batch Points tool to determine the locations for subbasin
divides. This created 76 subbasins within the Shenandoah River basin for use in the final HEC-
HMS hydrologic model. The area for all subbasins was recalculated and stored in the subbasin
attribute table. The final subbasin delineation is shown in Figure 3-5.
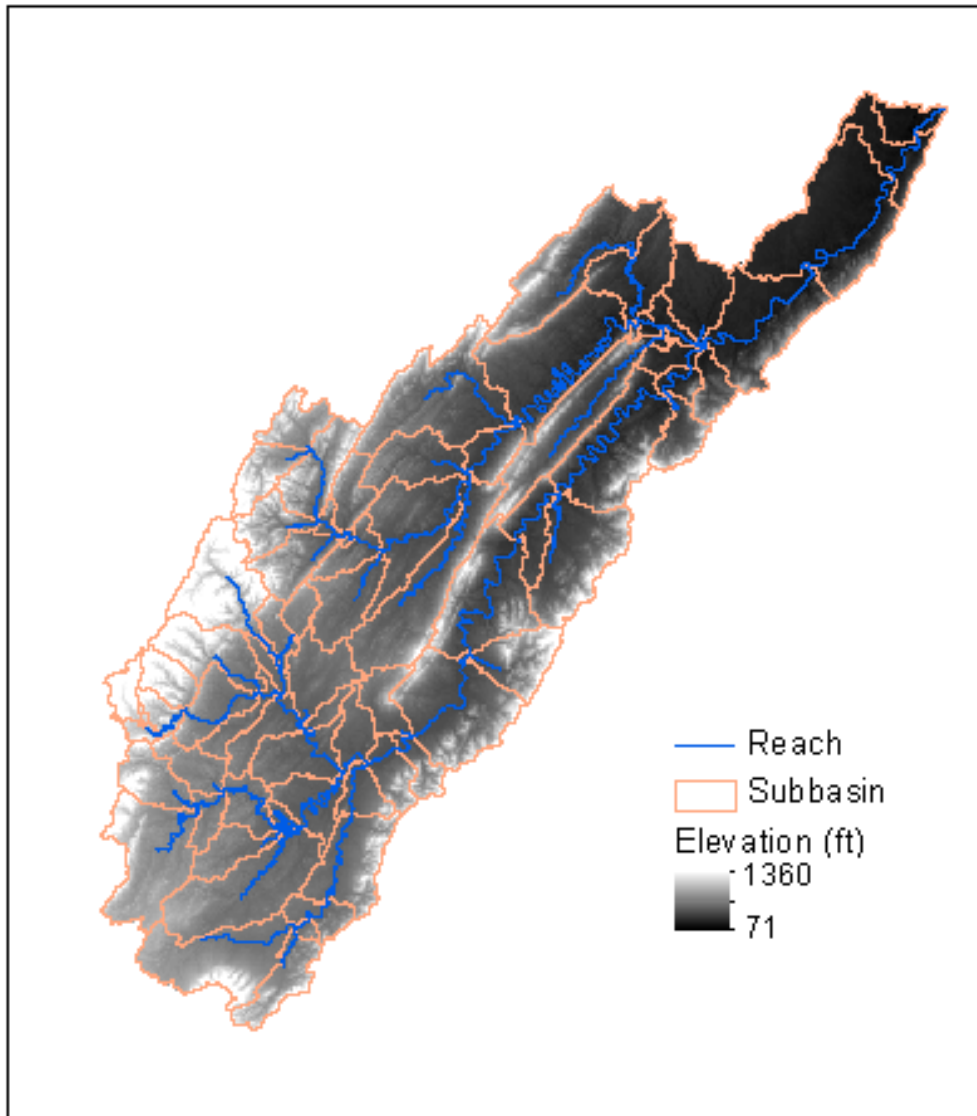
Figure 3-5: River and Subbasin Delineations for the Shenandoah Watershed after Adding USGS
Gages as Subbasin Outlets

3.1.5 Stream and Watershed Characteristics

Physical characteristics of the stream (reaches) and watersheds (subbasins) were completed

through the Characteristic menu. The characteristics, as appropriate, are stored in the attribute

table of either the river or subbasin polygons finalized during the basin processing. All of the

shapefiles created using the Characteristics menu must be created within a geodatabase to comply

with ArcGIS structuring and avoid errors. The following shapefiles were created using the Characteristics menu:

1. The length of each reach was determined by the River Length tool. The units are taken to be the units of the DEM, which is meters for this study.

2. The slope of each reach was determined by the River Slope tool. This tool uses the raw DEM and river shapefile by using the upstream and downstream elevation and length of each reach.

3. The average basin slope was determined using the Basin Slope tool. Before this can be completed however, a watershed slope grid was created using the raw DEM with the ArcHydro, Slope tool. The Slope tool finds the slope at each cell, while the Basin Slope tool finds the average slope across a subbasin. The basin slope was used to determine the CN lag time parameter if used in the hydrologic model.

4. The longest flow path was determined using the Longest Flow Path tool. Due to the size of the Shenandoah River basin, the Longest Flow Path tool failed to create the longest flow paths due to lack of available memory needed for processing. Therefore, the longest flow paths were created using the Interactive Longest Flow Path tool. Using the interactive tool, the approximate upstream location of the longest flow path was selected and ArcGIS determined the longest flow path based on the approximation. The units are taken to be the units of the DEM which is meters for this study.
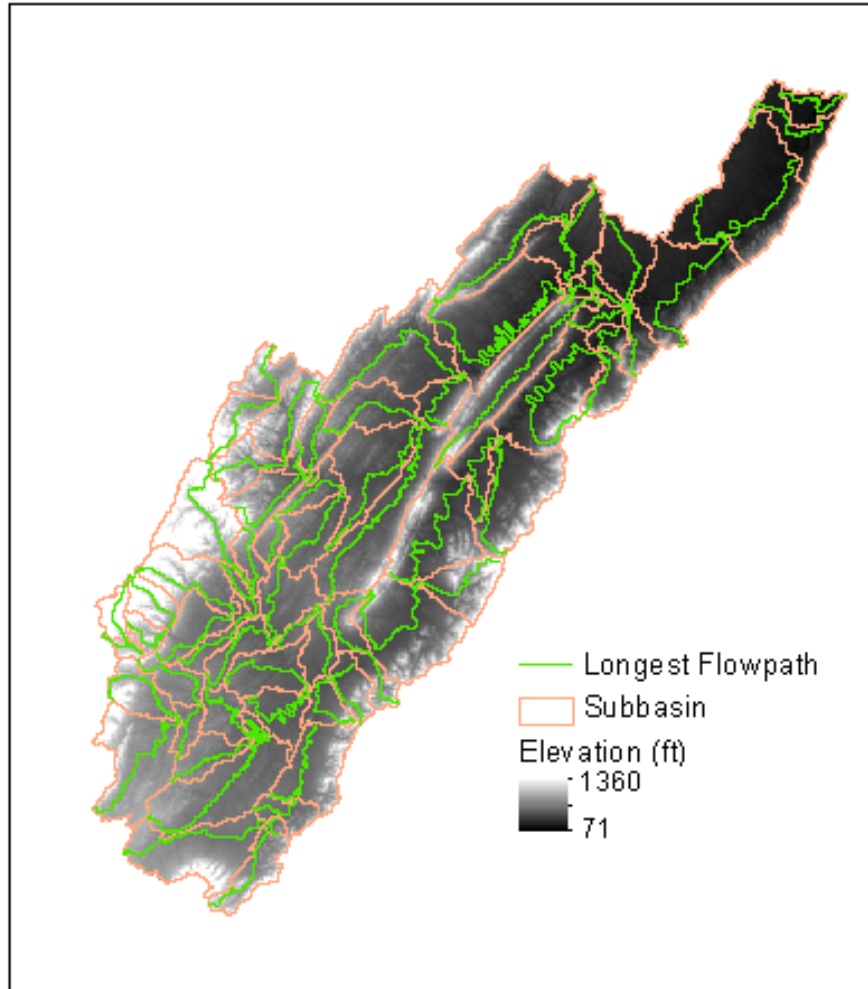
Figure 3-6: Longest Flow Paths for the Shenandoah Watershed

3.1.6 Hydrologic Parameter Estimation

After the physical characteristics of the reaches and subbasins had been derived, HEC-GeoHMS was used to derive several of the hydrologic parameters using the tools under the Parameter menu. However, prior to parameter estimation, the HEC-HMS processes were defined using the Select HMS Processes tool. The subbasin and reach processes as discussed in Chapter 2 are SCS CN and SMA loss methods, Clark's UH and ModClark transform method, linear reservoir baseflow method and Muskingum-Cunge routing method. These options were selected using the HEC-HMS user interface (Figure 3-7). Also, each reach and subbasin within the HEC-HMS model requires a unique name. The River and Basin Auto Name tool was used to

automatically generate reach and subbasin names from upstream to downstream and stores the information in their respective attribute tables.
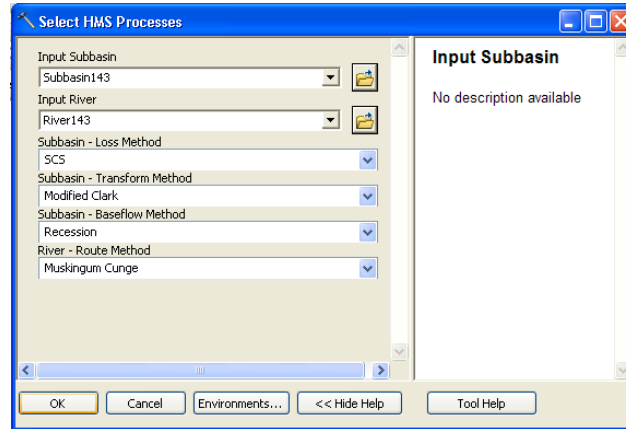
Figure 3-7: HEC-HMS Process Selections

Some hydrologic parameters can be estimated from elevation data, land cover and soil properties within ArcGIS using the HEC-GeoHMS tools. Three parameters that were estimated using HEC-GeoHMS capabilities are CN, percent impervious area, and T_c for each subbasin and channel geometry for reaches. They were estimated using the following methods:

First, the land cover raster dataset obtained from the MRLC and SSURGO raster dataset obtained from the USGS were used to compute the CN for the SCS CN loss method. The MLRC land cover data is classified into 15 land cover categories. These 15 land cover categories were reclassified into four land cover categories (Table 3-1) using the Reclass, Reclassify tool within the Spatial Analyst toolbox. The reclassified land cover grid was converted to a polygon shapefile using the From Raster, Raster to Polygon tool within the Conversion toolbox.

Table 3-1: Reclassification of Land Cover from MRLC

Original Classification		Revised Classification	
Number	Description	Number	Description
11	Open Water		
90	Woody Wetlands	1	Water
95	Emergent herbaceous wetlands		
21	Developed, open space		
22	Developed, low intensity	2	Medium Developed
23	Developed, medium intensity		
24	Developed, high intensity		
41	Deciduous forest		
42	Evergreen forest	3	Forested
43	Mixed forest		
31	Barren land (rock/sand/clay)		
52	Shrub/scrub		
71	Grassland/herbaceous	4	Agriculture
81	Pasture/hay		
82	Cultivated crops		

The SSURGO soil data is in tabular and spatial GIS shapefile format for each county. The county shapefiles contain the polygons of the soil type, but not the soil type itself. For determining the soil type, the tabular data and county polygon shapefiles were used. The tabular data was joined to the county shapefile by using the Join and Relates, Join command in ArcGIS. Both the shapefile and spatial data contain a MUKEY field which the join was based on. Once the tabular data was joined to the shapefile, the component.hydrp field in the spatial data was set equal to the soil type, A, B, C and/or D. Several features had "null" values for soil types. These features were reviewed and assigned a soil type based on other soil parameters given. Once the component.hydrp field was copied from the spatial data to the county shapefile, the join in ArcGIS was removed. Fields for percentage of A, B, C, and D soils were added to the shapefile and were calculated based on the component.hydrp field. This process was completed for all

counties. The soil type shapefiles were then merged into a single shapefile covering the
Shenandoah watershed using the Merge tool under the Geoprocessing menu bar.

The land cover and soil type shapefile of the Shenandoah watershed were merged into a
single shapefile using the Merge tool under the Geoprocessing menu bar. As a result of the
merge, features in the attribute table did not contain data. These were a result of a soil type
shapefile that extended beyond the limits of the land cover shapefile. Therefore, the features that
did not contain data were deleted.

A CN lookup table was created using the Create Table, Table tool within the Data
Management toolbox in order to compute the CN based on land cover and soil type. The CN
values shown in Figure 3-8 were obtained from the Urban Hydrology for Small Watershed, TR-
55 Manual (NRCS, 1986). The CN grid was created using the Generate CN Grid tool within the
Utility menu in HEC-GeoHMS. The DEM, merged land use and soil type polygon and CN
lookup table were specified as inputs and the resulting CN grid is a raster with a grid cell size of
10 x 10 meters (Figure 3-9).

The CN for each subbasin was calculated from the CN grid created by using the Subbasin
Parameters from Raster tool. This tool calculates the CN for each subbasin based on the gridded
information and stores the value in the subbasin attribute table.

OBJECTID *	LUValue	Description	A	B	C	D
1	1	Water	100	100	100	100
2	2	Medium Residential	57	72	81	86
3	3	Forest	30	58	71	78
4	4	Agricultural	67	77	83	87

Figure 3-8: Curve Number Table Lookup
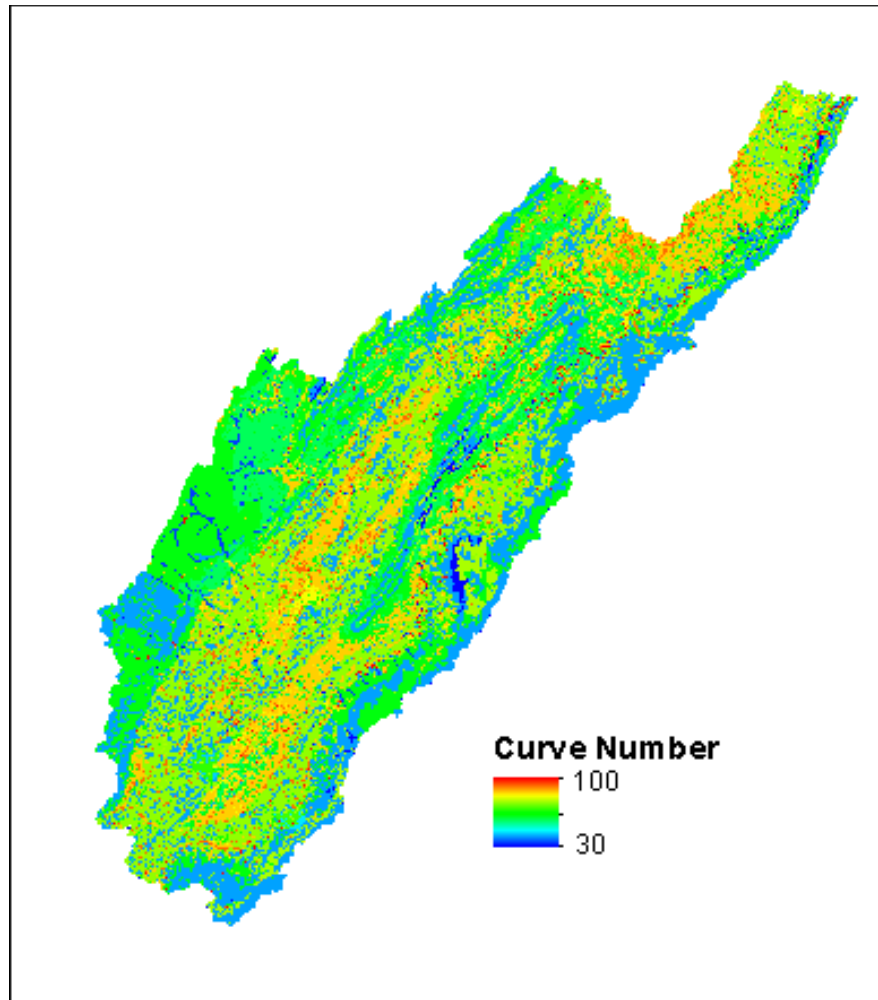
Figure 3-9: Curve Number Grid for the Shenandoah Watershed

Second, the percent impervious surface dataset obtained from the MRLC was used to calculate the percent impervious area for each subbasin. During the data collection and assembly stage, the percent impervious surface dataset was clipped to the Shenandoah River basin (Figure 3-10) so no further processing was necessary to be used for parameter estimation. The percent impervious area for each subbasin was calculated using the Subbasin from Raster tool. This tool calculates the percent impervious area for each subbasin based on the gridded information and stores the value in the subbasin attribute table.
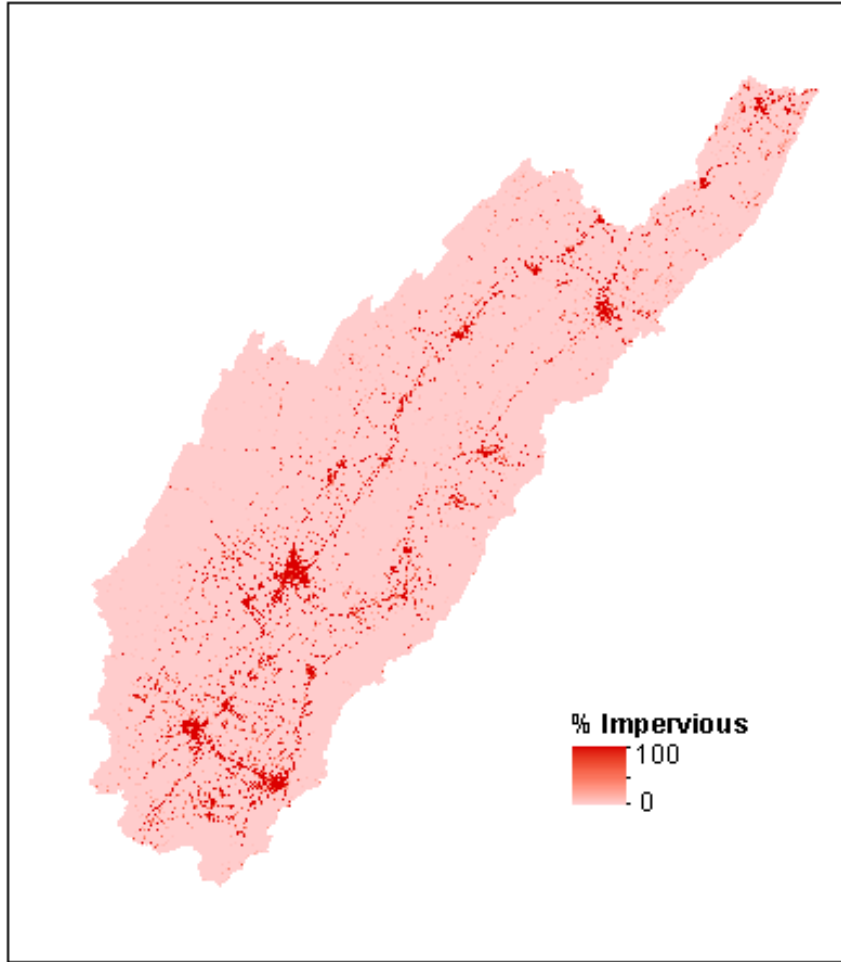
Figure 3-10: Percent Impervious Area Grid for the Shenandoah Watershed

Third, T_c was estimated using the NRCS TR-55 method. Prior to T_c computations, the 2-year, 24-hour rainfall (in.) must be defined. The 2-year, 24-hour rainfall (in.) values were obtained from NOAA Atlas 14 (http://hdsc.nws.noaa.gov). The latitude and longitude corresponding to the centroid of each subbasin was used to obtain the 2-year, 24-hour rainfall for each subbasin. These values were added to the subbasin attribute table. The TR55 Flow Path Segments tool should be used to compute the locational divides of the three NRCS flow regimes – sheet flow, shallow concentrated flow and channel flow. However, due to an unresolved system runtime error, the locational divides for the three flow regimes were completed outside the available GIS tools. A point shapefile was created and the locational divides between sheet,

shallow concentrated flow, and channel was defined as follows: sheet flow ends approximately 100 feet from the watershed divide and was identified as AA within each subbasin to be usable in future HEC-GeoHMS processes, shallow concentrated flow ends at the location where the longest flow path intersects with the main channel and was identified as BB within each subbasin. The TR-55 Flow Path Parameters tool was then used to calculate the flow length and slope of each flow regime. The flow path parameters were then exported to an excel file using the Export TR-55 Data tool.

Figure 3-11: TR55 Time of Concentration Computation Spreadsheet

Within the TR55 T_c computation spreadsheet (Figure 3-11) the bankfull cross-sectional flow area (ft^2), wetted perimeter (ft) and Manning's n values are user defined. The wetted perimeter was assumed to equal the bankfull top width as the variation between the two was assumed to be

small. These two parameters were estimated using drainage area and channel characteristic

relationships that are defined as (McCandless, 2003):

$$Cross-Sectional\ Area = 13.17 * Drainage\ Area^{0.75} \qquad \text{3-1}$$

$$Width = 13.87 * Drainage\ Area^{0.44} \qquad \text{3-2}$$

where drainage area (mi^2) is the cumulative drainage area for a give subbasin (McCandless,

2003). Manning's n values for the main channel and overbanks were estimated using FEMA's

Flood Insurance (FIS) reports of the counties located with the watershed. Channel Manning's n

values ranged from 0.05 to 0.08, while overbank Manning's n values ranged from 0.06 to 0.12.

Once all user specified parameters are defined, the TR55 computation spreadsheet calculates the

T_c which were imported into ArcGIS and stored within the subbasin attribute table.

Fourth, channel properties for the Muskingum-Cunge routing method were defined using the

Muskingum-Cunge and Kinematic Wave Parameters tool. Channel properties required for the

Muskingum-Cunge are dependent on the channel shape assumed. The Shenandoah River would

ideally be represented by an eight-point channel to capture the fluctuations and overbank areas of

natural streams. However, using a 10-meter DEM obtained from the USGS the fluctuations in

the stream would not adequately be captured. Due to this, all channels were assumed to be

trapezoidal in shape; overbank areas not considered. The fields completed in the Muskingum-

Cunge and Kinematic Wave Parameters were the Manning's n estimation, channel shape, bottom

width, reach length, channel slope, and side slope. The values for the reach length and channel

slope were previously computed and already stored within the reach attribute table. Channel

Manning's n values were estimated using FEMA's FIS reports of counties located with the

Shenandoah watershed and ranged from 0.05 to 0.08. Bottom widths were assumed to be

equivalent to the widths calculated using the McCandless (2003) equation described in the

previous section. Side slopes were assumed to be 0.5 ft/ft.

Fifth, a grid cell file, which is a grid-based representation of the watershed, was created for the HEC-HMS hydrologic model using gridded precipitation. The grid cell file was created through the Grid Cell Processing tool. The SHG grid cell method with a grid cell size of 2 x 2 km is suggested for use with radar rainfall data and was used for this study. The SHG grid uses the projection given in Figure 3-12.

```
Projected Coordinate System:
USA_Contiguous_Albers_Equal_Area_Conic_USGS_version
Projection: Albers
False_Easting:        0.00000000
False_Northing:       0.00000000
Central_Meridian: -96.00000000
Standard_Parallel_1:        29.50000000
Standard_Parallel_2:        45.50000000
Latitude_Of_Origin:         23.00000000
Linear Unit:          Meter

Geographic Coordinate System:    GCS_North_American_1983
Datum:        D_North_American_1983
Prime Meridian:    Greenwich
Angular Unit:        Degree
```

Figure 3-12: Geographic and Projected Coordinate System of Standard Hydrologic Grid Cell

Two grid cell polygons were created during this process, one projected to the SHG coordinate system and the other projected to the data's coordinate system, NAD1983 UTM Zone 18N. The resultant grid cell polygons contain the spatial location of each cell, cell area and travel length. The travel length is the average distance from the grid cell to the subbasin outlet and was used in the ModClark transform method. Only gridded parameters, i.e., precipitation, used in the HEC-HMS analysis need to be in the same projection as the grid cell file. All other parameters that did not require a specific projection were projected to the local projection. Figure 3-13 shows the SHG grid for the study region.
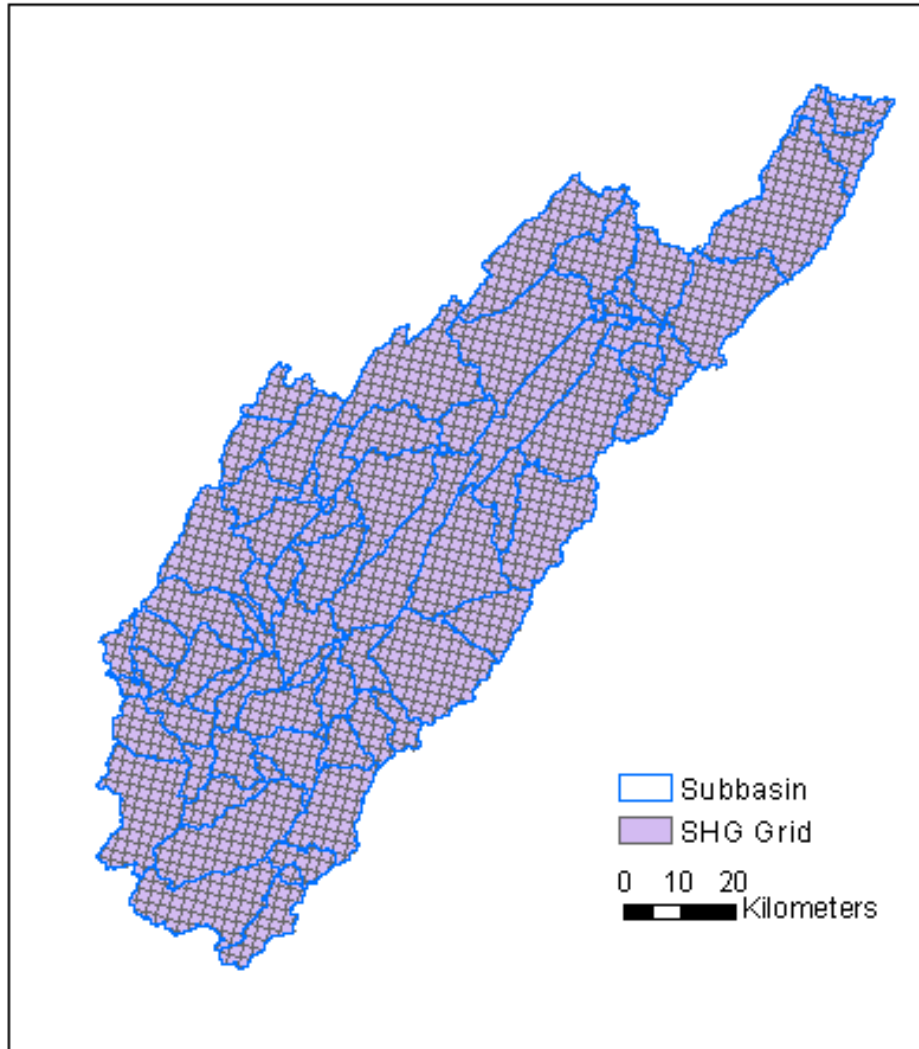
Figure 3-13: Grid Cell Polygon for the Shenandoah Watershed

3.1.7 HEC-HMS Model Setup

HEC-GeoHMS has the ability to set up the model files needed for HEC-HMS. The first step was to convert the units of the ArcGIS data into HEC-HMS units. This was completed through Map to HMS Units within the HMS menu. English units were selected for this study. Next the datasets created in HEC-GeoHMS were checked for consistency to ensure that there were no errors found in the hydrologic structure of the watershed. The data were checked through HEC Check Data within the HMS menu. Errors were not found. Next the HMS Basin Schematic was used with the HMS menu. This procedure builds the hydrologic network that contains the HEC-

HMS model nodes and reaches. Latitude and longitude coordinates are determined for data, such as gridded precipitation and inverse distance precipitation, through the Add Coordinates tool within the HMS menu. The final step before creating the setup files required for HEC-HMS was to use the Prepare Data for Model Export under the HMS menu. This tool gathers the details stored in the subbasin and reach attribute tables and prepares them for export into the HEC-HMS model file.

The HEC-HMS files which HEC-GeoHMS creates are the basin model file, grid cell file and meteorologic file. The basin model file contains all pertinent information related to the subbasins and reaches. This file was created through Basin Model File under the HMS menu. This tool creates an ASCII text file formatted for export into HEC-HMS. The grid cell file is required for gridded precipitation. This file contains the latitude and longitude, travel length and area of each SHG grid cell and the subbasin in which they are located. The grid cell file was created through Grid Cell File under the HMS menu. The meteorologic file was created through Met Model File under the HMS menu. This file is only required when gage precipitation data is utilized in the HEC-HMS hydrologic model. During this step the method by which subbasin precipitation is to be determined must be selected. This study uses the Inverse Distance method to determine precipitation values within the modeled subbasins. Rain gages which have unique Hydro IDs must be specified during this step.

Once these files have been made they can be exported into a HEC-HMS hydrologic model with no further reference to GIS software. When initially exporting the basin model file into HEC-HMS, an unknown error occurred. After troubleshooting the basin model file, it was determined that the ASCII text file cannot use scientific notation. Once all values in scientific notation were reformatted the basin model file was able to be exported into HEC-HMS.

3.2 Other Parameter Estimations

A number of model parameters could not be derived directly using HEC-GeoHMS. Several were estimated using methods from the literature and several were estimated through subjective optimization.

3.2.1 Storage Parameters

A canopy storage of 0.05 inches is recommended for subbasins whose ground is generally vegetated (McEnroe, 2010). Bennett (1998) suggested that maximum surface storage is a function of the subbasin slope and defined as shown in Table 3-2. With slopes in the Shenandoah watershed ranging from 5% to 40%, surface storage values used in the HEC-HMS model range from 0.04 to 0.50 inches. Surface storage capacity was expressed as two-piece linear function of slope, allowing a value to be found for each subbasin (Figure 3-14). The canopy and surface storages were assumed to be empty at the beginning of the simulation; therefore, the initial percent filled was set to 0 for both.

Table 3-2: Surface Storage Capacity as a Function of Subbasin Slope

Description	Slope (%)	Surface Storage (in)
Paved impervious areas	N/A	0.13 - 0.25
Steep, smooth slopes	> 30	0.04
Moderate to gentle slopes	5 - 30	0.50 - 0.25
Flat, furrowed land	0 - 5	2

Source: Bennett, 1998
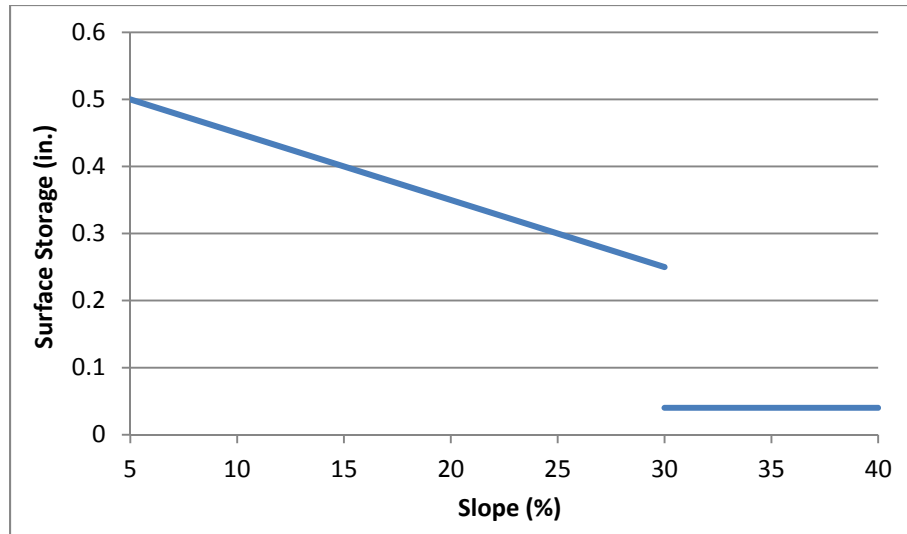
Figure 3-14: Graphical Representation of Table 3-2 for Storage Surface Capacity (in.) as a Function of Slope (%) within the Shenandoah Watershed

3.2.2 Soil Moisture Accounting Parameters

The maximum infiltration (in./hr) for the SMA loss method was approximated to be equal to the saturated hydraulic conductivity (ksat). Ksat values were obtained from the USDA Web Soil Survey (WSS) (http://websoilsurvey.sc.egov.usda.gov/App/WebSoilSurvey.aspx). WSS provides Ksat values for every soil type within an area of interest. The Ksat values for each subbasin were determined by taking an area weighted average of all soil types within subbasins.

The soil storage, S_S, (in.) and tension storage, S_T, (in.) were determined from the water content at saturation, θ_s, 1/3 bar (field capacity), $\theta_{1/3}$, and 15 bar (wilting point), θ_{15}, and soil depth, d (in.), using the following relationships (McEnroe, 2010):

$$S_S \ (in./in.) = (\theta_S - \theta_{15})d \qquad\qquad 3\text{-}3$$

$$S_T \ (in./in.) = \left(\theta_{1/3} - \theta_{15}\right)d \qquad\qquad 3\text{-}4$$

Water content at 1/3 and 15 bar are available from WSS as volumetric percentages for every soil type within an area of interest. The volumetric percentages were divided by 100, and then an area weighted average was determined for each subbasin. Water content at saturation is not directly available from WSS; however, bulk density is available. Water content at saturation is

equal to one minus the bulk density of the soil divided by the particle density (or specific gravity of soil), 2.65. Bulk densities (g/cm^3) are given for every soil type within an area of interest. An area weighted average was determined for subbasins. divided by 2.65, and subtracted from one to obtain water content at saturation. The soil depth was determined using the SSURGO horizon ASCII file in the tabular data. The soil depth was initially approximated to be equal to the depth of horizon 1 (top layer). Through subjective optimization by analyzing the water budget (precipitation = outflow + evapotranspiration + storage) and the predicted and observed hydrograph at the downstream reach of the Shenandoah watershed, this value was adjusted to 1.25 times the depth of horizon 1. The soil and tension storages were calculated using the equations given above.

Through subjective optimization, the initial soil, groundwater 1, and groundwater 2 storages (%); soil, groundwater 1, and groundwater 2 percolation (in./hr); groundwater 1 and 2 storage (in.); and groundwater 1 and 2 coefficients (hr) were determined. During the optimization runs, the values of these inputs were varied. The final values were chosen such that the predicted outflow and baseflow were a close match to observed outflow and baseflow at the downstream reach of the watershed by visual inspection. The initial soil, groundwater 1, and groundwater 2 storage (%) were set to 10%; soil and groundwater 1 percolation (in./hr) were assumed to be a function of the maximum infiltration rate and set to approximately 0.09% of the ksat value determined using SSURGO data; groundwater 2 percolation (in./hr) was set to 0; groundwater 1 and 2 storage (in.) were set to 0.8 in.; and groundwater 1 and 2 coefficient (hr) were set to 360 hrs.

3.2.3 Clark's UH/ModClark Parameters

Clark's UH/ModClark transform method requires two parameters, T_c and a storage coefficient, R. A report prepared for the Virginia Department of Highways and Transportation (VDOT) (Cruise & Yu, 1982) indicates R is a function of T_c. According to the VDOT report, R

is approximately 1.4 times T_c for subbasins located within the Shenandoah watershed. The

approximation, $R = 1.4 * T_c$, was adopted for this study. T_c was calculated utilizing HEC-

GeoHMS capabilities as described in Section 3.1.6.

3.2.4 Initial Baseflow

Initial baseflow for each subbasin was determined using USGS stream flow gage data.

Station 01636500, Shenandoah River at Millville, WV, is the most downstream gage and was

analyzed to determine the baseflow conditions. HEC-HMS requires the baseflow of each

individual subbasin, not the total baseflow of the contributing drainage area. The total baseflow

for each subbasin was determined by calculating an area weighted value based on the

contributing drainage area of a subbasin, the stream flow observed at USGS Station 01636500 on

October 1, 1995, and the contributing drainage area draining to USGS Station 01636500. The

individual baseflow for subbasins were then determined by subtracting the baseflow calculated

for the upstream subbasin from the baseflow calculated for that particular subbasin.

Groundwater 1 and 2 coefficients and reservoir number are also required for linear recession

baseflow in HEC-HMS. Through subjective optimization, the groundwater 1 and 2 coefficients

were set to 60 hrs. As with the SMA loss method parameters, the values of these inputs were

varied during optimization runs. The final values were chosen such that the predicted outflow

and baseflow was a close match to observed outflow and baseflow at the downstream reach of

the watershed by visual inspection.

3.2.5 Potential Evapotranspiration

Potential Evapotranspiration based Thornthwaite's method was obtained from the University

of Virginia's Climatology Office (University of Virginia (UVAb), undated). HEC-HMS

calculates actual evapotranspiration between events as a function of surface and soil storage, with

potential evapotranspiration as a maximum value.

Tables that contain all parameters inputted in the HEC-HMS hydrologic models appear in Appendix A.

3.3 Precipitation Processing

3.3.1 NLDAS

The NLDAS precipitation is available in grib or NetCDF format. Since NetCDF files are easily read into ArcGIS, the hourly NLDAS data was downloaded in NetCDF form using NASA's Mirador Earth Science Data Search Tool (http://mirador.gsfc.nasa.gov/). NetCDF files were downloaded for the 1995-1996 water year (October 1 to September 30) for the entire continental United States. This resulted in 8,748 NetCDF files. ArcGIS, in combination with python scripts, was used to process the NLDAS precipitation into a usable form for HEC-HMS. Gridded precipitation is read into HEC-HMS through HEC's Data Storage System (DSS). Each line in the HEC-DSS represents an ASCII file containing the hourly precipitation data. The following steps were taken to transform the NetCDF files into ASCII files and compiled in HEC-DSS.

1. Convert NetCDF file to raster using the Make NetCDF Raster Layer tool within the Multidimension toolbox in ArcGIS. The precipitation layer within the NetCDF file must be specified as the variable for extraction.

2. Clip the projected raster to the Shenandoah watershed using the Extract, Clip tool within the Analysis toolbox in ArcGIS. The shapefile that contains the watershed extent must be specified.

3. Project the precipitation raster to the same projection as the SHG grid cell file created for HEC-HMS through the Projections and Transformations tool within the Data Management toolbox in ArcGIS. The precipitation data were projected to the same coordinate system as the grid cell polygons, Albers Equal Area Conic.

4. Resample the cell size of the clipped raster to match the cell size of the grid cell created by HEC-GeoHMS. NLDAS grid cells are approximately 14 km x 14 km, while the grid cells in the SHG grid cell file created for HEC-HMS are 2 km x 2 km. The grid cell size of the NLDAS was resized using the Raster Processing, Resample tool within the Data Management toolbox in ArcGIS. The nearest neighbor was chosen as the resampling type to prevent interpolation of values. Figure 3-15 shows an example of this process.
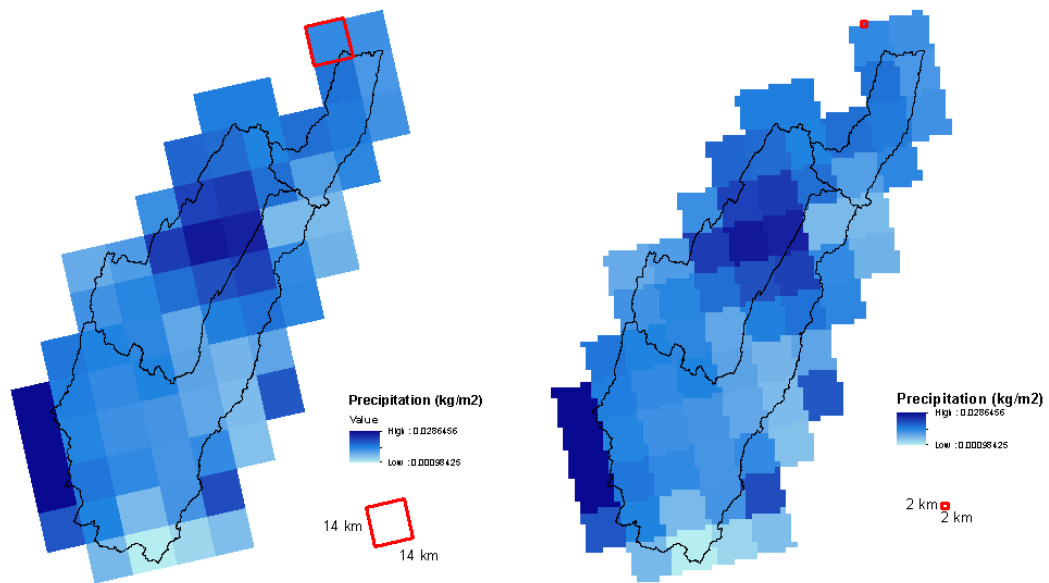
Figure 3-15: Example of original NLDAS precipitation grid (14 x 14 km) and resampled NDLAS precipitation grid (2 x 2 km)

5. Convert the forcing units, kg/m^2, of the NLDAS precipitation data to precipitation depth using the conversion 1 kg/m^2 = 0.0394 in of H_2O. The resampled raster was converted using the Raster Math, Times tool within the 3D analyst toolbox in ArcGIS.

6. Covert the precipitation depth raster to an ASCII file using the From Raster, Raster to ASCII tool within the Conversion toolbox.

Each of the processes described in the steps above were automated using python scripts written using commands to call the ArcGIS tools. The full python scripts are in included Appendix B. The resulting output was 8,748 ASCII files containing the precipitation depth in

inches. HEC-HMS cannot read ASCII files directly; therefore the files must be compiled into a HEC-DSS file. The 8,748 ASCII files were compiled into HEC-DSS using asc2dssGrid.exe command in a python script (Appendix B). A view of the resulting HEC-DSS file is shown in Figure 3-16.
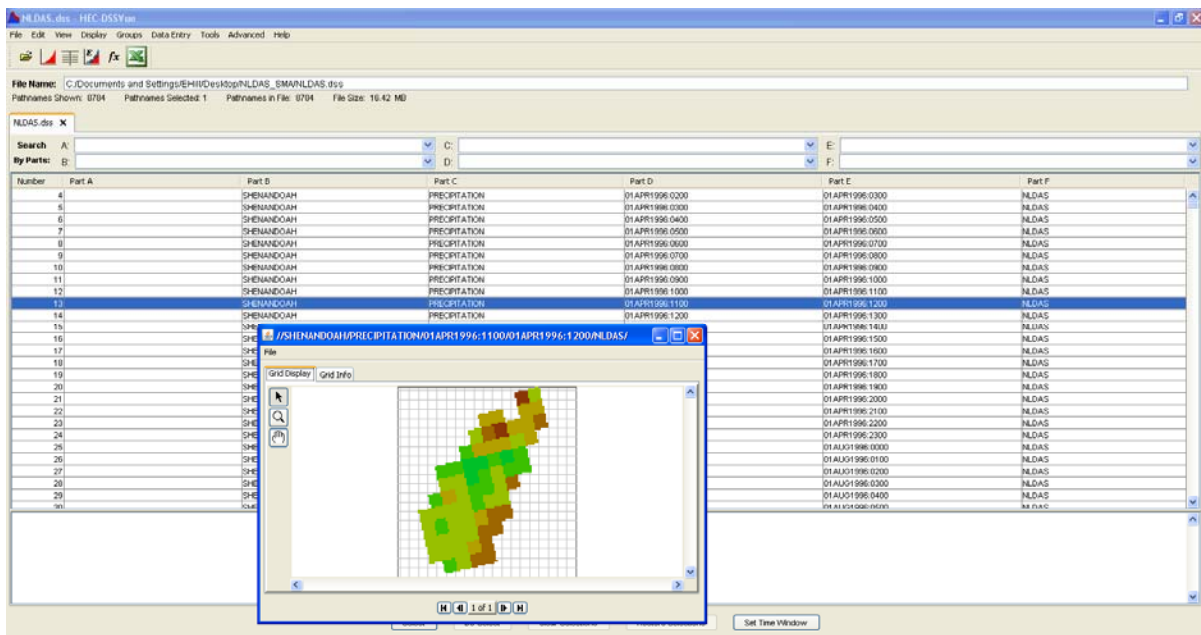
Figure 3-16: Hourly Precipitation Data Viewed in HEC-DSS

NLDAS precipitation data are backwards accumulated (total amount for the hour ending at the specified time) and referenced to Coordinated Universal Time (UTC). HEC-HMS applies precipitation data to the time step beginning at the specified model time. Eastern Standard Time (EST) is -4 hours from UTC. Therefore, a 5-hour time shift was applied to the HEC-HMS model. Note a time shift of -4 hours was tested to ensure the correct sign was applied. This resulted in the peak discharge being shifted 4 hours forward in time, not backwards.

3.3.2 Inverse Distance

Hourly rainfall gage data from the National Weather Service's CoOperative Observer Network (CoOp) were downloaded using NOAA's National Climatic Data Center (NCDC) online map interface (http://gis.ncdc.noaa.gov/map/viewer/#app=cdo). All gages with

precipitation data from October 1, 1995, to September 30, 1996, and within 30 miles of the

Shenandoah watershed were selected for download. Precipitation data from gages 442159,

442208, 445690, 445880, 446712, 448046, 448062, 448396, 461393, 466163 and 467730 were

downloaded and entered in HEC-HMS. Three gages, 442208, 448046 and 448062, are located

within the Shenandoah watershed (Figure 3-16). Missing gage data were left blank since the

inverse distance method has the ability to examine a nearby gage and determine if rainfall

occurred during that time step. A search distance of 35 miles for nearby gages was used to

ensure that all subbasins would have at least one gage from which to obtain precipitation data.
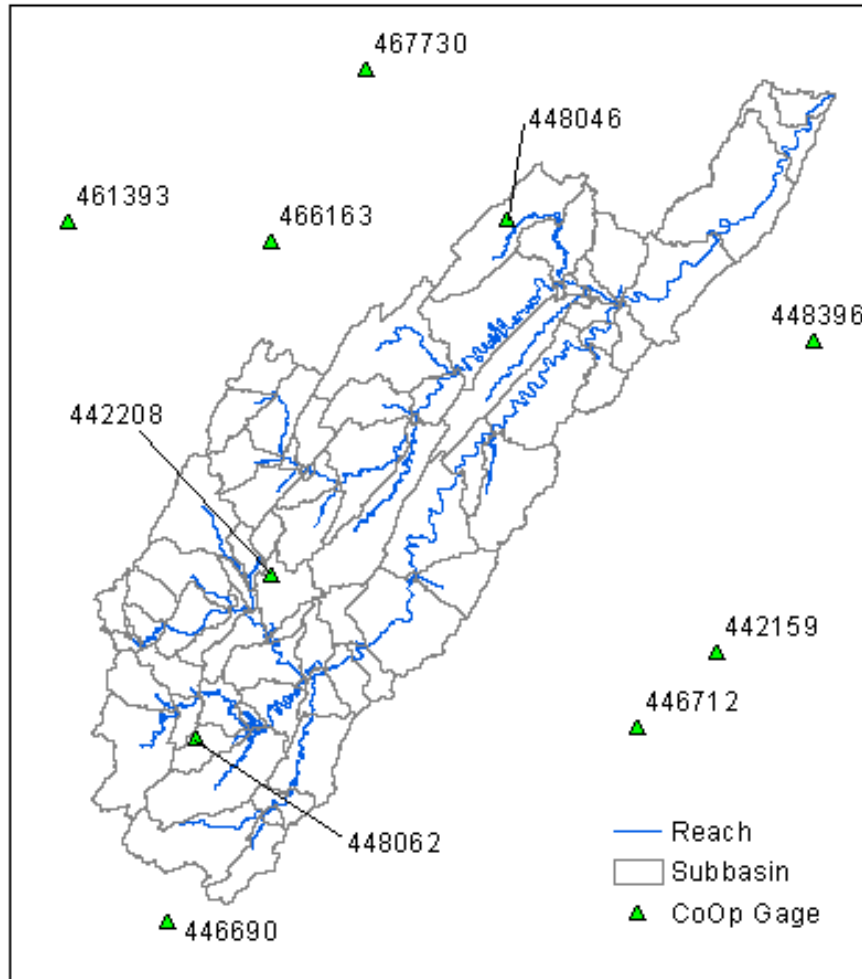
Figure 3-16: Precipitation Gages used in the HEC-HMS analysis

3.4 General Method for Model Analysis

The precipitation data, NLDAS and CoOp, and their resultant hydrologic responses modeled with HEC-HMS were analyzed using methods outlined in this section. The results of the modeling are presented in Chapter 4.

3.4.1 Precipitation Data

The NLDAS and interpolated CoOp data were analyzed to quantify differences between them and identify any spatial patterns or association with properties such as drainage area. These analyses were completely through simple difference calculations and plotting the data graphically and geographically.

In statistics, the cumulative distribution function (CDF) describes the probability that a variable, X, is less than or equal to a number, x (Wolfram, 2013). CDF curves of the hourly precipitation for the 76 subbasins were created in Excel by calculating the probability of precipitation values:

$$Probability\ (P \le x) \le \frac{Number\ of\ Occurences \le x}{Total\ Sample\ Size} \qquad \text{3-5}$$

The CDF curves are examined to determine the differences in the statistical distribution of hourly precipitation within the subbasins. The value probability $P \le 0$ gives the total amount of time that precipitation did not occur in the subbasin.

Differences in the precipitation input will result in differences in model hydrologic response. Model derived cumulative excess precipitation and direct runoff from the subbasins are compared (CoOp vs. NLDAS). Model predicted stream flow is can be compared to observations at the gauging stations in the basin.

3.4.2 Model Goodness-of-Fit Measures

The HEC-HMS hydrologic model used in this study has been subjectively optimized, but has not been calibrated or verified. However, model goodness-of-fit measures can be used to

compare how well the preliminary simulations (non-optimized) agree with observed hydrographs and whether that agreement changes when precipitation input is changed. USGS gage data were available for the 1995 to 1996 water year as daily mean discharge (cfs). The outflow data from the HEC-HMS hydrologic models were computed hourly. Therefore, the outflow from the HEC-HMS models was converted from hourly to daily mean discharge by averaging the outflow from 01:00 to 24:00 each day.

The coefficient of determination, R^2, is calculated to determine how well the model using the NLDAS and CoOp precipitation data compared to the observed hydrographs. R^2 provides as a measure of how well observed outcomes are replicated by the model, i.e., the proportion of the explained variation to total variation:

$$R^2 = (\frac{\sigma_{xy}}{\sigma_x \sigma_y})^2 \qquad\qquad 3\text{-}6$$

This provides information about the goodness of fit of each model by approximating how well the regression line approximates the measured data points. In regression, R^2 is a statistical measure of how well the regression line approximates the real data points. An R^2 of 1.0 indicates that the regression line perfectly fits the data (Ayyub & McCuen, 2011).

The mean error (ME), or mean bias, is used to measure the systematic error of the predicted outflows, x, to the observed outflows, y:

$$ME = \frac{\Sigma(x-y)}{N} \qquad\qquad 3\text{-}7$$

Mean error deprives a statistic result of representativeness by systematically distorting it (Ayyub and McCuen, 2011). It is one way to determine if the predicted values over or under predict the observed. The Root Mean Square Error (RMSE) is a goodness-of-fit statistic that describes the accuracy of a model:

$$RMSE = \sqrt{\frac{\Sigma(x-y)^2}{N-1}} \qquad\qquad 3\text{-}8$$

A RMSE value of 0 indicates that the model perfectly predicts the observed values. The larger

the RMSE, the greater the variation of the predicted values from the observed values (Stanford

University, 2000).

The Nash-Sutcliffe model efficiency coefficient (NSE) is used to assess the predictive power

of hydrological models:

$$NSE = 1 - \frac{\sum(y-x)^2}{\sum(y-\mu_y)^2}$$ 3-9

The NSE ranges from -∞ to 1. A NSE of 0 indicates that model predictions are only as accurate

as the observed mean. A NSE less than 0 occurs when the observed mean is a better predictor

than the predictor. A value of 1 denotes that the model predictions accurately represent the

observed data (Nash & Sutcliffe, 1970). It should be noted that NSE, as a single-value index, can

be sensitive to a number of factors, such as sample size, outliers, magnitude bias, and time off-set

bias (McCuen, Knight & Cutter, 2006).

The relative accuracy, Se/Sy, is used to assess the predictive power of a hydrologic model:

$$\frac{S_e}{S_y} = \frac{\sqrt{\frac{\sum(x-\bar{y})^2}{N-1}}}{\sigma_y}$$ 3-10

When Se/Sy is near 0, the model significantly improves the accuracy of prediction over

predictions made with the mean. When Se/Sy is near 1.0, the model provides little improvement

in prediction accuracy when compared to the mean (McCuen, 2002).

3.4.3 Other Criteria

Summary statistics of how well predicted observations match observed are not the only

criteria for evaluating hydrologic models. Other criteria of model performance that were

analyzed were the peak discharge and annual precipitation residuals. High flows result from a

large storm event or snowmelt. An accurate model would capture both the magnitude and timing

of the peak flow event. Discharge residuals are calculated at the annual predicted discharge (in.)

minus the annual observed discharge (in.). An accurate model would have discharge residuals

near 0.

Chapter 4

Model Results

4.1 Test of SCS Loss Method and Selection of SMA Loss Method

The SCS loss method within HEC-HMS was initially tested to determine if it would accurately represent the hydrology of the Shenandoah watershed. The SCS loss method relies on curve number (CN) to determine excess precipitation and losses within each subbasin. Based on the results at Station 01636500, BatchPoint20, the most downstream USGS gage, the SCS loss method results in a total residual (modeled outflow – observed outflow) of 49.95 inches for the 1995 to 1996 water year, October 1, 1995, to September 30, 1996 (Figure 4-1). A review of the HEC-HMS output for Subbasin 1970, the subbasin directly upstream of Station 01636500, and the hydrograph at BatchPoint20, revealed that the precipitation loss decreases to zero and does not reset through the simulation, causing an over prediction in outflow. Early rain events saturate the model surface; since there is no model mechanism to dry out the surface between events, the antecedent conditions are increasingly saturated for subsequent rain events, infiltration (loss) decreases to where all rainfall become excess (Figure 4-2), and the runoff overestimation grows through the simulation (Figure 4-3). Therefore, the SMA loss method was not used for the continuous modeling.
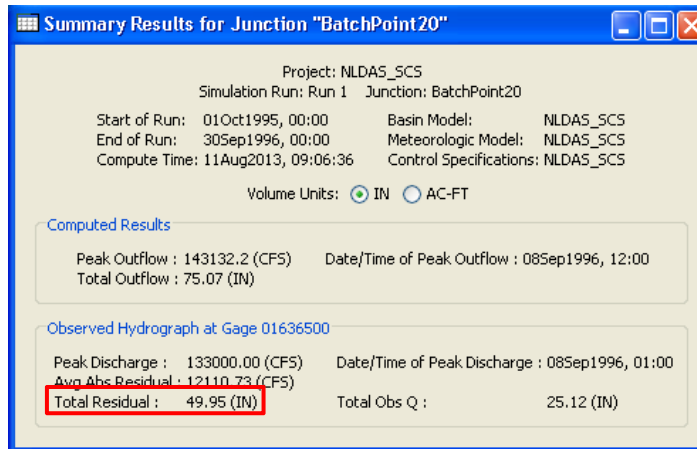
Figure 4-1: Summary of Results at USGS Station 01636500 Using SCS Loss Method
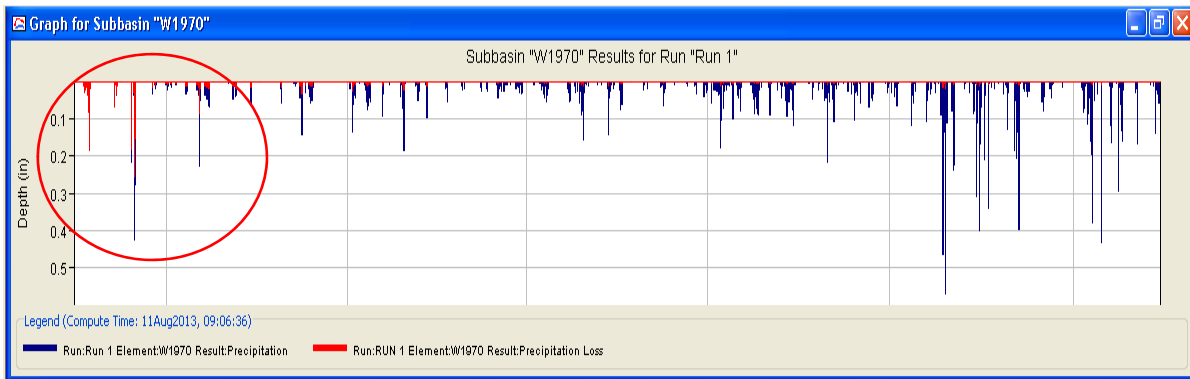
Figure 4-2: HEC-HMS Calculated Precipitation Excess and Precipitation Loss at Subbasin 1970 Using SCS Loss Method
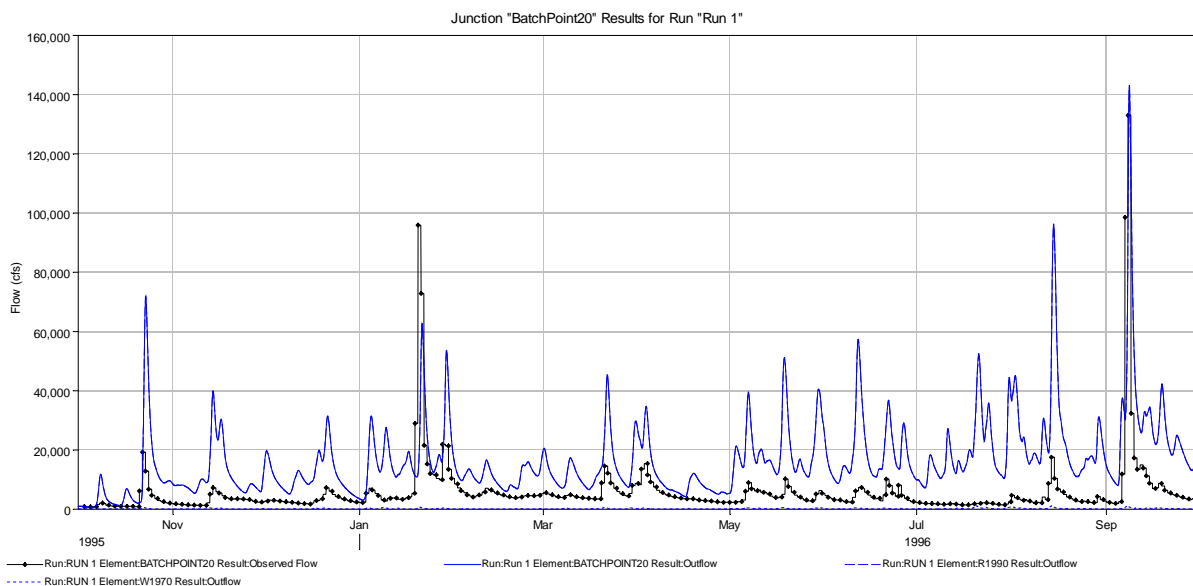
Figure 4-3: HEC-HMS Predicted Outflow (blue) and USGS Observed Outflow (black) at Station 01636500 (most downstream gage) Using SCS Loss Method

Initial investigations of the SMA loss method within HEC-HMS indicated that the total

modeled outflow (in. and cfs) was in close agreement with the observed outflow (in. and cfs) at

USGS Station 01636500 (Figure 4-4 and 4-5). In addition, the SMA loss method allows for

surface dry out between rain events, appropriately setting up antecedent conditions for

subsequent rain events (Figure 4-6). Therefore, the SMA loss method within HEC-HMS was

used for continuous modeling.
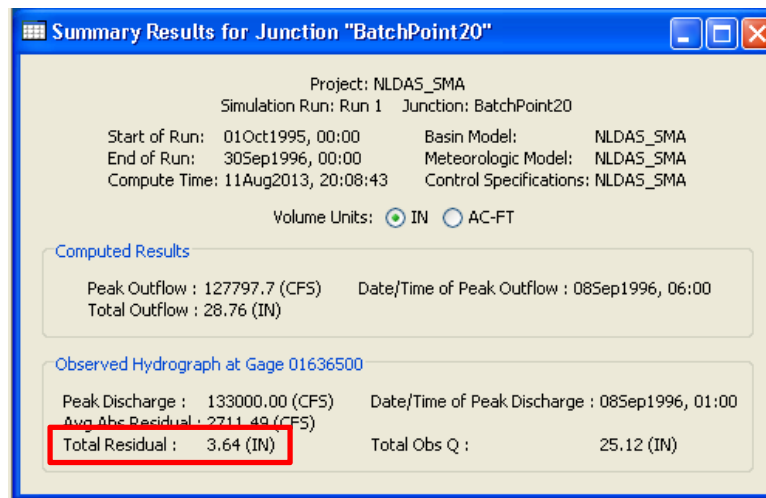
Figure 4-4: Summary of Results at USGS Station 01636500 Using SMA Loss Method
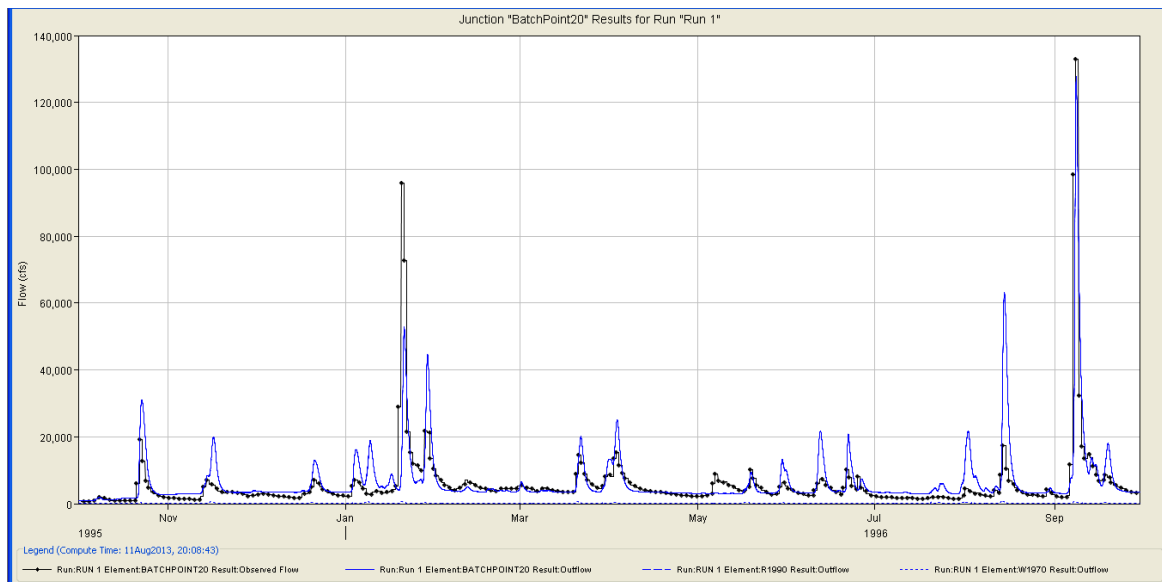
Figure 4-5: HEC-HMS Predicted Outflow (blue) and USGS Observed Outflow (black) at Station 01636500 (most downstream gage) Using SMA Loss Method
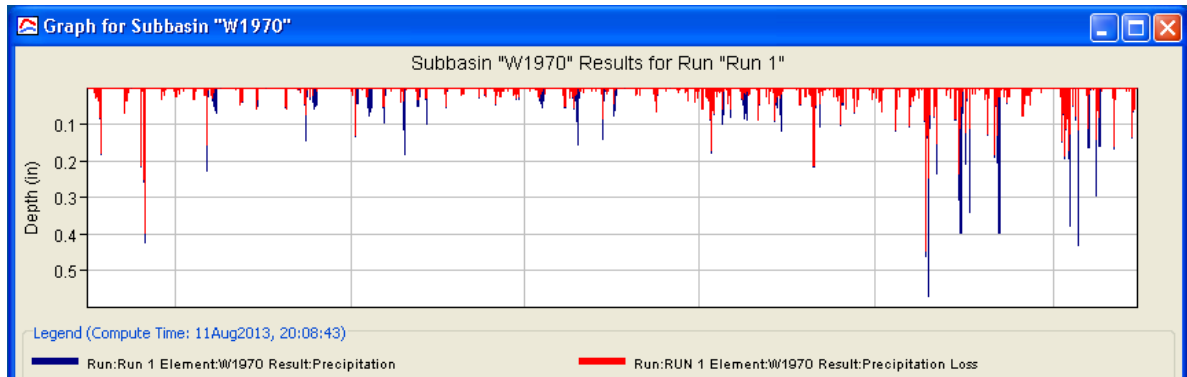
Figure 4-6: HEC-HMS Calculated Precipitation Excess and Precipitation Loss at Subbasin 1970 Using SMA Loss Method

4.2 Data and Model Analysis

4.2.1 Precipitation Data

On a subbasin basis, the NLDAS cumulative precipitation for the 1995 to 1996 water year ranges from 43.5 to 57.6 inches, with a yearly average of 49.1 inches throughout the Shenandoah watershed. Parts of Shenandoah and Frederick County, VA, located in the northwest portion of the watershed experienced 43.5 inches, while parts of Rockingham County, VA, located in the middle of the western portion had 57.6 inches. The CoOp cumulative precipitation for the 1995 to 1996 water year ranges from 27.4 to 69.9 inches, with a yearly average of 52.1 inches throughout the Shenandoah watershed. Parts of Page County, VA, located in the middle of the eastern portion of the watershed received 27.4 inches, while parts of Augusta County, VA, located in the southeast had 69.9 inches. Summary statistics appear in Table 4-1.

Table 4-1: NLDAS and CoOp Cumulative Precipitation Summary for Subbasins (n=76)

Precipitation	Maximum (in.)	Minimum (in.)	Average (in.)	Range (in.)
NLDAS	57.6	43.5	49.1	14.1
CoOp	69.9	27.4	52.1	42.5

The average cumulative precipitation for NLDAS and CoOp is comparable; however, the range of precipitation within the watershed varied greatly between the two. Cumulative

precipitation from both sources is compared by subbasin in Figure 4-7. The majority of points lie above the line of equality, indicating that CoOp precipitation is greater than NLDAS for those subbasins. The variation in the CoOp precipitation data can be attributed to the lack of data within the Shenandoah watershed and missing data at the CoOp gages. The inverse distance method in HEC-HMS can account for insufficient and/or missing data by searching for nearby gages. Due the location of the Shenandoah watershed in a rain shadow between the Blue Ridge and Appalachian Mountains, obtaining data from outside the watershed would potentially create false high records of precipitation. In general, gaps in the record would lead to errors in the gaged precipitation data.
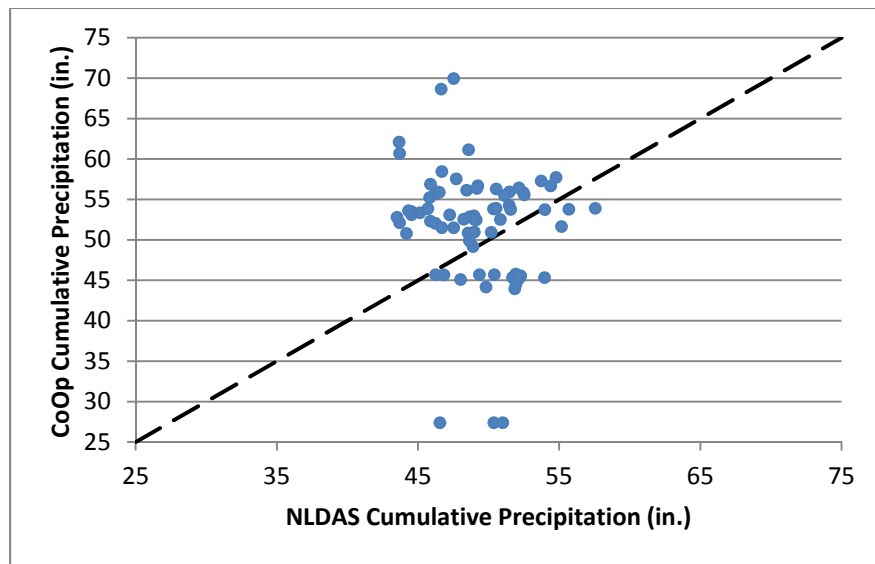
Figure 4-7: CoOp versus NLDAS Cumulative Precipitation for Subbasins (n=76). Each point represents one subbasin.

On average, the CoOp precipitation by subbasin is 3.0 inches higher than the NLDAS precipitation. The variation in cumulative precipitation appears greater for drainage areas more than 75 mi^2 in size (Figure 4-8). However, since fewer than 20% of the subbasins are larger than 75 mi^2, a relationship between the cumulative precipitation differences and subbasin size is not conclusive.
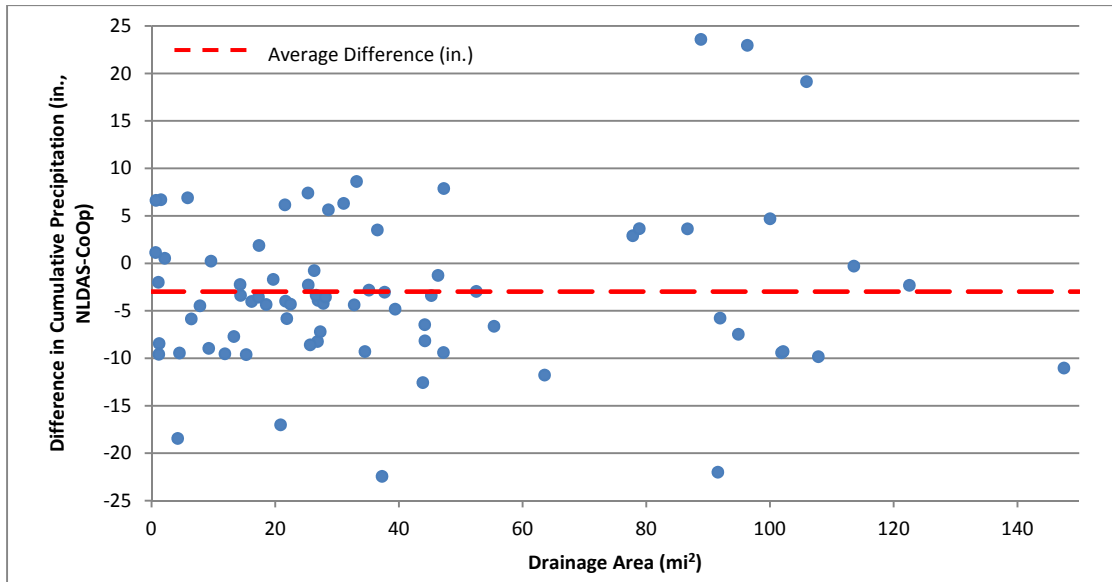
Figure 4-8: Differences in Cumulative Precipitation (NLDAS – CoOp) for Subbasins (n=76)

A Cumulative Distribution Function (CDF) curve was constructed for the hourly precipitation in each subbasin; examples are shown in Figure 4-9. The y-intercept of each curve gives the probability that hourly precipitation is less than or equal to 0, in other words the fraction of total hours in which that subbasin did not receive precipitation. The CDF curves showed an average deviation of approximately 7% in the probability of zero precipitation within a subbasin, with the probability of zero precipitation being consistently higher using the CoOp precipitation data. The probability of zero precipitation was approximately 88% for the NLDAS precipitation data and 96% for the CoOp precipitation data. This indicates that the CoOp precipitation data had more dry hours, hours where rainfall did not occur, than NLDAS. Since CoOp precipitation data is given in 0.1 inch increments, the CDF curves for the CoOp precipitation are not smooth as with the NLDAS precipitation data.
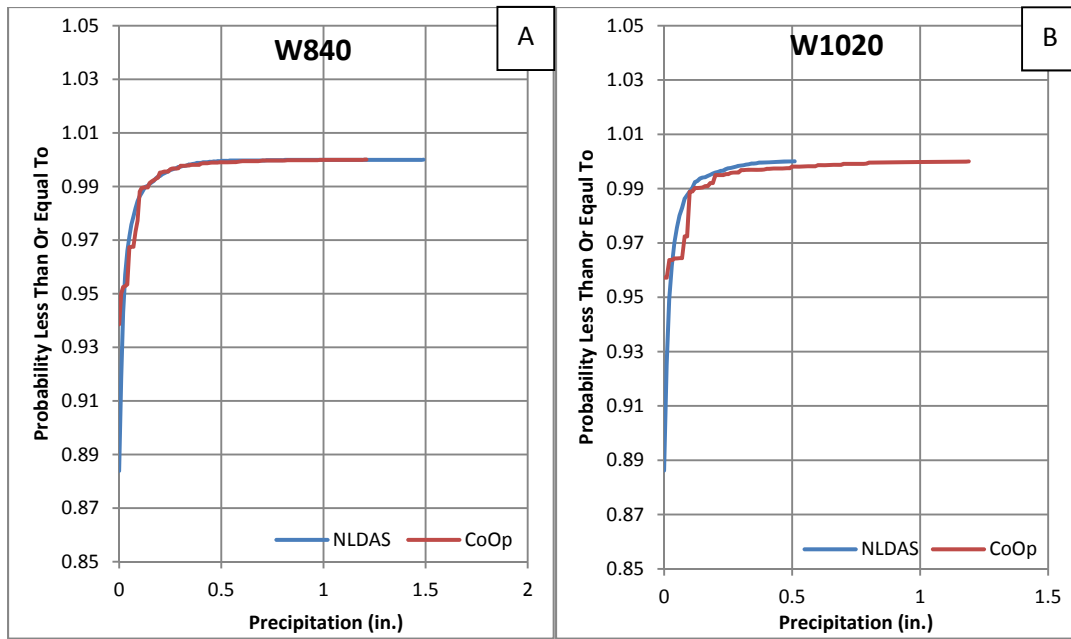
Figure 4-9: Example CDF Curves for NLDAS and CoOp Precipitation. The Y-intercept gives the probability that hourly precipitation is equal to 0, which equals the fraction of hours when no precipitation occurred in the subbasin.

As with cumulative precipitation, the CoOp precipitation data showed a wider range of cumulative excess precipitation (Table 4-1, Figures 4-10 and 4-11). The maximum cumulative excess precipitation occurred in the same subbasins where the maximum cumulative precipitation, while the minimum cumulative excess precipitation occurred within the middle portion of the Shenandoah watershed. This was due to the fact that cumulative excess precipitation is not only dependent on subbasin area, but also on watershed characteristics and the distribution of rainfall over time. On average, the CoOp cumulative excess precipitation is 2.5 inches greater than the NLDAS.

Table 4-2: NLDAS and CoOp Cumulative Excess Precipitation Summary for Subbasins (n=76)

Precipitation	Maximum (in.)	Minimum (in.)	Average (in.)	Range (in.)
NLDAS	21.1	9.4	15.3	11.7
CoOp	33.9	7.0	17.8	26.8
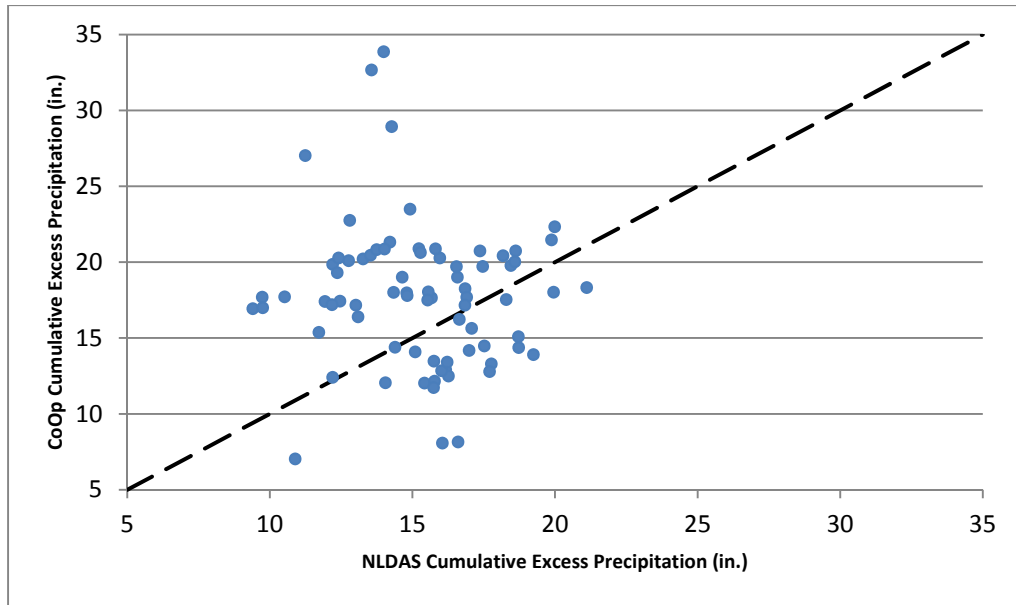
Figure 4-10: CoOp versus NLDAS Cumulative Excess Precipitation for Subbasins (n=76)
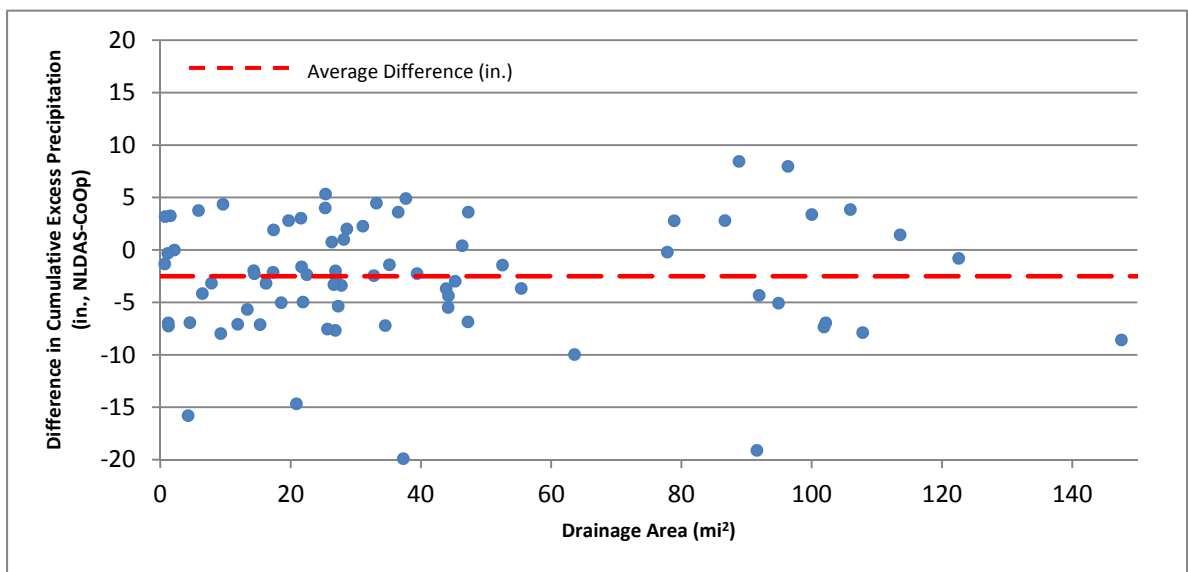
Figure 4-11: Differences in Cumulative Excess Precipitation (NLDAS – CoOp) for Subbasins (n=76)

The NLDAS cumulative precipitation is greater than the CoOp cumulative precipitation in the middle portion of the Shenandoah Watershed along the Massanutten Mountain in the Ridge and Valley Appalachians (Figure 4-12). The CoOp cumulative precipitation is greater in all other areas of the Shenandoah watershed. The CoOp cumulative precipitation is larger in the southern and larger portions of the watershed likely due to the use of the inverse distance method in HEC-

HMS to interpolate precipitation to subbasins. At the northern and southern extents of the watershed there are more CoOp gages that fall within the search distance of each subbasin; therefore increasing the potential precipitation within these subbasins. Given that the CoOp cumulative precipitation is greater than the NLDAS cumulative precipitation over much of the Shenandoah watershed, it was expected that the HEC-HMS CoOp model would over predict the discharge for many of the subbasins.
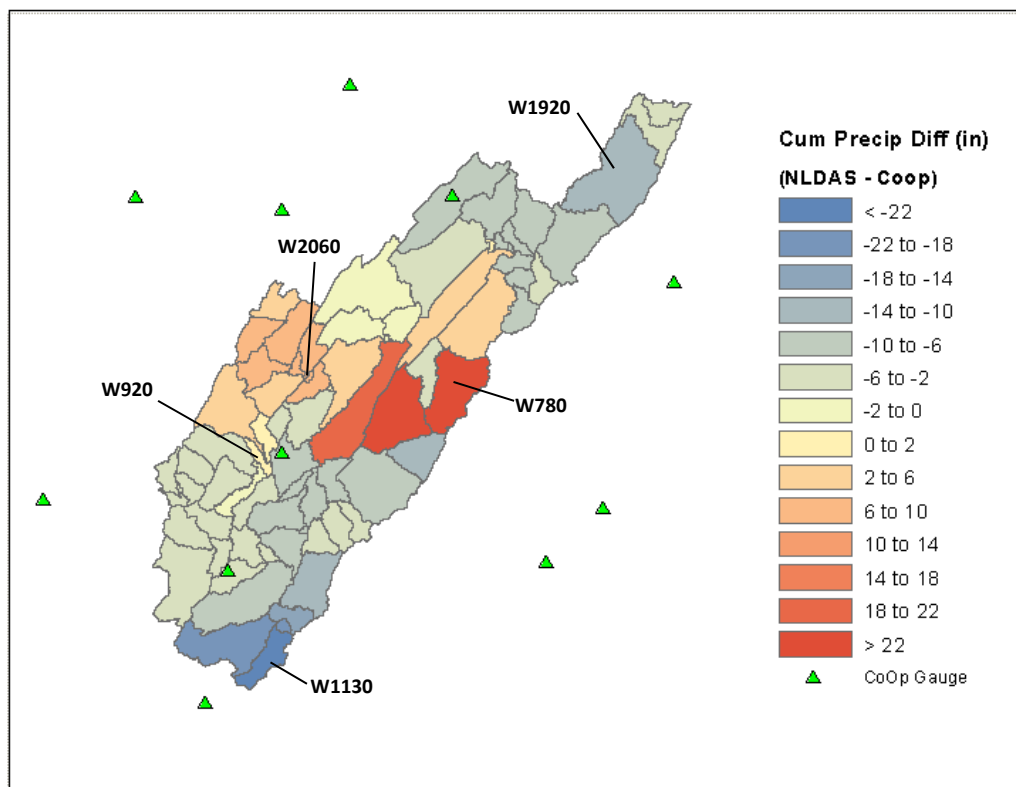
Figure 4-12: Geographic Difference in Cumulative Precipitation, NLDAS – CoOp

In order to determine the impact that the NLDAS and CoOp precipitation data has on the predicted hydrology with a subbasin, the direct runoff was examined for selected subbasins. Subbasins for which the direct runoff was examined in closer detail are identified in Figure 4-12 and listed in Table 4-3.

Table 4-3: Subbasins at which Direct Runoff Comparisons Were Made

Subbasin	Drainage Area (mi²)	Reason Subbasin Was Chosen
W780	88.8	Largest positive difference in cumulative precipitation
W920	9.6	Smallest difference in cumulative precipitation
W1130	37.3	Largest negative difference in cumulative precipitation
W1920	147.5	Largest drainage area
W2060	0.7	Smallest drainage area
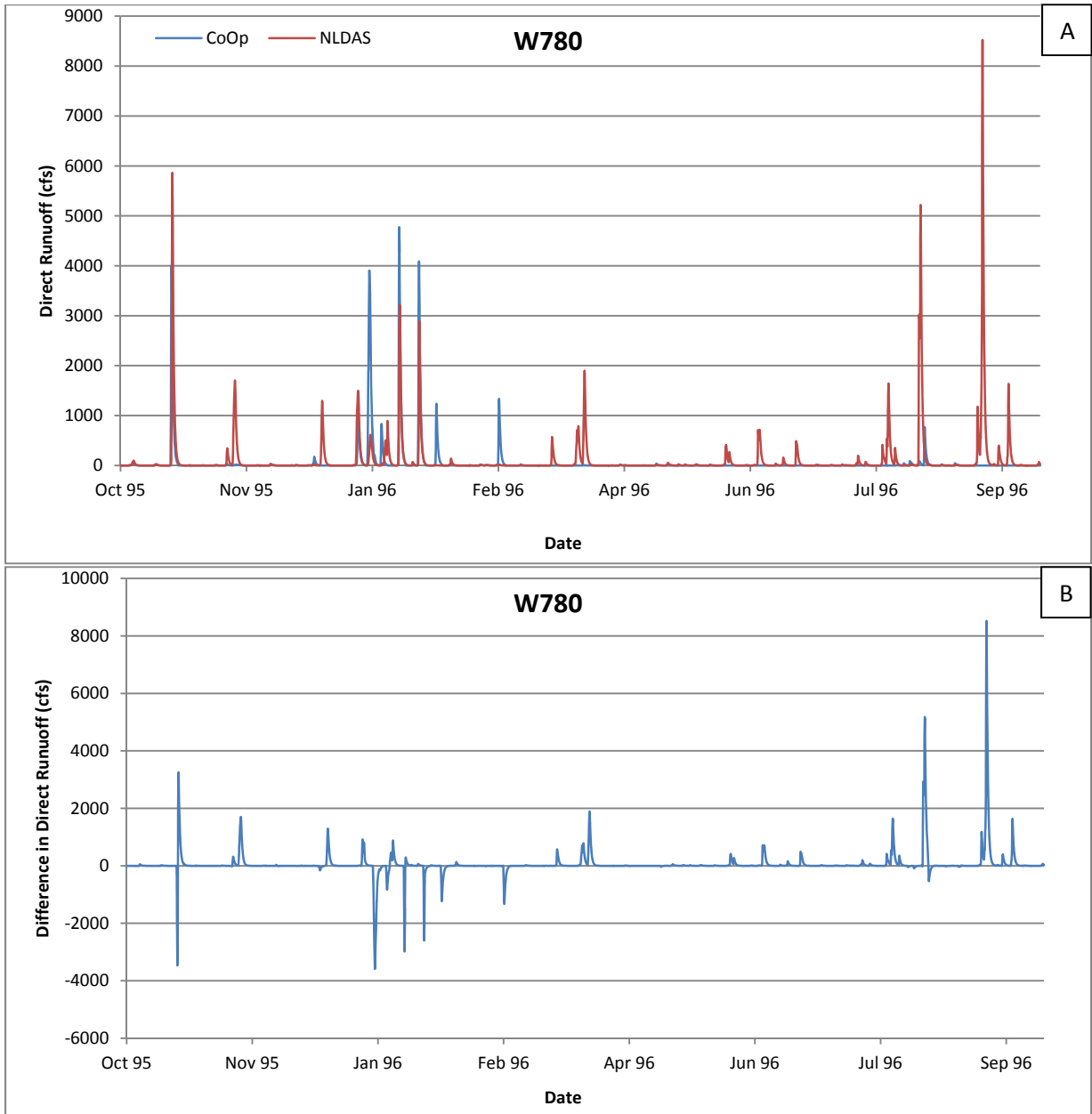
Figure 4-13: HEC-HMS Calculated Direct Runoff and Differences in Direct Runoff (NLDAS – CoOp) for Subbasin W780. This subbasin had the greatest positive difference in cumulative precipitation (NLDA – CoOp)
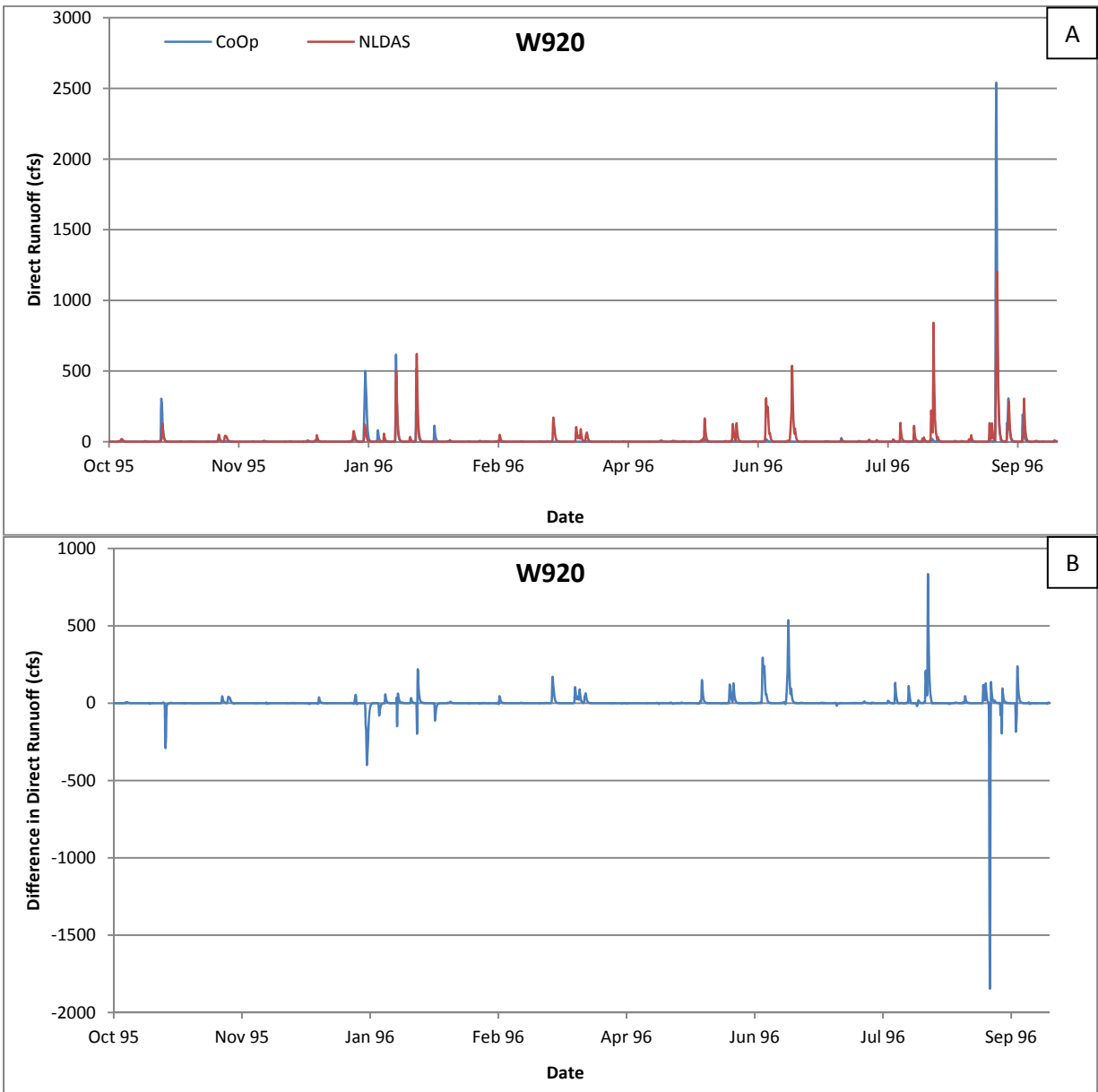
Figure 4-14: HEC-HMS Calculated Direct Runoff and Differences in Direct Runoff (NLDAS – CoOp) for Subbasin W920. This subbasin had the smallest difference in cumulative precipitation (NLDAS – CoOp).
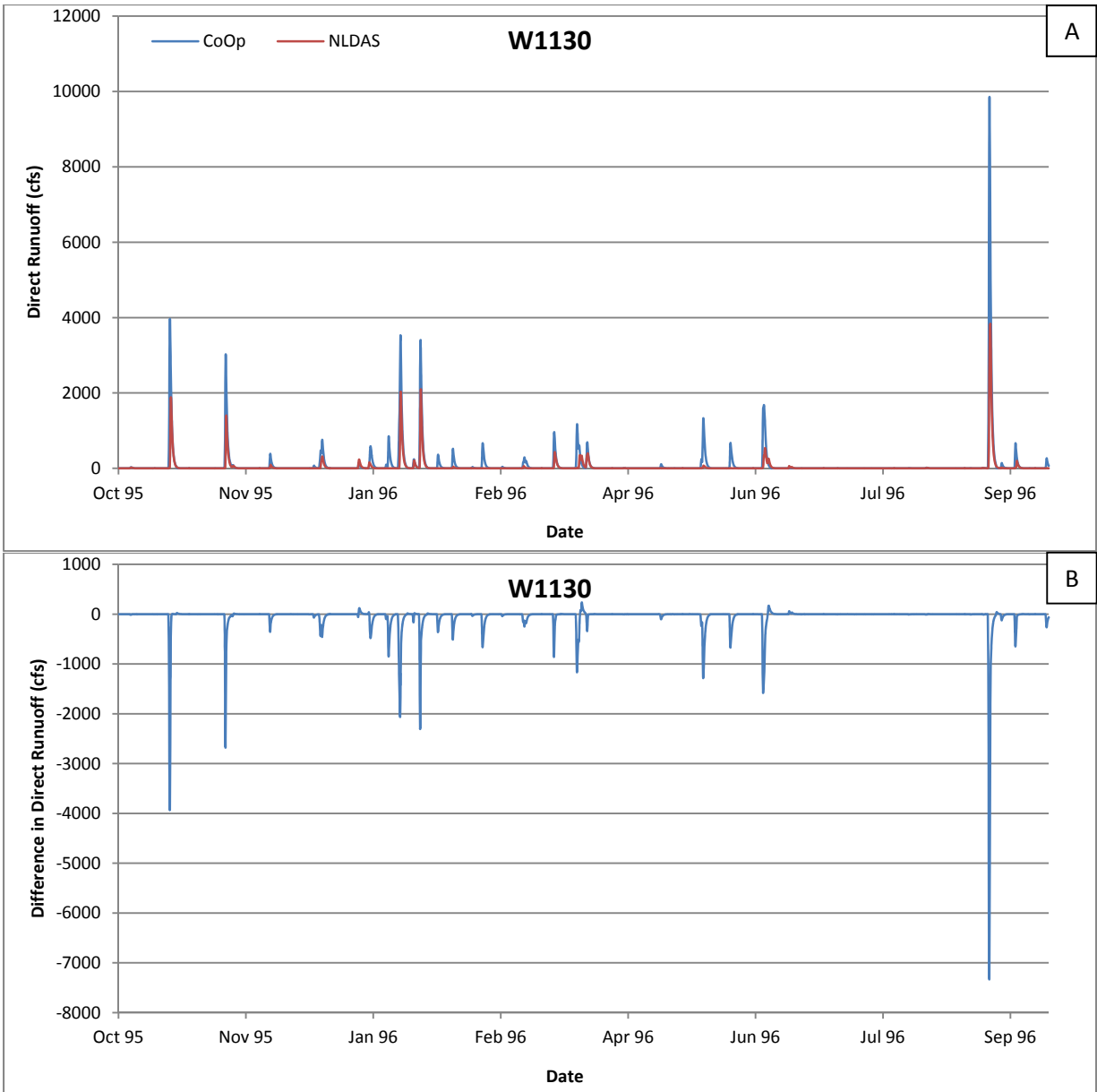
Figure 4-15: HEC-HMS Calculated Direct Runoff and Differences in Direct Runoff (NLDAS – CoOp) for Subbasin W1130. This subbasin had the greatest negative difference in cumulative precipitation (NLDAS – CoOp).
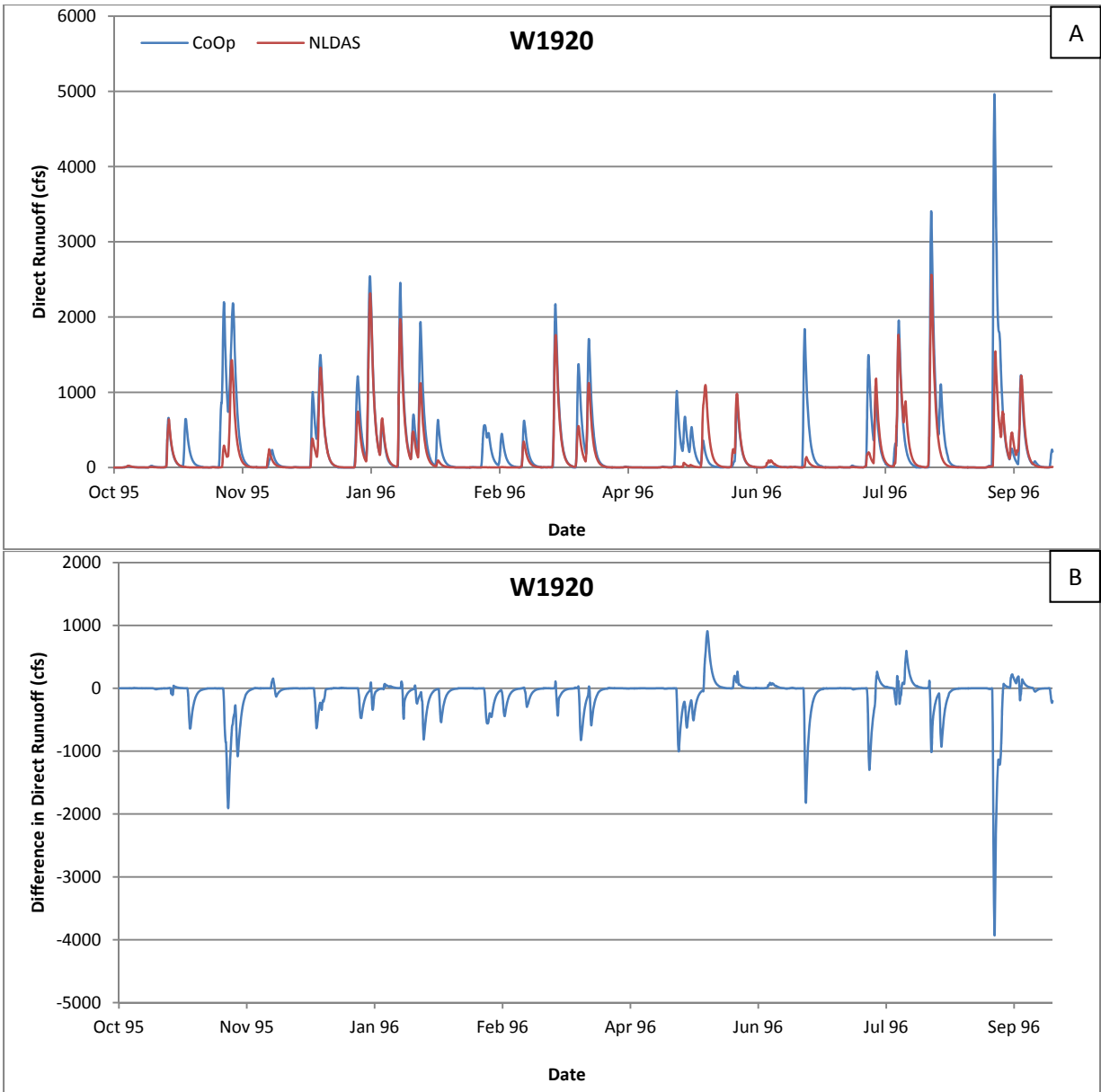
Figure 4-16: HEC-HMS Calculated Direct Runoff and Differences in Direct Runoff (NLDAS – CoOp) for Subbasin W1920. This subbasin had the largest drainage area.
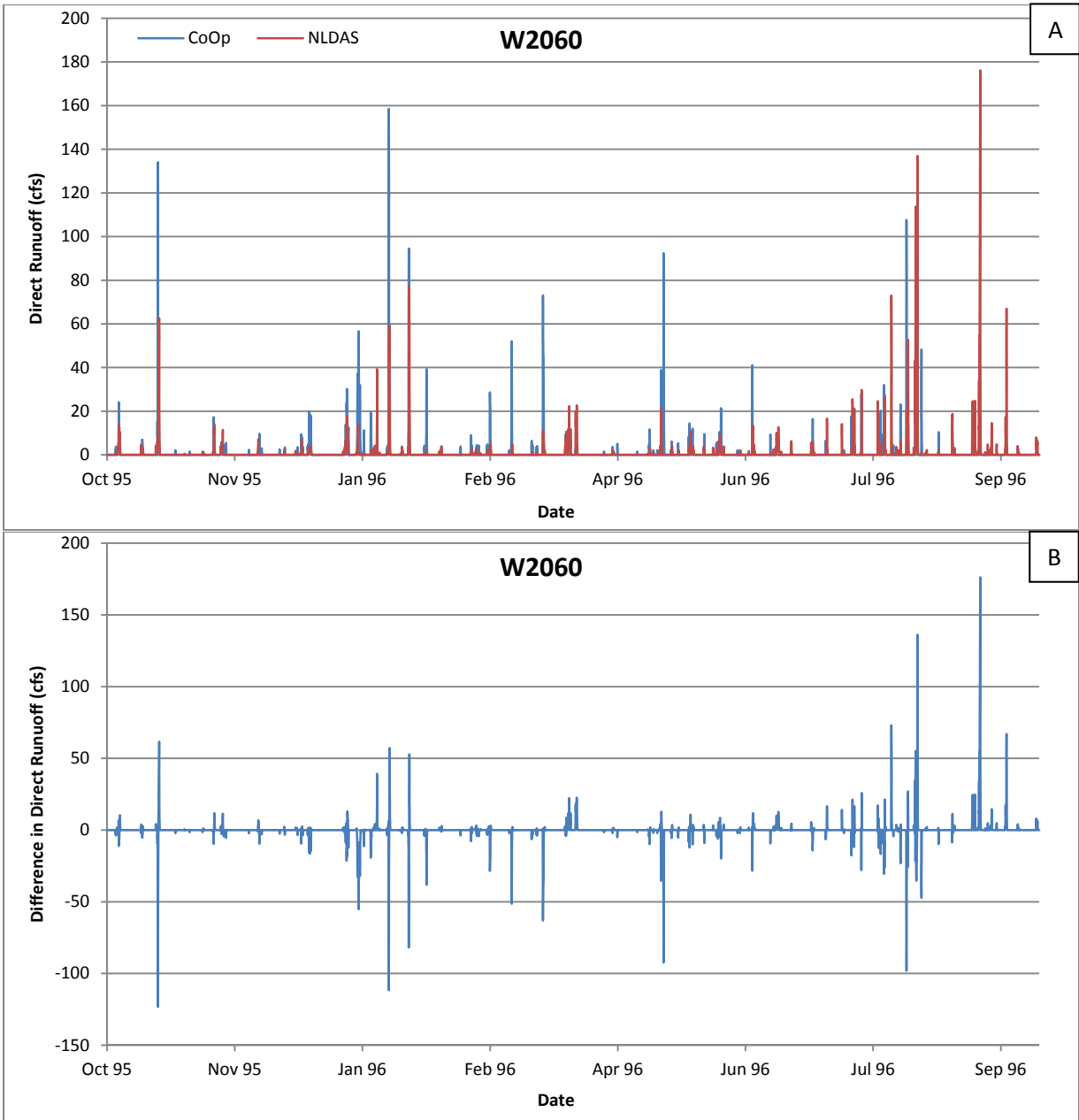
Figure 4-17: HEC-HMS Calculated Direct Runoff and Differences in Direct Runoff (NLDAS – CoOp) for Subbasin W2060. This subbasin has the smallest drainage area.

Table 4-4: Direct Runoff Results for Subbasins W780, W920, W1130, W1920, and W2060 for the 1995 to 1996 Water Year

Subbasin	Drainage Area (mi^2)	Source	Difference in Cumulative Precipitation (in., NLDAS - CoOp)	Maximum Runoff (cfs)	Average Yearly Difference (cfs, NLDAS-CoOp)	Runoff Ratio, *direct runoff / precipitation* (in./in.)
W780	88.8	NLDAS	23.60	8521.5	55.3	0.33
		CoOp		4771.1		0.30
W920	9.6	NLDAS	0.24	1204.1	3.1	0.35
		CoOp		2539.9		0.27
W1130	37.3	NLDAS	-22.42	3834.6	-54.5	0.29
		CoOp		9855.1		0.48
W1920	147.5	NLDAS	-11.02	2561.1	-92.3	0.33
		CoOp		4961.8		0.41
W2060	0.7	NLDAS	1.15	174.6	-0.07	0.39
		CoOp		157.1		0.43

Results of the cumulative precipitation and direct runoff comparisons are summarized in Table 4-4. As expected, if the difference in the cumulative precipitation is positive, subbasins where the NLDAS precipitation is greater, the average yearly difference in direct runoff is positive. The exception to this is Subbasin W2060 where the average yearly difference is negligible, 0.07 cfs. Conversely, if the difference in the cumulative precipitation was negative, subbasins where the CoOp cumulative precipitation is greater, then the average yearly difference in direct runoff was negative.

An important observation based on Figures 4-13 through 4-17 is that for several subbasins, specifically W780 and W2060, there are known rainfall events where the HEC-HMS CoOp model shows no direct runoff. For the September 8, 1996 storm event Subbasins W780 and W2060 in the HEC-HMS CoOp model show that no precipitation fell within these basins; however, given historic knowledge it is known that these subbasins experienced rainfall during the September storm. This is a good example of where using CoOp precipitation can lead to errors in the inputs and errors in the predicted hydrologic responses.

The ratio of cumulative direct runoff to cumulative precipitation is given in Table 4-4 for both precipitation data sources in each subbasin; generally the ratio is greater for the precipitation source which had the greater cumulative precipitation. The difference in runoff ratio for Subbasin W780 is relatively small, while the difference in cumulative precipitation is large, and the difference in runoff ratio for Subbasin W920 is relatively large, while the difference in cumulative precipitation is relatively small. Due to these observations, no other identifiable relationship between direct runoff and cumulative precipitation was realized. This means that direct runoff is impacted by numerous factors beyond cumulative precipitation. These factors include evapotranspiration, slope, soil properties, and land cover of the subbasin.

4.2.2 Comparison to Observed Stream Flow

Stream flow as predicted by both models was compared at USGS Stations 0162200, 0162600, 0163100, 01633000, 01634500 and 01636500 (Figure 4-18). Station 01636500 is the most downstream gage located in the Shenandoah watershed.

Discharge is given as mean daily discharge at the USGS Stations, while the outflow predictions given by HEC-HMS are computed hourly. Therefore, the outflows from the HEC-HMS models were converted from hourly to daily mean discharge by averaging the outflows from 01:00 to 23:00 each day.

Hydrographs and difference graphs are presented in Figures 4-19 through 4-24. The goodness-of-fit measures, i.e., R^2, MA, Se/Sy, RMSE, and NSE, were calculated for both models at each station.
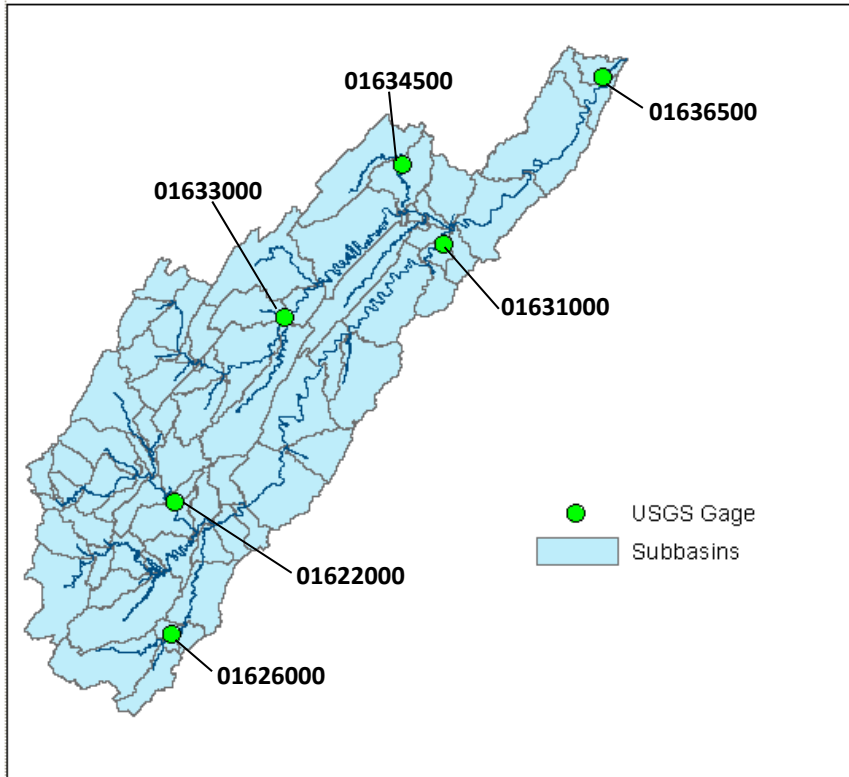
Figure 4-18: USGS Gage Locations within the Shenandoah Watershed

During the October 1, 1995, to September 30, 1996, water year, there were two major high flow events in the Shenandoah watershed, from snowmelt on January 21, 1996, and from rainfall on September 8, 1996. The HEC-HMS hydrologic model used in this study is not set up for snowmelt therefore it is expected that there will be a significant discrepancy in discharge during the January 1996 event.
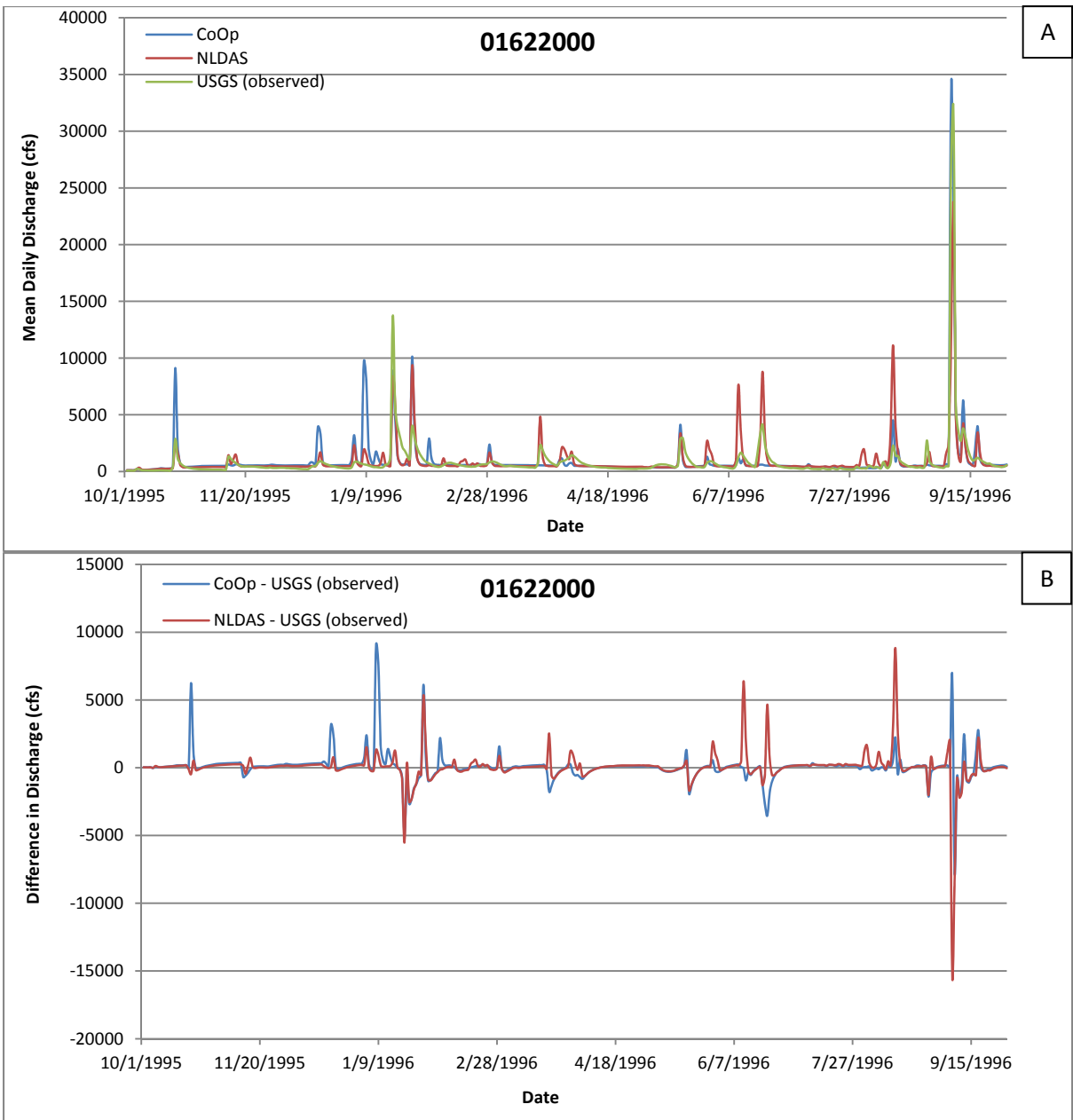
Figure 4-19: Results at USGS Station 01622000: Observed (USGS) and Modeled (CoOp and NLDAS) Mean Daily Discharge (A) and Discharge Differences (B)
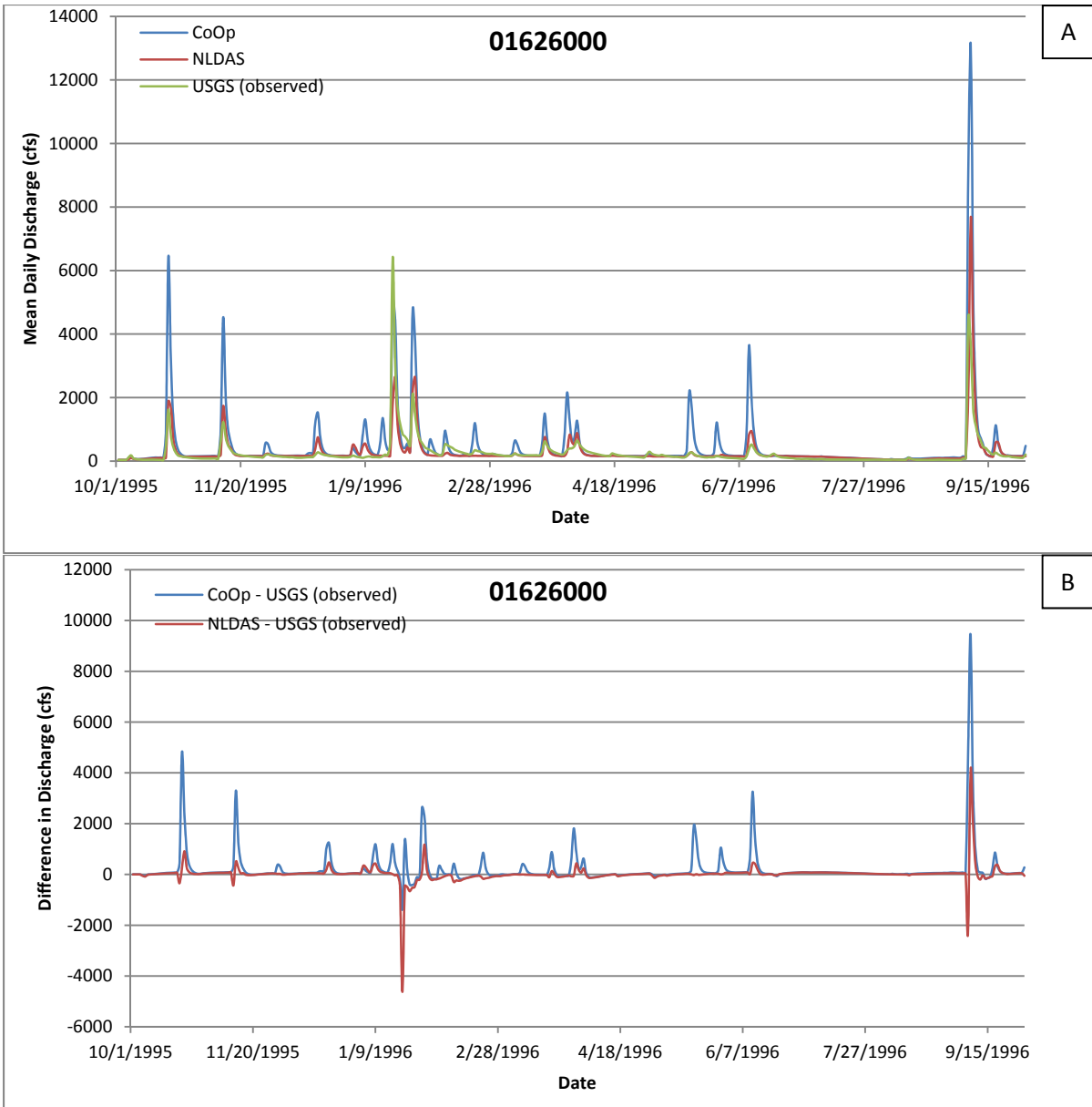
Figure 4-20: Results at USGS Station 01626000: Observed (USGS) and Modeled (CoOp and NLDAS) Mean Daily Discharge (A) and Discharge Differences (B)
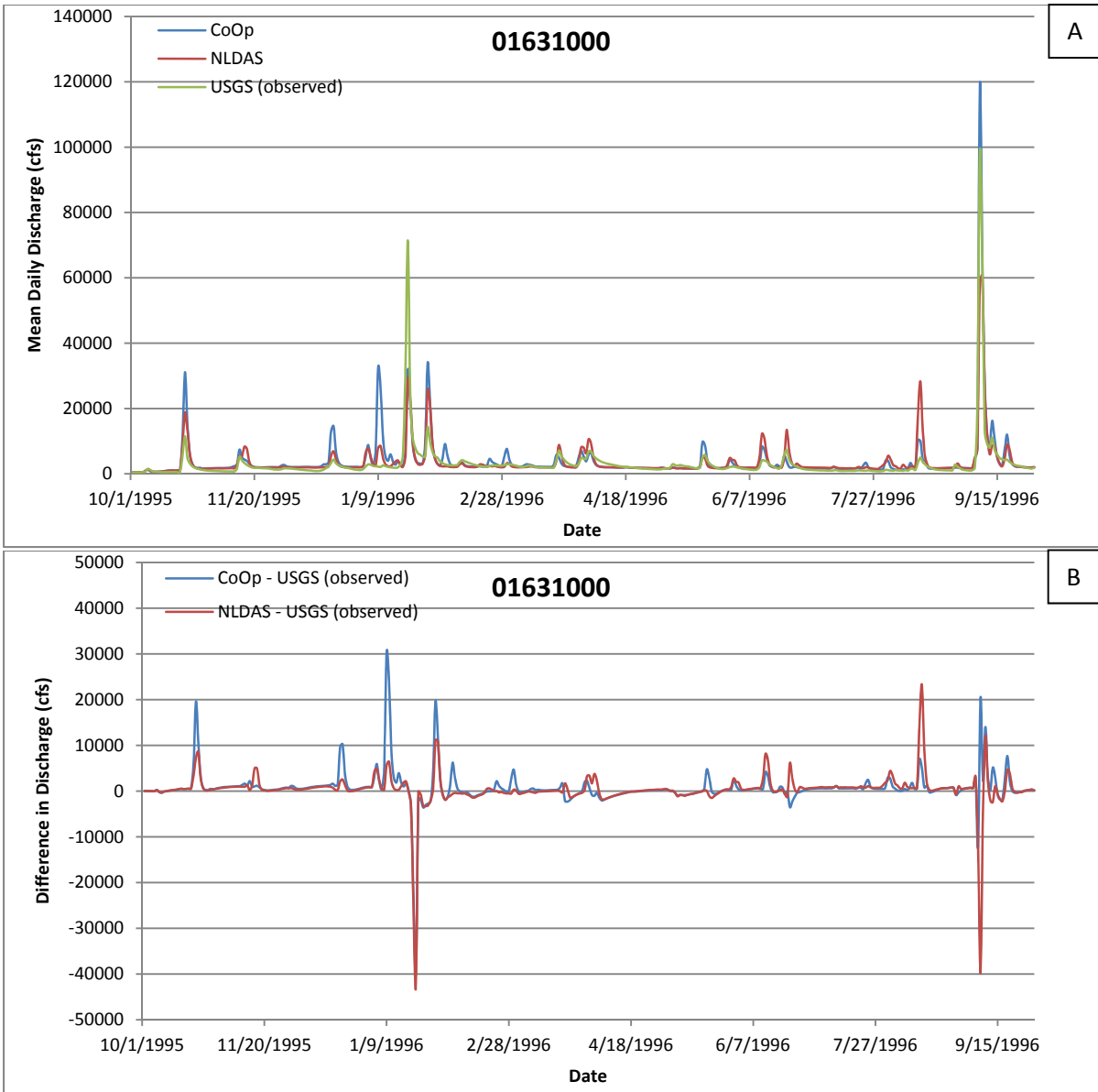
Figure 4-21: Results at USGS Station 01631000: Observed (USGS) and Modeled (CoOp and NLDAS) Mean Daily Discharge (A) and Discharge Differences (B)
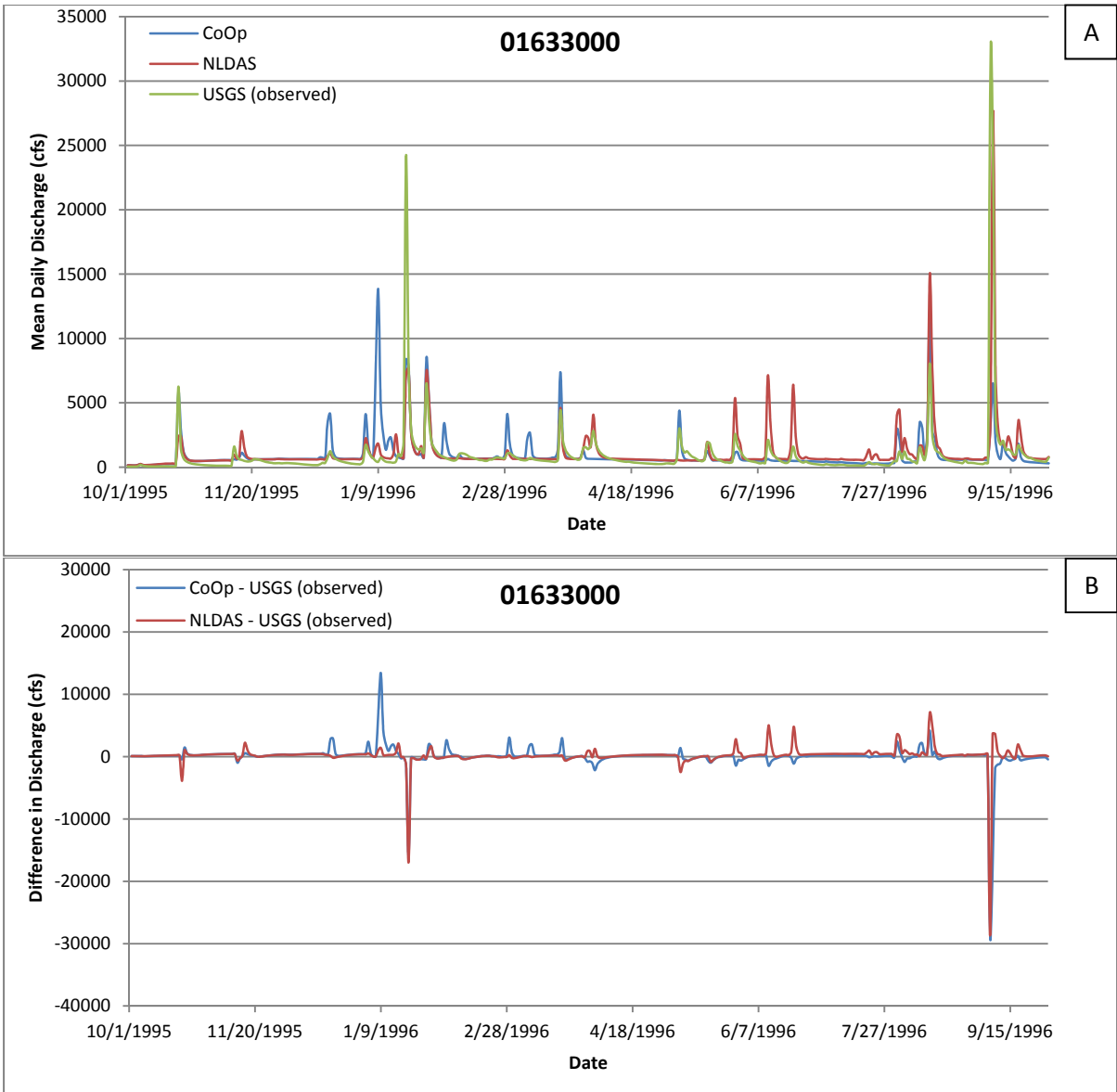
Figure 4-22: Results at USGS Station 01633000: Observed (USGS) and Modeled (CoOp and NLDAS) Mean Daily Discharge (A) and Discharge Differences (B)
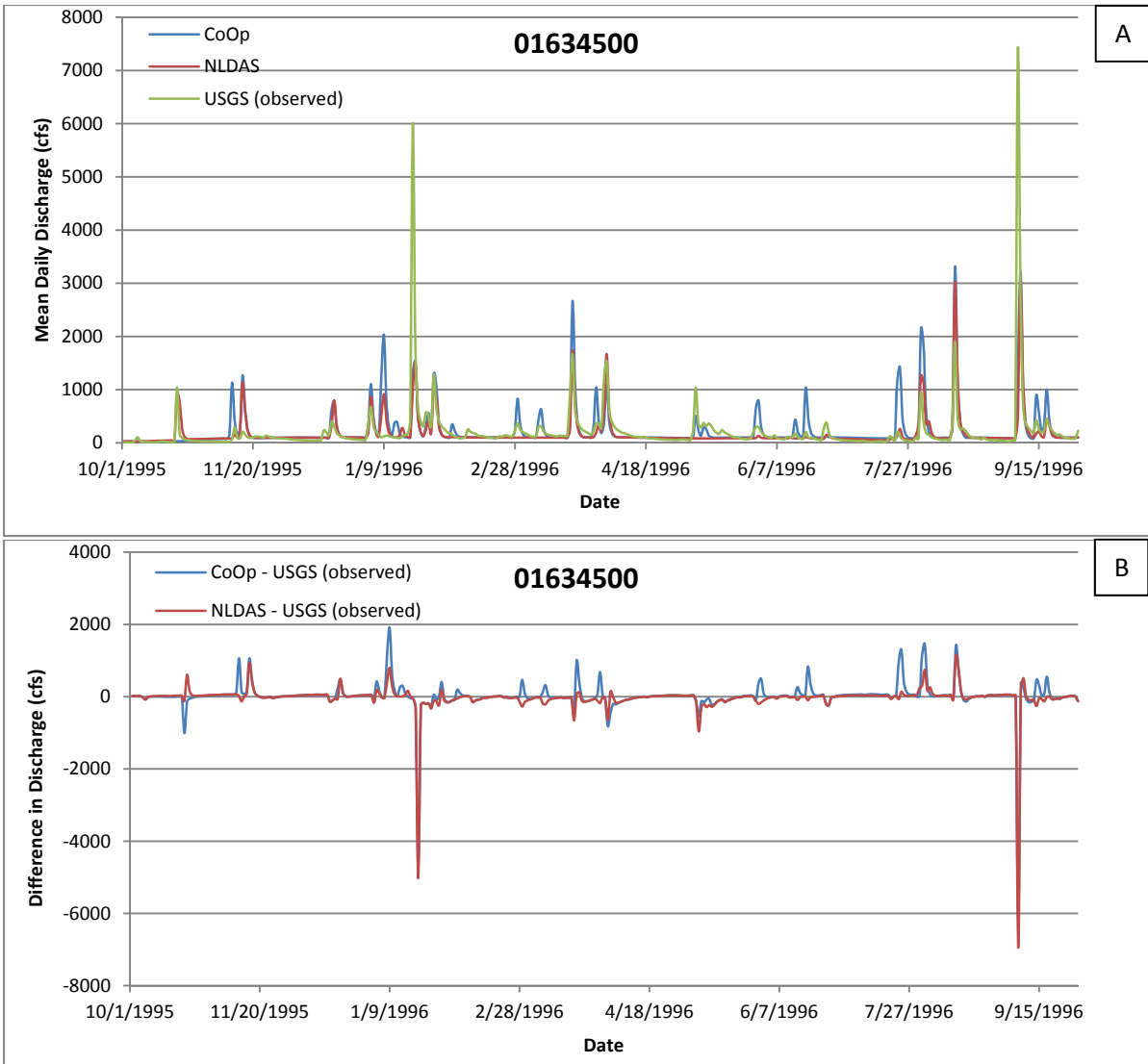
Figure 4-23: Results at USGS Station 01634500: Observed (USGS) and Modeled (CoOp and NLDAS) Mean Daily Discharge (A) and Discharge Differences (B)
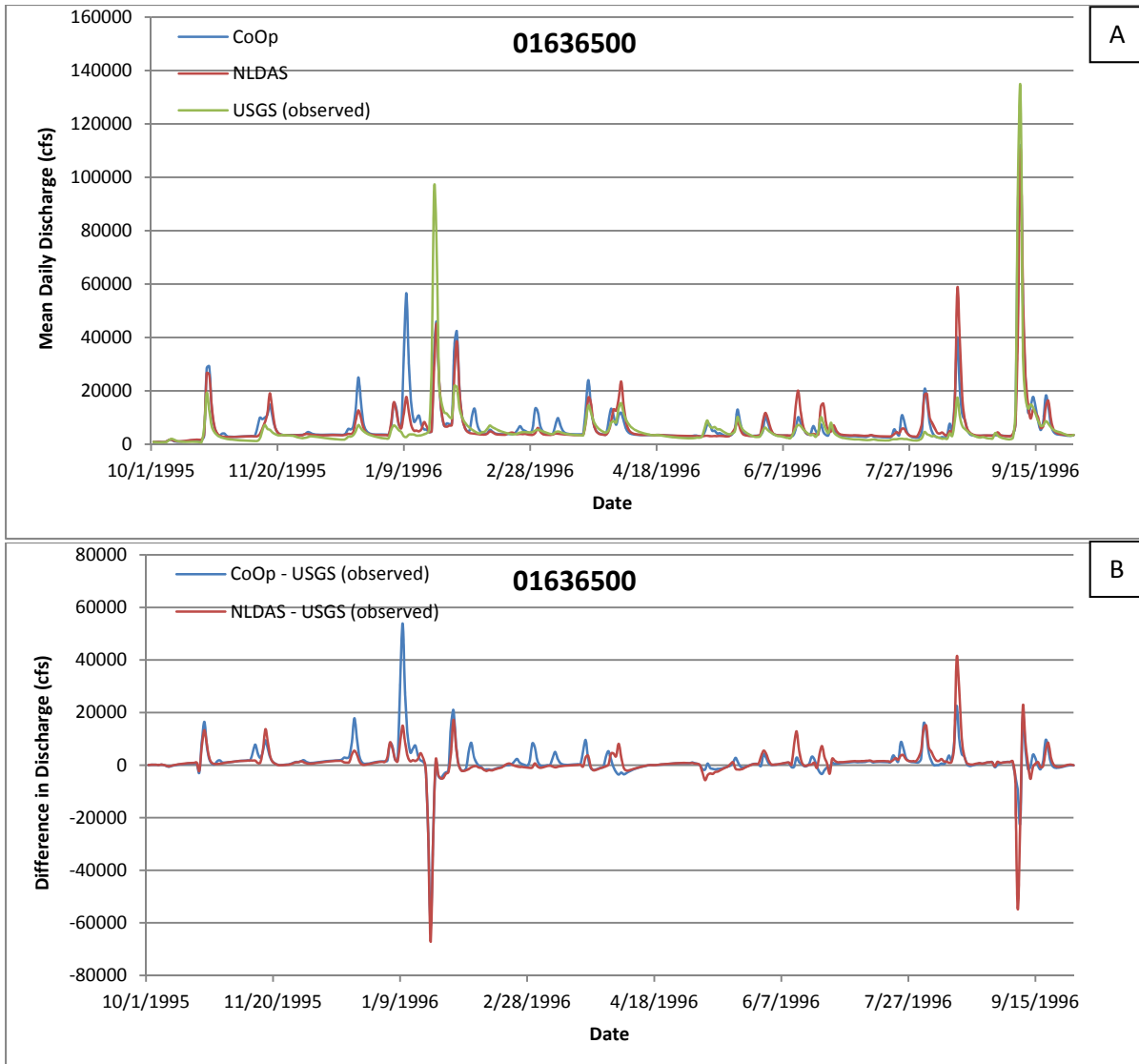
Figure 4-24: Results at USGS Station 01636500: Observed (USGS) and Modeled (CoOp and NLDAS) Mean Daily Discharge (A) and Discharge Differences (B)

Both the NLDAS and CoOp HEC-HMS model under predict the snowmelt event in January 1996 at all locations. The NLDAS model over predicted the mean daily discharge during the September 8, 1996, rainfall event at USGS Gage 01626000 and under predicted the mean daily discharge at USGS Gages 01622000, 01631000, 01633000, 01634500, and 01636500. The CoOp model over predicted the mean daily discharge during the September 8, 1996, rainfall event at USGS Gages 01622000, and 0162600 and under predicted the mean daily discharge at

USGS Gages 01631000, 0163300, 01634500, and 01636500. Generally, both the NLDAS and CoOp model over predict the mean daily discharge during low flow events.

The NLDAS model over predicted the mean daily discharge over the 1995 to 1996 water year at five stations and under predicted the mean daily discharge at Station 01634500 (Table 4-5). The NLDAS model over predicted the mean daily discharge by 232 cfs on average based on the six USGS Gages investigated. The CoOp model over predicted the mean daily discharge over the 1995 to 1996 water year at all six stations. The CoOp model over predicted the mean daily discharge by 405 cfs on average based on the six USGS Gages investigated.

Table 4-5: Average Bias in NLDAS and CoOp HEC-HMS models over the 1995 to 1996 Water Year

USGS Gage	Source	Average Yearly Bias (cfs)
01622000	NLDAS	46.9
	CoOp	68.1
01626000	NLDAS	11.4
	CoOp	209
01631000	NLDAS	370.4
	CoOp	765.6
01633000	NLDAS	183.7
	CoOp	50.62
01634500	NLDAS	-35.9
	CoOp	21.83
01636500	NLDAS	814.9
	CoOp	1312.2

If the model objective is to predict the daily mean discharge for purposes such as water supply decisions, the NLDAS would be a better predictor. The NLDAS model over predicted the mean daily discharge by an average of 230 cfs over the 1995 to 1996 water year. The CoOp model over predicted the mean daily discharge by an average of 404 cfs over the 1995 to 1996 water year.

The NLDAS precipitation data are spatially varying throughout larger subbasins and have the ability to represent a storm moving through a subbasin. The CoOp precipitation inputs are uniform across a subbasin and cannot account for spatial changes in rainfall across a subbasin due to a moving storm. Due to this, it is expected to see a slower rate of increase along the rising limb of the hydrograph in response to the NLDAS input. This would explain the deviations from the NDLAS to USGS discharges seen in the hydrographs during the September 8, 1996, event (Figures 4-19 through 4-24).

Based on the hydrographs and the difference graphs it is difficult to assess the accuracy of the models driven by NLDAS and CoOp precipitation data. Therefore goodness-of-fit measures, i.e., residuals, R^2, ME, Se/Sy, RMSE, and NSE, were computed to assess the NLDAS and CoOp HEC-HMS model accuracy to predict discharge for the 1995 to 1996 water year. In addition, a comparison of peak outflow as computed by HEC-HMS without consideration to timing was reviewed.

ME and RMSE are hydrological values, while R^2 and NSE are statistical values. The following are the criteria used for each goodness-of-fit measure to assess the models' accuracy when compared to USGS discharge data.

1. ME – smallest absolute value is considered to be less biased.

2. RMSE – smallest value represents less deviation from the observed.

3. Se/Sy – smallest value represents model with better predictive power.

4. R^2 – smallest deviation from 1.0 is considered to be a better predictor of the observed.

5. NSE – smallest deviation from 1.0 is considered to be a better predictor of the observed.

Table 4-6: Goodness-of-Fit Measures for CoOp and NLDAS HEC-HMS Models (n=365)

USGS Gage	Source	ME (cfs)	RMSE (cfs)	Se/Sy	R^2	NSE
1622000	CoOp	68.13	1161.12	1.03	0.78	0.76
	NLDAS	46.87	1305.29	0.76	0.7	0.69
1626000	CoOp	208.99	777.9	2.13	0.66	-1.25
	NLDAS	11.35	390.04	1.04	0.53	0.43
1631000	CoOp	765.61	4195.27	1.09	0.75	0.69
	NLDAS	370.39	4154.12	0.75	0.7	0.69
1633000	CoOp	50.62	2222.07	0.58	0.25	0.24
	NLDAS	183.72	1948.65	0.76	0.43	0.42
1634500	CoOp	21.83	481.48	0.73	0.29	0.25
	NLDAS	-35.86	477.35	0.57	0.27	0.26
1636500	CoOp	1312.17	6441.17	0.92	0.67	0.65
	NLDAS	814.86	6592.32	0.81	0.64	0.63

Table 4-7: Goodness-of-Fit (GOF) Measures Assessment. X represents the model with the better GOF value based on the criteria given above.

USGS Gage	Source	ME(cfs)	RMSE (cfs)	Se/Sy	R^2	NSE
1622000	CoOp		X		X*	X
	NLDAS	X*		X		
1626000	CoOp				X	
	NLDAS	X	X	X		X
1631000	CoOp				X*	-
	NLDAS	X	X*	X		-
1633000	CoOp	X*		X		
	NLDAS		X		X	X
1634500	CoOp	X			-	-
	NLDAS		X*	X	-	-
1636500	CoOp		X		-	-
	NLDAS	X		X	-	-

*Indicates that the goodness of fit measure was slightly better; - Indicates the goodness of measures was not significantly different

Based on the goodness-of-fit measures, it was determined that HEC-HMS hydrologic model that utilizes the NLDAS precipitation data provides a better representation of the hydrologic processes in the Shenandoah watershed at two of the six USGS stations analyzed, Stations 01626000 and 01633000. At Stations 01632000 the HEC-HMS hydrologic model utilizing the

CoOp precipitation data appears to be a better representation. However, it should be noted that in previous studies of the Shenandoah watershed the calibrated model discharge did not match well with the observed discharge at Station 01634500 (Kim, 2012). Based on these measures alone at Stations 1631000, 1634500 and 1636500 the bias and predictive accuracy of the precipitation datasets are equal.

4.2.3 Other Criteria

The peak outflow and outflow residuals as calculated by HEC-HMS were analyzed to determine the accuracy of the models. The time to peak events was not analyzed since the USGS data is in daily increments and the model data is in hourly. The following criteria were used:

1. Peak outflow – model with smallest deviation from the observed discharge is considered to be more accurate.

2. Residuals (predicted outflow (in.) – observed outflow (in.)) – model with smallest absolute residual is considered to be a better representation of the observed. Residuals are computed in HEC-HMS for each junction.

Based on the six sites shown in Figure 4-16 analyzed, the NLDAS HEC-HMS model under predicted the peak discharge at Stations 0163100, 01634500, and 01636500 by 6.3, 47.9, and 3.9%, respectively, and over predicted at Stations 01622000, 01626000, and 0163300 by 23.1, 37.3, and 31.1%, respectively. On average the NLDAS model over predicted the peak discharge by 5.6%. The CoOp HEC-HMS model under predicted the peak discharge at Stations 1633000 and 1634500 by 41.9 and 32.2%, respectively, and over predicted at Stations 01622000,01626000, 1631000, and 0163300 by 103.4, 184.3, 49.5, and 13.0%, respectively. On average the CoOp model over predicted the peak discharge by 50.0%.

Table 4-7: HEC-HMS Outputs for the 1995 to 1996 Water Year at USGS Gages Shown in Figure 4-16

USGS Gage	Precipitation	Peak Outflow (cfs)	Residual (in.)	% Difference in Peak Outflow (Predicted – Observed)
01622000	CoOp	72,733	2.46	127.29
	NLDAS	39,383	1.69	23.07
	USGS	32,000	-	-
01626000	CoOp	18,166	21.31	184.29
	NLDAS	8,775	1.16	37.32
	USGS	6,390	-	-
01631000	CoOp	146,826	6.35	49.52
	NLDAS	92,048	3.07	-6.26
	USGS	98,200	-	-
01633000	CoOp	18,707	1.35	-41.90
	NLDAS	42,207	4.90	31.08
	USGS	32,200	-	-
01634500	CoOp	5,014	2.90	-32.24
	NLDAS	3,852	-4.77	-47.95
	USGS	7,400	-	-
01636500	CoOp	150,265	5.86	12.98
	NLDAS	127,798	3.64	-3.91
	USGS	133,000	-	-

If the model objective is to capture peak flow events such as that seen on September 8, 1996, for applications such as floodplain management and planning, decisions based on the CoOp model would be inaccurate since the model over predicted high flow events. The NLDAS model would lead to better decisions given its ability to better predict high flow events.

Based on the outflow residuals, the NLDAS model is a better predictor of the outflow at Stations 01622000, 01626000, 01631000, and 01636500. The CoOp model is a better predictor of the outflow at Stations 01633000, and 01634500.

Chapter 5

Conclusions and Discussion

5.1 Conclusions

The objective of this study was to determine the sensitivity of hydrologic responses in the Shenandoah watershed to distributed NLDAS precipitation data and assess if the NLDAS precipitation data can be used for predictive stream flow analyses. Given advancements in hydrologic model and the increasing availability of gridded data it is important to understand the implications of using NLDAS precipitation data over traditional point data.

To fulfill the objectives, a hydrologic model of the Shenandoah watershed was built in the HEC-HMS modeling environment using open source data from federal entities. Due to the size of the watershed and limited data availability, assumptions regarding estimations of parameters were made based on local and similar studies. This led to parameter estimations, including Manning's n and SMA loss method parameters, across the Shenandoah watershed that should not be taken as accurate without further examination. The parameter estimates are appropriate for a sensitivity study as they capture the general hydrologic behavior of the watershed. Holding the parameters constant for both simulations ensure that differences in the modeling output are due to the variation in precipitation data, not due to differences in parameter estimations via calibration. In addition, as the modeling process progressed, additional parameters were required to adequately represent the watershed. While the inclusion of watershed parameters can improve model accuracy, it can also lead to unreasonable results if the parameters included are not calibrated and not based on attainable physical values.

Due to the significant amount of time required to build a hydrologic model of this magnitude and the computation time needed calibrate a hydrologic model, the HEC-HMS models used in this study were subjectively optimized, but uncalibrated. While the study was useful to

determine the potential impacts of using different precipitation datasets, the models should be calibrated to more fully determine the models' accuracy for predicting hydrologic responses.

Based on the NLDAS and CoOp precipitation data used in this study the following observations are made:

1. The CoOp precipitation data appears to over predict the precipitation in the southern and northern extents and under predict the precipitation in the middle portion of the Shenandoah watershed. The over estimation of precipitation is believed to be partly due to the lack of CoOp gauging stations within the Shenandoah watershed. The under prediction of precipitation is believe to be due to missing precipitation data and the fact that CoOp gages do not record values below a tenth of an inch. If precipitation data are missing, this could erroneously result in a subbasin not accounting for precipitation when in reality rainfall occurred. The NLDAS data appears to be a better representation of precipitation in the Shenandoah watershed.

2. Unlike the CoOp precipitation data, the NLDAS data has the ability to replicate a storm event that moves through a subbasin given its gridded nature. This leads to a change in the predicted hydrograph shape and creates a slower rate of development of the rising limb. This is due to the fact that precipitation is spatially distributed and routed through each subbasin and not assumed to be evenly distributed within the subbasin.

3. Comparing subjectively optimized models, the NLDAS precipitation data represents the hydrologic processes of the Shenandoah watershed better than the CoOp data. This assessment was determined through inspection of the hydrographs and goodness-of-fit measures. The NLDAS model better predicted the observed daily mean discharge and the September 8, 1996, storm event. The goodness-of-fit measures indicated that the NLDAS model was less biased and a better predictor of the observed at two of the six

USGS stations investigated. At three of the six USGS stations investigated both the

CoOp and NLDAS models showed similar abilities to predict the observed.

It is recommended that the HEC-HMS hydrologic model utilizing the NLDAS precipitation

data be calibrated and further analyzed to determine its true predictive accuracy. Based on the

results of this study, it is believed based on the results of this study that the NLDAS precipitation

data can be used to improve stream flow forecasts within the Shenandoah watershed, when

compared to gaged data. It should be noted that processing the NLDAS precipitation data for use

in hydrologic models is time consuming, therefore it is important to define your model objectives

early.

5.2 Future Research

5.2.1 Calibration and Verification

The HEC-HMS hydrologic models used in the study were subjectively optimized but not

calibrated. The models should be calibrated if intended to be used for stream flow predictions. It

is suggested that the model which utilizes the NLDAS precipitation data be calibrated and it

appears the data is an improvement over gaged data. Some of the parameters within the HEC-

HMS model which lend themselves well to calibration are: 1. Manning's n value used in the

reach routing method and T_c calculations; 2. The SMA parameters, not including percent

impervious. A majority of these parameters were estimated based on similar studies and/or

through subjective calibration. The subsurface storage and baseflow parameters were assumed to

be the same for all subbasins, despite their physical differences. Further research could

determine if these parameters can be estimated from measurable or observable watershed

characteristics. In addition, the interaction of the subsurface layers and their impact on the

hydrologic model is not fully understood as small changes in values during the subjective

optimization process created large changes in resultant hydrologic responses (i.e., discharge);

100

3. Storage coefficient used in the transform method; and 4. Groundwater parameters used in the baseflow method.

5.2.2 Timing differences

It was noted during the study that there were timing differences in peak events, large and small, between the CoOp and NLDAS models. Given that the observed data were provided as mean daily discharge it is difficult to determine which peak time is more accurate. If the modeler is only concerned about peak values, i.e., for water demand, without regard to time this, is not an issue. However, if timing of the peaks is important, i.e., for reservoir/dam management, this issue should be investigated further.

5.2.3 Gridded SMA method

For this study since gaged precipitation data was utilized as well as gridded precipitation, the lumped SMA loss method was used. This would allow for the only change in models to be the precipitation and routing method. A lumped SMA loss method approach assumes that the soil saturation is identical throughout a subbasin at a given time step. Using the gridded SMA method would allow for the losses to be discretized across a subbasin and could potentially improve model accuracy.

Appendix A

Shenandoah River Basin Physical Characteristics and Hydrologic Parameters

General Watershed Parameters:

Subbasin	Reach	Length (ft)	Area (mi²)	Average Slope (ft/ft)	Subbasin	Reach	Length (ft)	Area (mi²)	Average Slope (ft/ft)
W1000	R10	80077	55	0.00204	W1960	R260	62035	89	0.00322
W1020	R100	95459	114	0.00421	W1970	R270	6599	1	0.00318
W1050	R110	2977	29	0.00243	W2010	R280	148445	106	0.00150
W1060	R1170	32597	17	0.00327	W2020	R290	57012	33	0.00136
W1070	R1190	62	14	0.02007	W2060	R30	15472	47	0.00147
W1080	R120	8871	1	0.00552	W2070	R300	24179	44	0.00689
W1090	R1220	40669	14	0.00933	W610	R310	81092	79	0.00867
W1100	R1260	10727	8	0.01119	W620	R330	45410	53	0.00956
W1110	R1280	87	17	0.05869	W640	R340	16698	10	0.00484
W1120	R130	17163	31	0.00717	W650	R350	19356	20	0.00211
W1130	R1330	13230	9	0.00108	W670	R360	2156	25	0.01251
W1140	R1390	95227	35	0.00066	W680	R370	70685	38	0.00476
W1160	R140	60571	26	0.00164	W690	R380	17364	44	0.00222
W1180	R1430	14357	4	0.00208	W700	R390	32787	28	0.00172
W1210	R1480	30434	21	0.00160	W710	R40	28869	22	0.00169
W1250	R150	27117	46	0.00492	W720	R410	82591	108	0.00123
W1270	R1540	80979	64	0.00142	W730	R420	10621	27	0.00327
W1310	R1580	20316	27	0.00118	W740	R430	23621	19	0.00090
W1320	R160	7203	1	0.00055	W750	R440	27611	26	0.00073
W1360	R1640	133771	96	0.00111	W760	R450	52592	44	0.00092
W1370	R1690	36081	13	0.00059	W770	R460	10186	27	0.00306
W1420	R170	172990	100	0.00101	W780	R470	20287	35	0.00474
W1470	R1740	259351	123	0.00100	W800	R480	28308	16	0.00205
W1510	R1790	98456	102	0.00283	W810	R490	11548	1	0.00068
W1520	R180	52466	47	0.00488	W820	R50	30017	12	0.00072
W1560	R1840	131923	87	0.00341	W830	R500	53011	6	0.00096
W1570	R1880	117336	95	0.00050	W840	R510	84162	27	0.00156
W1610	R190	23922	33	0.00886	W870	R520	17290	28	0.00268
W1620	R1940	113244	148	0.00046	W890	R530	73596	92	0.00263
W1660	R1990	50040	39	0.00098	W900	R540	105257	102	0.00164
W1670	R20	15596	5	0.00039	W910	R550	42960	22	0.00224
W1710	R200	1899	25	0.00184	W920	R560	87676	92	0.00159
W1720	R2030	7292	2	0.00292	W930	R570	26849	37	0.00448
W1760	R2090	36224	45	0.00303	W940	R60	6201	22	0.00005
W1770	R210	17194	6	0.00336	W950	R70	19926	15	0.00056
W1810	R220	6008	1	0.00361	W960	R80	14624	27	0.01624
W1820	R230	99721	78	0.00161	W970	R90	13750	2	0.00010
W1870	R240	20253	22	0.00227					
W1920	R250	28315	37	0.00552					

SCS Loss Method Parameters:

Subbasin	SCS CN	Impervious (%)
W1000	73.74	9.36
W1020	77.72	1.53
W1050	71.49	0.69
W1060	74.44	4.89
W1070	72.98	2.33
W1080	69.77	1.17
W1090	71.72	0.71
W1100	78.78	1.60
W1110	75.41	3.46
W1120	73.32	12.05
W1130	64.97	0.87
W1140	69.59	2.18
W1160	73.60	2.32
W1180	74.79	1.05
W1210	65.32	0.07
W1250	70.05	0.07
W1270	63.84	0.05
W1310	75.25	2.19
W1320	74.72	2.70
W1360	79.09	1.68
W1370	78.12	2.14
W1420	67.77	4.65
W1470	69.74	15.17
W1510	70.98	3.16
W1520	67.93	2.19
W1560	69.30	0.44
W1570	69.45	0.67
W1610	73.18	1.85
W1620	69.01	1.49
W1660	73.20	4.25
W1670	67.95	2.07
W1710	69.73	0.58
W1720	73.61	2.16
W1760	73.53	1.17
W1770	69.19	0.16
W1810	72.40	1.19
W1820	67.93	0.23
W1870	70.85	0.88
W1920	75.65	0.95

Subbasin	SCS CN	Impervious (%)
W1960	74.68	6.80
W1970	73.19	3.01
W2010	72.71	6.43
W2020	70.87	0.59
W2060	79.80	25.07
W2070	78.43	1.92
W610	76.49	2.12
W620	75.38	2.81
W640	78.48	3.09
W650	65.76	5.97
W670	70.64	0.80
W680	68.20	0.37
W690	62.73	0.24
W700	73.16	1.89
W710	70.38	0.16
W720	69.44	0.09
W730	67.82	0.24
W740	72.62	0.78
W750	76.70	1.25
W760	74.83	1.94
W770	73.94	1.52
W780	68.82	2.01
W800	68.47	0.09
W810	74.19	1.11
W820	69.10	0.14
W830	71.29	0.35
W840	69.63	0.22
W870	69.54	0.30
W890	70.39	2.31
W900	69.06	0.44
W910	64.86	0.56
W920	76.12	3.47
W930	74.62	1.13
W940	71.04	0.91
W950	76.68	3.11
W960	60.38	0.02
W970	78.08	15.74

SMA Loss Method Parameters:

Subbasin	Initial Soil/ GW 1/ GW 2 (%)	Maximum Infiltration (in/hr)	Impervious (%)	Soil Storage (in)	Tension Storage (in)	Soil/GW 1 Percolation (in/hr)	GW 1/GW 2 Storage (in)	GW 1/GW 2 Coefficient (hr)	GW 2 Percolation (in/hr)
W1000	10	4.47	9.36	3.71	0.98	0.00402	0.80	360	0
W1020	10	4.47	1.53	3.71	0.98	0.00402	0.80	360	0
W1050	10	4.14	0.69	3.41	0.98	0.00373	0.80	360	0
W1060	10	4.14	4.89	3.41	0.98	0.00373	0.80	360	0
W1070	10	4.14	2.33	3.41	0.98	0.00373	0.80	360	0
W1080	10	4.14	1.17	3.41	0.98	0.00373	0.80	360	0
W1090	10	4.14	0.71	3.41	0.98	0.00373	0.80	360	0
W1100	10	4.14	1.60	3.41	0.98	0.00373	0.80	360	0
W1110	10	4.14	3.46	3.41	0.98	0.00373	0.80	360	0
W1120	10	4.14	12.05	3.41	0.98	0.00373	0.80	360	0
W1130	10	4.14	0.87	3.41	0.98	0.00373	0.80	360	0
W1140	10	4.14	2.18	3.41	0.98	0.00373	0.80	360	0
W1160	10	4.47	2.32	3.71	0.98	0.00402	0.80	360	0
W1180	10	4.47	1.05	3.71	0.98	0.00402	0.80	360	0
W1210	10	4.14	0.07	3.41	0.98	0.00373	0.80	360	0
W1250	10	4.14	0.07	3.41	0.98	0.00373	0.80	360	0
W1270	10	4.14	0.00	3.41	0.98	0.00373	0.80	360	0
W1310	10	4.14	2.19	3.41	0.98	0.00373	0.80	360	0
W1320	10	4.47	2.70	3.71	0.98	0.00402	0.80	360	0
W1360	10	4.14	1.68	3.41	0.98	0.00373	0.80	360	0
W1370	10	4.14	2.14	3.41	0.98	0.00373	0.80	360	0
W1420	10	4.14	4.65	3.41	0.98	0.00373	0.80	360	0
W1470	10	4.14	15.17	3.41	0.98	0.00373	0.80	360	0
W1510	10	4.14	3.16	3.41	0.98	0.00373	0.80	360	0
W1520	10	4.14	2.19	3.41	0.98	0.00373	0.80	360	0
W1560	10	4.47	0.44	3.71	0.98	0.00402	0.80	360	0
W1570	10	4.47	0.67	3.71	0.98	0.00402	0.80	360	0
W1610	10	3.81	1.85	3.55	1.07	0.00343	0.80	360	0
W1620	10	3.81	1.49	3.55	1.07	0.00343	0.80	360	0
W1660	10	3.60	4.25	3.17	1.06	0.00324	0.80	360	0
W1670	10	3.60	2.07	3.17	1.06	0.00324	0.80	360	0
W1710	10	2.88	0.58	3.47	1.10	0.00259	0.80	360	0
W1720	10	2.88	2.16	3.47	1.10	0.00259	0.80	360	0
W1760	10	3.44	1.17	3.60	1.08	0.00310	0.80	360	0
W1770	10	2.88	0.16	3.47	1.10	0.00259	0.80	360	0
W1810	10	3.60	1.19	3.17	1.06	0.00324	0.80	360	0
W1820	10	2.88	0.23	3.47	1.10	0.00259	0.80	360	0
W1870	10	3.60	0.88	3.17	1.06	0.00324	0.80	360	0
W1920	10	2.61	0.95	3.70	1.20	0.00235	0.80	360	0
W1960	10	2.08	6.80	3.49	1.13	0.00188	0.80	360	0
W1970	10	2.08	3.01	3.49	1.13	0.00188	0.80	360	0
W2010	10	4.47	6.43	3.71	0.98	0.00402	0.80	360	0
W2020	10	4.47	0.59	3.71	0.98	0.00402	0.80	360	0
W2060	10	4.47	25.07	3.71	0.98	0.00402	0.80	360	0
W2070	10	4.47	1.92	3.71	0.98	0.00402	0.80	360	0
W610	10	3.60	2.12	3.17	1.06	0.00324	0.80	360	0
W620	10	3.60	2.81	3.17	1.06	0.00324	0.80	360	0
W640	10	3.44	3.09	3.60	1.08	0.00310	0.80	360	0
W650	10	3.60	5.97	3.17	1.06	0.00324	0.80	360	0
W670	10	2.88	0.80	3.47	1.10	0.00259	0.80	360	0
W680	10	3.81	0.37	3.55	1.07	0.00343	0.80	360	0
W690	10	3.60	0.24	3.17	1.06	0.00324	0.80	360	0
W700	10	2.88	1.89	3.47	1.10	0.00259	0.80	360	0
W710	10	4.47	0.16	3.71	0.98	0.00402	0.80	360	0
W720	10	4.47	0.09	3.71	0.98	0.00402	0.80	360	0

Subbasin	Initial Soil/ GW 1/GW 2 (%)	Maximum Infiltration (in/hr)	Impervious (%)	Soil Storage (in)	Tension Storage (in)	Soil/GW 1 Percolation (in/hr)	GW 1/GW 2 Storage (in)	GW 1/GW 2 Coefficient (hr)	GW 2 Percolation (in/hr)
W730	10	4.47	0.24	3.71	0.98	0.00402	0.80	360	0
W740	10	2.88	0.78	3.47	1.10	0.00259	0.80	360	0
W750	10	2.88	1.25	3.47	1.10	0.00259	0.80	360	0
W760	10	4.47	1.94	3.71	0.98	0.00402	0.80	360	0
W770	10	4.47	1.52	3.71	0.98	0.00402	0.80	360	0
W780	10	3.81	2.01	3.55	1.07	0.00343	0.80	360	0
W800	10	4.47	0.09	3.71	0.98	0.00402	0.80	360	0
W810	10	4.47	1.11	3.71	0.98	0.00402	0.80	360	0
W820	10	4.47	0.14	3.71	0.98	0.00402	0.80	360	0
W830	10	4.47	0.35	3.71	0.98	0.00402	0.80	360	0
W840	10	4.47	0.22	3.71	0.98	0.00402	0.80	360	0
W870	10	4.47	0.30	3.71	0.98	0.00402	0.80	360	0
W890	10	4.47	2.31	3.71	0.98	0.00402	0.80	360	0
W900	10	4.47	0.44	3.71	0.98	0.00402	0.80	360	0
W910	10	3.81	0.56	3.55	1.07	0.00343	0.80	360	0
W920	10	4.47	3.47	3.71	0.98	0.00402	0.80	360	0
W930	10	4.14	1.13	3.41	0.98	0.00373	0.80	360	0
W940	10	4.14	0.91	3.41	0.98	0.00373	0.80	360	0
W950	10	4.14	3.11	3.41	0.98	0.00373	0.80	360	0
W960	10	4.14	0.02	3.41	0.98	0.00373	0.80	360	0
W970	10	4.47	15.74	3.71	0.98	0.00402	0.80	360	0

Clark UH/ModClark Transform Method Parameters:

Subbasin	Tc (hr)	R (hr)	Subbasin	Tc (hr)	R (hr)
W1000	12.51	16.26	W1960	9.34	12.14
W1020	12.95	16.84	W1970	1.07	1.39
W1050	4.85	6.31	W2010	31.47	40.91
W1060	6.16	8.01	W2020	12.02	15.63
W1070	4.08	5.30	W2060	18.27	23.75
W1080	1.33	1.73	W2070	6.38	8.29
W1090	3.99	5.19	W610	10.27	13.35
W1100	2.56	3.33	W620	6.57	8.54
W1110	6.19	8.05	W640	6.59	8.57
W1120	7.97	10.36	W650	14.27	18.55
W1130	7.61	9.89	W670	4.68	6.08
W1140	20.22	26.29	W680	9.73	12.65
W1160	5.38	6.99	W690	16.83	21.88
W1180	2.19	2.85	W700	17.63	22.92
W1210	7.01	9.11	W710	10.88	14.14
W1250	10.54	13.70	W720	10.95	14.24
W1270	15.28	19.86	W730	9.04	11.75
W1310	5.50	7.15	W740	4.21	5.47
W1320	3.01	3.91	W750	9.39	12.21
W1360	12.02	15.63	W760	14.01	18.21
W1370	3.45	4.49	W770	9.49	12.34
W1420	15.84	20.59	W780	7.63	9.92
W1470	28.13	36.57	W800	8.30	10.79
W1510	13.89	18.06	W810	2.70	3.51
W1520	7.39	9.61	W820	7.62	9.91
W1560	18.20	23.66	W830	9.05	11.77
W1570	15.65	20.35	W840	11.60	15.08
W1610	4.82	6.27	W870	12.86	16.72
W1620	24.31	31.60	W890	17.26	22.44
W1660	21.48	27.92	W900	28.59	37.17
W1670	2.57	3.34	W910	5.62	7.31
W1710	6.09	7.92	W920	21.90	28.47
W1720	0.89	1.16	W930	9.97	12.96
W1760	14.01	18.21	W940	6.69	8.70
W1770	2.79	3.63	W950	6.46	8.40
W1810	0.66	0.86	W960	4.31	5.60
W1820	20.18	26.23	W970	0.98	1.27
W1870	5.28	6.86			
W1920	6.72	8.74			

Baseflow Parameters:

Subbasin	Initial GW 1 /GW 2 Baseflow (cfs)	GW 1/GW 2 Coefficient (hr)	GW 1 /GW 2 Reservoirs	Subbasin	Initial GW 1 /GW 2 Baseflow (cfs)	GW 1/GW 2 Coefficient (hr)	GW 1 /GW 2 Reservoirs
W1000	3.99	60	1	W1920	21.91	60	1
W1020	3.81	60	1	W1960	3.22	60	1
W1050	4.00	60	1	W1970	5.85	60	1
W1060	4.00	60	1	W2010	3.20	60	1
W1070	2.41	60	1	W2020	0.23	60	1
W1080	5.22	60	1	W2060	0.10	60	1
W1090	13.66	60	1	W2070	6.72	60	1
W1100	0.96	60	1	W610	0.67	60	1
W1110	15.13	60	1	W620	1.77	60	1
W1120	4.13	60	1	W640	7.01	60	1
W1130	5.54	60	1	W650	3.34	60	1
W1140	13.60	60	1	W670	16.87	60	1
W1160	2.58	60	1	W680	14.85	60	1
W1180	2.13	60	1	W690	4.05	60	1
W1210	2.14	60	1	W700	3.91	60	1
W1250	1.17	60	1	W710	4.25	60	1
W1270	2.57	60	1	W720	4.62	60	1
W1310	6.56	60	1	W730	7.02	60	1
W1320	1.38	60	1	W740	6.88	60	1
W1360	0.19	60	1	W750	0.17	60	1
W1370	5.13	60	1	W760	11.56	60	1
W1420	0.63	60	1	W770	15.73	60	1
W1470	3.10	60	1	W780	13.19	60	1
W1510	3.25	60	1	W800	4.93	60	1
W1520	9.44	60	1	W810	0.87	60	1
W1560	2.76	60	1	W820	3.76	60	1
W1570	3.96	60	1	W830	0.11	60	1
W1610	4.87	60	1	W840	5.43	60	1
W1620	14.31	60	1	W870	11.72	60	1
W1660	2.28	60	1	W890	16.01	60	1
W1670	1.98	60	1	W900	7.80	60	1
W1710	0.32	60	1	W910	6.52	60	1
W1720	18.20	60	1	W920	1.43	60	1
W1760	8.23	60	1	W930	2.93	60	1
W1770	15.17	60	1	W940	5.60	60	1
W1810	0.18	60	1	W950	4.18	60	1
W1820	12.87	60	1	W960	3.77	60	1
W1870	14.09	60	1	W970	6.57	60	1

Muskingum-Cunge Routing Method:

Reach	Length (ft)	Average Slope (ft/ft)	Manning's n	Width (ft)	Side Slope (H:V)	Reach	Length (ft)	Average Slope (ft/ft)	Manning's n	Width (ft)	Side Slope (H:V)
R10	80077	0.00204	0.05	67.54	0.5	R210	17194	0.00336	0.06	469.87	0.5
R1170	32597	0.00327	0.06	44.74	0.5	R220	6008	0.00361	0.07	472.58	0.5
R120	8871	0.00552	0.07	74.71	0.5	R230	99721	0.00161	0.06	74.22	0.5
R1220	40669	0.00933	0.07	111.27	0.5	R240	20253	0.00227	0.06	57.46	0.5
R1260	10727	0.01119	0.07	128.50	0.5	R270	6599	0.00318	0.07	145.83	0.5
R1330	13230	0.00108	0.06	57.31	0.5	R290	57012	0.00136	0.05	106.19	0.5
R1390	95227	0.00066	0.08	220.06	0.5	R340	16698	0.00484	0.05	99.39	0.5
R140	60571	0.00164	0.08	145.36	0.5	R350	19356	0.00211	0.06	63.47	0.5
R1430	14357	0.00208	0.08	75.00	0.5	R370	70685	0.00476	0.07	60.67	0.5
R1480	30434	0.00160	0.07	148.12	0.5	R390	32787	0.00172	0.07	69.96	0.5
R1540	80979	0.00142	0.07	296.53	0.5	R40	28869	0.00169	0.07	79.25	0.5
R1580	20316	0.00118	0.08	330.38	0.5	R410	82591	0.00123	0.07	353.28	0.5
R160	7203	0.00055	0.06	124.26	0.5	R430	23621	0.00090	0.07	357.27	0.5
R1640	133771	0.00111	0.08	258.47	0.5	R440	27611	0.00073	0.07	127.23	0.5
R1690	36081	0.00059	0.08	98.79	0.5	R450	52592	0.00092	0.07	48.61	0.5
R170	172990	0.00101	0.06	108.36	0.5	R480	28308	0.00205	0.07	62.90	0.5
R1740	259351	0.00100	0.08	183.80	0.5	R490	11548	0.00068	0.06	119.33	0.5
R180	52466	0.00488	0.07	64.75	0.5	R50	30017	0.00072	0.07	107.91	0.5
R1880	117336	0.00050	0.06	75.62	0.5	R500	53011	0.00096	0.07	186.60	0.5
R1940	113244	0.00046	0.06	73.22	0.5	R510	84162	0.00156	0.06	188.56	0.5
R1990	50040	0.00098	0.06	94.78	0.5	R550	42960	0.00224	0.05	206.38	0.5
R20	15596	0.00039	0.06	99.87	0.5	R60	6201	0.00005	0.06	333.89	0.5
R2030	7292	0.00292	0.06	281.38	0.5	R70	19926	0.00056	0.07	459.56	0.5
						R90	13750	0.00010	0.07	152.24	0.5

<p style="text-align: center;">**Appendix B**</p>

Python Scripts

Extract NetCDF files in ArcGIS and save as a raster:

```
# Import arcpy module
import arcpy
from arcpy import env
from arcpy.sa import *

# Check out any necessary licenses
arcpy.CheckOutExtension("3D")
arcpy.CheckOutExtension("Spatial")

# Sources:
arcpy.env.overwriteOutput = True
arcpy.env.workspace = "C:\\Documents and Settings\\EHill\\Desktop\\Shenandoah\\NLDAS"
outputfolder = "C:\\Documents and Settings\\EHill\\Desktop\\Shenandoah\\NLDAS\\extract"

# Loop:
NCFiles = arcpy.ListFiles("*.nc")
for filename in NCFiles:
    print("Processing:" + filename)
    inNCFiles = arcpy.env.workspace + "/" + filename
    fileroot = filename[0:(len(filename)-3)]
    TempLayerFile = "precip"
    outNCFiles = outputfolder + "/" + fileroot

    # Process: Make NetCDF Raster Layer:
    arcpy.MakeNetCDFRasterLayer_md(inNCFiles, "APCPsfc_110_SFC_acc1h", "lon_110",
"lat_110", TempLayerFile, "", "", "BY_VALUE")

    # Process: Copy Raster:
    arcpy.CopyRaster_management(TempLayerFile, outNCFiles + ".tif", "", "", "", "NONE",
"NONE", "")
```

Clip projected raster to watershed:

```
# Import arcpy module
import arcpy
from arcpy import env
from arcpy.sa import *

# Check out any necessary licenses
arcpy.CheckOutExtension("3D")
arcpy.CheckOutExtension("Spatial")

# Sources:
```

```
arcpy.env.overwriteOutput = True
arcpy.env.workspace = "C:\\Documents and
Settings\\EHill\\Desktop\\Shenandoah\\NLDAS\\projected"
outputfolder = "C:\\Documents and Settings\\EHill\\Desktop\\Shenandoah\\NLDAS\\clipped"
NLDAS_Grid_Reference = "swtshd.shp"

# Loop:
rasters = arcpy.ListRasters()
for inRaster in rasters:
    outRaster = outputfolder + "/" + inRaster

    # Process: Extract by Mask
    arcpy.gp.ExtractByMask_sa(inRaster, NLDAS_Grid_Reference, outRaster)
```

Resample NLDAS grid cells to match cell size of grid cells in HEC-HMS:

```
import arcpy
from arcpy import sa
arcpy.gp.overwriteOutput=True
arcpy.CheckOutExtension("spatial")
import glob

Input=glob.glob("C:\\Documents and
Settings\\EHill\\Desktop\\Shenandoah\\NLDAS\\final\\*tif")

for i in Input:
    arcpy.Resample_management(i, i+"_2000.tif", "2000", "NEAREST")
```

Project raster:
```
# Import arcpy module
import arcpy
from arcpy import env
from arcpy.sa import *

# Check out any necessary licenses
arcpy.CheckOutExtension("3D")
arcpy.CheckOutExtension("Spatial")

arcpy.env.overwriteOutput = True
arcpy.env.workspace = "C:\\Documents and
Settings\\EHill\\Desktop\\Shenandoah\\NLDAS\\resample"
outputfolder = "C:\\Documents and Settings\\EHill\\Desktop\\Shenandoah\\NLDAS\\projecta"

# Loop:
rasters = arcpy.ListRasters()
for inRaster in rasters:
    outRaster = outputfolder + "/" + inRaster
```

```
   # Process: Project Raster
   arcpy.ProjectRaster_management(inRaster, outRaster,
"PROJCS['USA_Contiguous_Albers_Equal_Area_Conic_USGS_version',GEOGCS['GCS_Nort
h_American_1983',DATUM['D_North_American_1983',SPHEROID['GRS_1980',6378137.0,29
8.257222101]],PRIMEM['Greenwich',0.0],UNIT['Degree',0.0174532925199433]],PROJECTIO
N['Albers'],PARAMETER['False_Easting',0.0],PARAMETER['False_Northing',0.0],PARAMET
ER['Central_Meridian',-
96.0],PARAMETER['Standard_Parallel_1',29.5],PARAMETER['Standard_Parallel_2',45.5],PA
RAMETER['Latitude_Of_Origin',23.0],UNIT['Meter',1.0]]", "NEAREST", "2000", "", "",
"PROJCS['NAD_1983_UTM_Zone_18N',GEOGCS['GCS_North_American_1983',DATUM['D
_North_American_1983',SPHEROID['GRS_1980',6378137.0,298.257222101]],PRIMEM['Green
wich',0.0],UNIT['Degree',0.0174532925199433]],PROJECTION['Transverse_Mercator'],PARA
METER['false_easting',500000.0],PARAMETER['false_northing',0.0],PARAMETER['central_m
eridian',-
75.0],PARAMETER['scale_factor',0.9996],PARAMETER['latitude_of_origin',0.0],UNIT['Meter'
,1.0]]")
```

Convert forcing units to depth of precipitation:
```
# Import arcpy module
import arcpy
from arcpy import env
from arcpy.sa import *

# Check out any necessary licenses
arcpy.CheckOutExtension("3D")
arcpy.CheckOutExtension("Spatial")

# Sources:
arcpy.env.overwriteOutput = True
arcpy.env.workspace = "C:\\Documents and
Settings\\EHill\\Desktop\\Shenandoah\\NLDAS\\clipped"
outputfolder = "C:\\Documents and Settings\\EHill\\Desktop\\Shenandoah\\NLDAS\\final"
constant = "0.03937"

# Loop:
rasters = arcpy.ListRasters()
for inRaster in rasters:
   outRaster = outputfolder + "/" + inRaster

   # Process: Times
   arcpy.Times_3d(inRaster, constant, outRaster)
```

Convert raster to ascii:
```
import arcpy
from arcpy import sa
arcpy.gp.overwriteOutput=True
arcpy.CheckOutExtension("spatial")
import glob
```

Input=glob.glob("C:\\Documents and
Settings\\EHill\\Desktop\\Shenandoah\\NLDAS\\projecta*tif")

for i in Input:
    arcpy.RasterToASCII_conversion(i, i+".asc")

Compile ascii files into DSS:
import os

os.system(r"asc2dssGrid.exe INPUT=nldas_fora0125_h.a19951001.0000.002.tif_2000.tif.asc
PATHNAME=//SHENANDOAH/PRECIPITATION/30SEP1995:2300/01Oct1995:0000/NLDA
S/ DSSFILE=NLDAS.dss GRIDTYPE=SHG DTYPE=PER-CUM DUNITS=IN")
.
.
.
os.system(r"asc2dssGrid.exe INPUT=nldas_fora0125_h.a19960930.2300.002.tif_2000.tif.asc
PATHNAME=//SHENANDOAH/PRECIPITATION/30Sep1996:2200/30Sep1996:2300/NLDAS
/ DSSFILE=NLDAS.dss GRIDTYPE=SHG DTYPE=PER-CUM DUNITS=IN")

References

Ajami, N., Gupta, H., Wagener, T., & Sorooshian, S. (2004). Calibration of a semi-distributed hydrologic model for streamflow estimation along a river system. *Journal of Hydrology*, *298*(1), 112-135.

American Rivers. (2006). America's Most Endangered Rivers of 2006. Retrieved June 23, 2013, from http://crca.caloosahatchee.org/crca_docs/MER_full.pdf.

Ayyub, B. M., & McCuen, R. (2011). *Probability, statistics, and reliability for engineers and scientists*. Taylor & Francis US.

Bennett, T. H. (1998). *Development and application of a continuous soil moisture accounting algorithm for the Hydrologic Engineering Center Hydrologic Modeling System (HEC-HMS)* (Masters thesis, University of California, Davis).

Cruise, J., & Yu, S. L. (1982) *Determination of Rainfall Losses in Virginia, Phase II: Final Report*. Virginia Highway & Transportation Research Council.

Daly, C., Neilson, R. P., & Phillips, D. L. (1994). A statistical-topographic model for mapping climatological precipitation over mountainous terrain. *Journal of applied meteorology*, *33*(2), 140-158.

Da Silva, R. V., Yamashiki, Y., & Takara, K. (2010). Distributed TOPMODEL approach for rainfall-runoff routing modeling in large-scale basins. *Disaster Prevention Research Institute Annuals. B*, *53*(B), 37-44.

Duan, Q., Gupta, H. V., Sorooshian, S., Rousseau, A. N., & Turcotte, R. (2003). *Calibration of watershed models* (Vol. 6, pp. 1-345). American Geophysical Union.

Fulton, R. A., Breidenbach, J. P., Seo, D. J., Miller, D. A., & O'Bannon, T. (1998). The WSR-88D rainfall algorithm. *Weather and Forecasting*, *13*(2), 377-395.

Gao, H., Tang, Q., Shi, X., Zhu, C., Bohn, T. J., Su, F., ... & Wood, E. F. (2010). Water budget record from Variable Infiltration Capacity (VIC) model. *Algorithm Theoretical Basis Document for Terrestrial Water Cycle Data Records*.

Goddard Earth Sciences Data and Information Services Center (GES DISC). (2013). *README Document for North American Land Data Assimilation System Phase 2 (NLDAS-2) Products*. Technical Reference Document. National Aeronautics and Space Administration (NASA), Greenbelt, Maryland.

Hydrologic Engineering Center (HEC). (2000). *Hydrologic Modeling System, HEC-HMS*. Technical Reference Manual. U.S. Army Corps of Engineers, Davis, California.

Hydrologic Engineering Center (HEC). (2010a). *Hydrologic Modeling System, HEC-HMS*. User's Manual. U.S. Army Corps of Engineers, Davis, California.

Hydrologic Engineering Center (HEC). (2010b). *HEC-GeoHMS, Geospatial Hydrologic Modeling Extension.* User's Manual. U.S. Army Corps of Engineers, Davis, California.

Interstate Commission on the Potomac River Basin. (2012). *Facts.* Retrieved on June 26, 2013, from http://www.potomacriver.org/2012/facts-a-faqs.

Kim, S. (2012). Response of hydrologic calibration to replacing gage-based with NEXRAD-based precipitation data in the USEPA Chesapeake Bay Watershed model. (PhD Dissertation, University of Maryland, College Park)

Knebl, M. R., Yang, Z. L., Hutchison, K., & Maidment, D. R. (2005). Regional scale flood modeling using NEXRAD rainfall, GIS, and HEC-HMS/RAS: a case study for the San Antonio River Basin Summer 2002 storm event. *Journal of Environmental Management*, *75*(4), 325-336.

Kull, D. W., & Feldman, A. D. (1998). Evolution of Clark's unit graph method to spatially distributed runoff. *Journal of Hydrologic Engineering*, *3*(1), 9-19.

Lancaster University. (2005). *TOPMODEL Freeware.* Retrieved on June 29, 2013, from http://www.es.lancs.ac.uk/hfdg/freeware/hfdg_freeware_top.htm.

Leavesley, G.H., Litchy, R.W., Troutman, B.M., & Saindon, L.G. (1983). *Precipitation-Runoff Modeling System.* User's Manual. U.S. Geological Survey, Denver, Colorado.

Liang, X., Lettenmaier, D. P., Wood, E. F., & Burges, S. J. (1994). A simple hydrologically based model of land surface water and energy fluxes for general circulation models. *Journal of Geophysical Research: Atmospheres (1984–2012)*, *99*(D7), 14415-14428.

Lohmann, D., NOLTE-HOLUBE, R. A. L. P. H., & Raschke, E. (1996). A large-scale horizontal routing model to be coupled to land surface parametrization schemes. *Tellus A*, *48*(5), 708-721.

Lohmann, D., Raschke, E., Nijssen, B., & Lettenmaier, D. P. (1998). Regional scale hydrology: I. Formulation of the VIC-2L model coupled to a routing model. *Hydrological Sciences Journal*, *43*(1), 131-141.

Luo, L., Robock, A., Mitchell, K. E., Houser, P. R., Wood, E. F., Schaake, J. C., ... & Tarpley, J. D. (2003). Validation of the North American Land Data Assimilation System (NLDAS) retrospective forcing over the southern Great Plains. *Journal of Geophysical Research*, *108*(D22), 8843.

McCandless, T. L. (2003). Maryland stream survey: Bankfull discharge and channel characteristics of streams in the Coastal Plain hydrologic region. *US Fish and Wildlife Service, Chesapeake Bay Field Office, CBFO-S03-02*.

McCuen, R. H. (2002). *Modeling hydrologic change: statistical methods*. CRC Press.

McCuen, R. H., Knight, Z., & Cutter, A. G. (2006). Evaluation of the Nash–Sutcliffe efficiency index. *Journal of Hydrologic Engineering*, *11*(6), 597-602.

McEnroe, Bruce M. (2010) Guidelines for Continuous Simulation of Streamflow in Johnson County, Kansas, with HEC-HMS. Report to Johnson County Public Works and Infrastructure Stormwater Management Program. Retrieved August 6, 2013, from http://publicworks.jocogov.org/files/documents/handbook/continuous-simulation-with-HEC-HMS.pdf.

McMillan, H., Jackson, B., Clark, M., Kavetski, D., & Woods, R. (date unknown). Input Uncertainty in Hydrological Models: An Evaluation of Error Models for Rainfall. For Submission to: Journal of Hydrometeorology: Special Collection on the State of the Science of Precipitation Research. Retrieved June 29, 2013, from http://www.hilandtom.com/hilarymcmillan/McMillan_RainfallVariability_Proof.pdf.

Montesinos-Barrios, P. & Beven, K. (date unknown). *Evaluation of TOPMODEL*. Retrieved on June 29, 2013, from http://s1004.okstate.edu/S1004/Regional-Bulletins/Modeling-Bulletin/TOPMODEL.html.

Neary, V. S., Habib, E., & Fleming, M. (2004). Hydrologic modeling with NEXRAD precipitation in middle Tennessee. *Journal of Hydrologic Engineering*, *9*(5), 339-349.

Nan, Z., Wang, S., Liang, X., Adams, T. E., Teng, W., & Liang, Y. (2010). Analysis of spatial similarities between NEXRAD and NLDAS precipitation data products. *Selected Topics in Applied Earth Observations and Remote Sensing, IEEE Journal of*, *3*(3), 371-385.

Nash, J., & Sutcliffe, J. V. (1970). River flow forecasting through conceptual models part I—A discussion of principles. *Journal of Hydrology*, *10*(3), 282-290.

National Aeronautics and Space Administration (NASA). (2013a). *Land Information System (LIS)*. Retrieved June 26, 2013 from http://lis.gsfc.nasa.gov/.

National Aeronautics and Space Administration (NASA). (2013b). *NLDAS-2 Forcing Dataset Information*. Retrieved June 25, 2013 from http://ldas.gsfc.nasa.gov/nldas/NLDAS2forcing.php.

National Center for Atmospheric Research (NCAR). (date unknown). *Atmospheric Reanalysis: Overview & Comparison Tables*. Retrieved on August 12, 2013 from https://climatedataguide.ucar.edu/reanalysis/atmospheric-reanalysis-over.

National Oceanic and Atmospheric Administration (NOAAa). (date unknown). *Reading GRIB Files*. Retrieved August 12, 2013 from http://www.cpc.ncep.noaa.gov/products/wesley/reading_grib.html.

National Oceanic and Atmospheric Administration (NOAAb). (date unknown). *Data Resources: What is netCDF?* Retrieved June 26, 2013 from http://www.esrl.noaa.gov/psd/data/gridded/whatsnetCDF.html.

Natural Resources Conservation Service (NRCS). (date unknown). *Description of Soil Survey Geographic (SSURGO) Database*. Retrieved June 28, 2013, from http://soils.usda.gov/survey/geography/ssurgo/description.html.

Natural Resources Conservation Service (NRCS). (1986). *Small Watershed Hydrology, Win-TR55*. User Guide. United States Department of Agriculture, Washington, DC.

Nourani, V., Roughani, A., & Gebremichael, M. (2011). TOPMODEL capability for rainfall-runoff modeling of the Ammameh watershed at different time scales using different terrain algorithms. *Journal of Urban and Environmental Engineering*, *5*(1), 1-15.

Pan, M., Sheffield, J., Wood, E. F., Mitchell, K. E., Houser, P. R., Schaake, J. C., ... & Tarpley, J. D. (2003). Snow process modeling in the North American Land Data Assimilation System (NLDAS): 2. Evaluation of model simulated snow water equivalent. *Journal of Geophysical Research*, *108*(D22), 8850.

Paudel, M., Nelson, E. J., & Downer, C. W. (2009, May). Assessment of Lumped, Quasi-Distributed and Distributed Hydrologic Models of the US Army Corps of Engineers. In *World Environmental and Water Resources Congress 2009 Great Rivers* (pp. 5932-5942). ASCE.

Pechlivanidis, I. G., Jackson, B. M., Mcintyre, N. R., & Wheater, H. S. (2011). Catchment scale hydrological modelling: a review of model types, calibration approaches and uncertainty analysis methods in the context of recent developments in technology and applications. *Global Nest Journal*, *13*(3), 193-214.

Potomac Conservancy. (2013). *Potomac Conservancy's Priority Watersheds*. Retrieved June, 26, 2013, from http://www.potomac.org/site/priorities/#shenandoah.

Shah, S. M. S., O'Connell, P. E., & Hosking, J. R. M. (1996). Modelling the effects of spatial variability in rainfall on catchment response. 1. Formulation and calibration of a stochastic rainfall field model. *Journal of Hydrology*, *175*(1), 67-88.

Smith, M. B., Seo, D. J., Koren, V. I., Reed, S. M., Zhang, Z., Duan, Q., & Cong, S. (2004). The distributed model intercomparison project (DMIP): motivation and experiment design. *Journal of Hydrology*, *298*(1), 4-26.

Song-James, Z. (date unknown). Hydrologic Modeling Applications in National Flood Insurance Program. Retrieved June 27, 2013, from http://www.gcmrc.gov/library/reports/physical/fine_sed/8thfisc2006/3rdfihmc/10f_song-james.pdf.

Sullivan, J., & Maidment, D. R. (2013). Soil moisture mapping of drought in Texas. Report for Integrated Drought Information System (IDISII). Retrieved July 24, 2013, from http://www.twdb.state.tx.us/publications/reports/contracted_reports/doc/1200011387_final%20report.pdf.

Stanford University. (2000). *RMS Error*. Retrieved on August 12, 2013, from http://www-stat.stanford.edu/~susan/courses/s60/split/node60.html.

Tiruneh, N. (2007). Basin-wide Annual Baseflow Analysis for the Fractured Bedrock Unit in the Potomac. Report for the Interstate Commission on the Potomac River, ICPRB Report No. 07-6.

The University of Arizona. (2013, January 23). *What is a Watershed?* Retrieved June 30, 2013, from http://cals.arizona.edu/watershedsteward/resources/module/Intro/intro_p.

University of Saskatchewan. (2004). *MAGS Glossary*. Retrieved August 11, 2013, from http://www.usask.ca/geography/MAGS/Glossary_e.html.

University of Delaware Water Resources Agency. (date unknown). *What is a watershed and why should I care?* Retrieved June 30, 2013, from http://info.geography.siu.edu/people/oyana/Teaching/381_550/watershed.

University of Virginia (UVAa) Climatology Office. (date unknown). *Virginia's Climate*. Retrieved June 26, 2013, from http://climate.virginia.edu/description.htm.

University of Virginia (UVAb) Climatology Office. (date unknown). *Potential Evapotranspiration, Annual Precipitation, and Annual Precipitation Minus Potential Evapotranspiration*. Retrieved July 27, 2013, from http://climate.virginia.edu/va_pet_prec_diff.htm.

University of Washington. (2009a). *Variable Infiltration Capacity (VIC)Macroscale Hydrologic Model, VIC Model Overview*. Retrieved on June 26, 2013, from http://www.hydro.washington.edu/Lettenmaier/Models/VIC/Overview/ModelOverview.shtml.

University of Washington. (2009b). *Variable Infiltration Capacity (VIC)Macroscale Hydrologic Model,Distributed Precipitation Formulation*. Retrieved on June 26, 2013, from http://www.hydro.washington.edu/Lettenmaier/Models/VIC/Overview/DistPrecText.shtml.

U.S. Environmental Protection Agency (EPA). (2012). *What is a Watershed?* Retrieved June 30, 2013, from http://water.epa.gov/type/watersheds/whatis.cfm.

U.S. Geological Survey (USGS). (2012). *Frequently Asked Questions, Multi-Resolution Land Characterization (MRLC) Consortium*. Retrieved June 28, 2013, from http://mrlc.gov/faq.php.

U.S. Geological Survey (USGS). (2013a). *Elevation*. Retrieved June 28, 2013, from http://nationalmap.gov/elevation.html.

U.S. Geological Survey (USGS). (2013b). *National Hydrography Dataset*. Retrieved June 28, 2013, from http://nhd.usgs.gov.

Virginia Employment Commission. (2013). Virginia Community Profile, Shenandoah Valley (LWIA IV). Retrieved June 29, 2013, from http://virginiascan.yesvirginia.org/communityprofiles/createPDF.aspx?id=231.

Wang, Y. (2011). *Calibrating Shenandoah watershed SWAT model using a nonlinear groundwater algorithm* (Masters thesis, University of Maryland, College Park).

Weisstein, E. W. (date unknown). *Distribution Functions*. Mathworld-A Wolfram Web Resource . Retrieved August 11, 2013 from http://mathworld.wolfram.com/DistributionFunction.html.

Xia, Y., Ek, M., Wei, H., & Meng, J. (2012). Comparative analysis of relationships between NLDAS-2 forcings and model outputs. *Hydrological Processes*, *26*(3), 467-474.

Zhang, H. L., Wang, Y. J., Wang, Y. Q., Li, D. X., & Wang, X. K. (2013). The effect of watershed scale on HEC-HMS calibrated parameters: a case study in the Clear Creek watershed in Iowa, US. *Hydrology and Earth System Sciences*, *17*(7), 2735-2745.